

The Synthesis and Spectroscopic Study of a Spirooxazine-Functionalized  
Poly(phenylenevinylene)

Jordan Thomas Walk

Tazewell, Virginia

Bachelor of Science, The College of William & Mary, 2008

A Thesis presented to the Graduate Faculty  
of the College of William and Mary in Candidacy for the Degree of  
Master of Science

Department of Chemistry

The College of William and Mary  
August, 2009

## APPROVAL PAGE

This Thesis is submitted in partial fulfillment of  
the requirements for the degree of

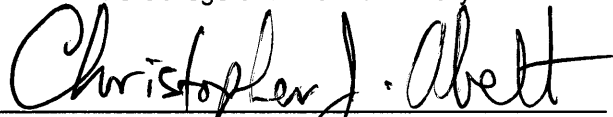
Master of Science

  
Jordan Thomas Walk

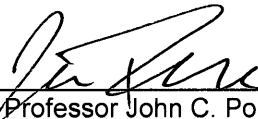
Approved by the Committee, July, 2009



Committee Chair  
Professor Elizabeth J. Harbron  
The College of William and Mary



Professor Christopher J. Abelt  
The College of William and Mary



Professor John C. Poutsma  
The College of William and Mary

## ABSTRACT PAGE

The synthesis and fluorescence studies of two spirooxazine-functionalized poly(phenylenevinylene) derivatives is presented. One of the polymers, a 50% spirooxazine-functionalized PPV derivative, exhibits reversible quenching of its fluorescence upon exposure to ultraviolet light. Poor solubility of this polymer was overcome by the synthesis of a 25% spirooxazine-functionalized PPV derivative, which unfortunately displayed no quenching. Synthesis of the polymers was completed using the Heck coupling reaction between two benzene monomers bearing aryl bromines and ethenyl groups, respectively. The monomers contained alkoxy groups to improve the solubility of the resulting polymers. One of the monomers was functionalized with a spirooxazine via a decyloxy group. Synthesis of the diethenylbenzene monomer was achieved using the Wittig reaction after attempts at a Stille coupling were unsuccessful. The groundwork has been laid for future experiments to improve the efficiency of reversible, selective PPV quenching by modification of the polymer as necessary.

## TABLE OF CONTENTS

Table of Contents	i
Table of Figures	ii
Dedication	iii
Acknowledgments	iv
Background	1
Results and Discussion	15
Monomer Synthesis	15
Polymerizations	28
Early Fluorescence Studies	31
Alternate Synthetic Routes	36
Conclusion	46
Experimental	49
References	61
Appendix (NMR Spectra)	65

## TABLE OF FIGURES

Figure 1 – Backbone of Poly(phenylene vinylene)	2
Figure 2 – Poly(2,5-bis(decyloxy)-1,4-phenylenevinylene)	2
Figure 3 – Jablonski Diagram Showing Fluorescence	4
Figure 4.– Isomerization of Azobenzene	9
Figure 5 – Overlap of Azobenzene Absorption and PPV Emission	9
Figure 6 – Different Conformations of Spiropyran and Spirooxazine	10
Figure 7 – Gilch Polymerization Overview	12
Figure 8 – Gilch Polymerization Mechanism	12
Figure 9 – Heck Reaction Overview	13
Figure 10 – Heck Reaction Mechanism	14
Figure 11 – Synthesis of SO-PPV	15
Figure 12 – Synthesis of 1,4-bis(decyloxy)-2,5-diethenylbenzene	16
Figure 13 – Methylbromination Mechanism	17
Figure 14 – Acetyloxymethyl Mechanism	18
Figure 15 – LAH Ester Reduction Mechanism	19
Figure 16 – PCC Oxidation Mechanism	20
Figure 17 – Wittig Reaction Mechanism	21
Figure 18 – Synthesis of Hydroxyspirooxazine	22
Figure 19 – Nitrosation Mechanism	23
Figure 20 – Spirooxazine Condensation Mechanism	24
Figure 21 – Synthesis of <b>5</b>	25
Figure 22 – <b>14</b> Forming Mechanism	25
Figure 23 – Difunctionalized Side Product from <b>14</b> Synthesis	26
Figure 24 – Bromination mechanism	26
Figure 25 – Synthesis of Control Polymer <b>15</b>	28
Figure 26 – Synthesis of 25% Functionazlied PPV <b>16</b>	30
Figure 27 – Absorption and Emission Spectra of <b>15</b>	31
Figure 28 – Absorption and Emission Spectra of SO-PPV <b>1</b>	32
Figure 29 – UV Effects on Fluorescence of <b>1</b>	33
Figure 30 – UV Effects of Absorption of <b>1</b>	34
Figure 31 – Absorption and Emission Spectra of	35
Figure 32 – Diethenylbenzene Synthesis Using Stille Coupling	36
Figure 33 – Stille Coupling Mechanism	37
Figure 34 – Palladium Catalyst	38
Figure 35 – Synthesis of <b>18</b> Using Bis(pyridine)iodonium Tetrafluoroborate	39

## Table of Figures (Cont.)

Figure 36 – Iodination Mechanism Using Bis(pyridine)Iodonium Tetrafluoroborate	39
Figure 37 – Synthesis of <b>18</b> Using Mercury Acetate	40
Figure 38 – Iodination Mechanism Using Mercury Acetate	41
Figure 39 – Stille Coupling Using <b>18</b> as Starting Material	42
Figure 40 – Attempted Routes to Aldehyde <b>10</b>	42
Figure 41 – Oxidation Mechanism Using Hexamine	43
Figure 42 – Oxidation Mechanism Using Pyridine N-oxide	44
Figure 43 – Oxidation Mechanism Using DMSO	44
Figure 44 – <sup>1</sup> H NMR Spectrum of <b>7</b>	65
Figure 45 – <sup>13</sup> C NMR Spectrum of <b>7</b>	66
Figure 46 - <sup>1</sup> H NMR Spectrum of <b>8</b>	67
Figure 47 - <sup>13</sup> C NMR Spectrum of <b>8</b>	68
Figure 48- <sup>1</sup> H NMR Spectrum of <b>9</b>	69
Figure 49 - <sup>13</sup> C NMR Spectrum of <b>9</b>	70
Figure 50 - <sup>1</sup> H NMR Spectrum of <b>10</b>	71
Figure 51 - <sup>13</sup> C NMR Spectrum of <b>10</b>	72
Figure 52 - <sup>1</sup> H NMR Spectrum of <b>3</b>	73
Figure 53 - <sup>13</sup> C NMR Spectrum of <b>3</b>	74
Figure 54 - <sup>1</sup> H NMR Spectrum of <b>4</b>	75
Figure 55 - <sup>13</sup> C NMR Spectrum of <b>4</b>	76
Figure 56 - <sup>1</sup> H NMR Spectrum of <b>14</b>	77
Figure 57 - <sup>13</sup> C NMR Spectrum of <b>14</b>	78
Figure 58 - <sup>1</sup> H NMR Spectrum of <b>5</b>	79
Figure 59 - <sup>13</sup> C NMR Spectrum of <b>5</b>	80
Figure 60 - <sup>1</sup> H NMR Spectrum of <b>2</b>	81
Figure 61 - <sup>13</sup> C NMR Spectrum of <b>2</b>	82
Figure 62 - <sup>1</sup> H NMR Spectrum of <b>18</b>	83
Figure 63 - <sup>13</sup> C NMR Spectrum of <b>18</b>	84

## DEDICATION

In loving memory of my dad, who couldn't do organic chemistry.

## ACKNOWLEDGEMENTS

First and foremost, I'd like to express my gratitude to Elizabeth Harbron for offering me a position in her lab. Her personal and professional advice over the past year has been invaluable and much of what I accomplish in the future can no doubt be attributed to things I've learned under her tutelage. Further thanks go to Chris Abelt and JC Poutsma, who've had a role in both my undergraduate and graduate research here at the College, for serving on this committee. As I head off on further adventures, I do so with the fondest memories of the last four years. Every member of this faculty has had some hand in my journey and has made my time here extremely worthwhile. They will all be dearly missed. Finally, I'd also like to thank my fellow labmates Christina Davis, Brooklynd Saar, Becca Allred, Marissa Kovary, Chris Lee, Josh Campbell, and Katie Peth. I hope my next lab will be half as entertaining as you all have been.

## Background

Conjugated polymers are very useful in a wide variety of technologies due to their delocalized  $\pi$ -electron bonding (1). Modification of these polymers can result in a myriad of optical, mechanical, and semiconducting properties (1, 2). Conjugated polymers can be found in LED's, photodiodes, field-effect transistors, polymer grid triodes, light-emitting electrochemical cells, optocouplers, solid state lasers, field-effect transistors, photovoltaics, and flexible displays (1, 3, 4). The fluorescence of conjugated polymers is of particular interest to the Harbron lab (5-10). In the past, azobenzene has been covalently attached to poly(phenylene vinylene) (PPV) and used to quench its fluorescence. While azobenzene is suitable for some PPV fluorescence quenching, other molecules have better spectral overlap with PPV and thus can quench fluorescence more strongly. This work describes both the synthesis of a PPV-bound spirooxazine dye and some of the resulting optical properties, with the aim of improving the efficiency of PPV quenching via an energy transfer mechanism.

PPV is a polymer with repeating units consisting of a vinyl group attached to a phenyl group. The vinyl attachments to the phenyl group can be at any location on the ring, but they are most often seen para to each other. Early attempts at PPV synthesis produced the powder form of the polymer, which is insoluble in common solvents (11, 12). This is due to the high dielectric constant created by the delocalization of electrons along the polymer backbone (13). Insolubility was improved by adding alkoxy groups to the phenyl group (Figure 2) (11-13). The most widely used alkoxy group has been the 2-

ethylhexyloxy group, though others with at least six carbons have been shown to increase solubility (14).

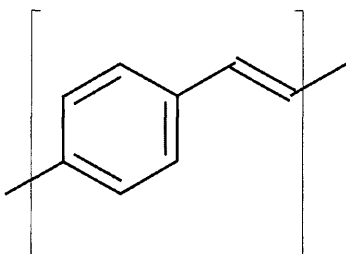


Figure 1 – Backbone of Poly(phenylene vinylene)

Alkoxy groups also have the effect of lowering the melting point of polymers (13).

Furthermore, the added steric hindrance from the alkoxy groups greatly extends the

polymer and prevents it from coiling (15). Coils in a polymer have the effect of

shortening chromophores due to bends which break the conjugation (13). Therefore,

when alkoxy groups are added to PPV the end result is longer chromophores.

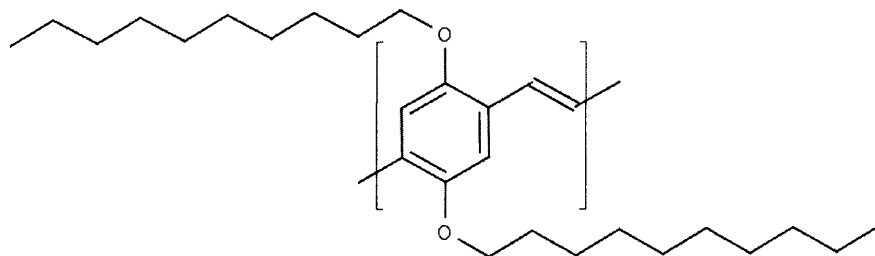


Figure 2 – Poly(2,5-Bis(decyloxy)-1,4-phenylene vinylene)

The delocalized  $\pi$ -bonding of PPV results in some interesting properties. Its ability to conduct electricity creates a useful material that combines the processability of a polymer with the ability to act as a semiconductor (13). PPV and its derivatives have thus been incorporated into several new technologies and their physics and chemistry

studied further by taking advantage of these properties (1, 3, 4). It is also highly fluorescent. The fluorescence of PPV results from the combination of its rigid aromatic character and its planar conjugated segments (16). A goal of the Harbron lab is to control the fluorescence of PPV and its derivatives by covalently attaching photochromic molecules to the polymer backbone.

Fluorescence is the radiative relaxation of an excited-state atomic or molecular electron to the ground state. While fluorescence had been observed for millennia, it was Sir George Stokes in the 19<sup>th</sup> century who began the modern study of the process (17). The sensitivity of fluorescence is so high that the minute amount of quinine found in tonic water can visibly fluoresce in broad daylight. In fact, the fluorescent molecule fluorescein was dissolved into the Danube river to prove that it and the Rhine river are connected by underground tunnels (17). Fluorescence occurs when a molecule's vibrational degrees of freedom are limited, usually seen in rigid, aromatic structures. These compounds tend to have many degenerate vibrational modes.

Spectroscopic transitions give information about the differences in energy between quantum states of an atom or molecule (16). Upon absorption of a photon of the correct energy, a molecule is typically found in both an excited electronic state as well as an excited vibrational state (Figure 3) (18). Absorption spectra of solutions are not simple thin lines due to the transition to different vibrational levels (16). If the excited state molecule is in solution, it typically loses its vibrational energy to heat in collisions with solvent molecules (18). This is called an internal conversion and occurs on a time scale

of about  $10^{-12}$  seconds (17). The time scale of fluorescence, typically between  $10^{-7}$  and  $10^{-10}$ , is much longer and so it usually occurs from the ground vibrational state of an excited electronic state (16, 17).

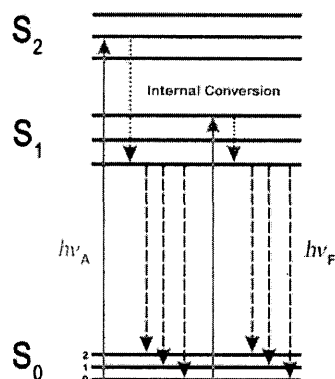


Figure 3 (19) – Fluorescence Via a Jablonski Diagram

Aliphatic and other non-rigid compounds can relax to the electronic ground state in collisions with other molecules, resulting in increased translational, rotational, and vibrational energies (18). Due to the decreased degrees of freedom, aromatic and other rigid molecules lack the vibrations necessary to undergo this radiationless deactivation. Instead, they spontaneously emit a photon and drop down to the ground electronic state (18). A molecule is typically returned to the ground state in an excited vibrational state (17). Therefore, fluorescence spectra in solution resemble absorption spectra in that they too have broad peaks instead of narrow lines.

Since fluorescence occurs from the ground vibrational state and an excited electronic state, fluorescence spectra tend to be mirror images of absorption spectra and almost always occur at a longer wavelength (18). The mirror image is due to the fact that

the vibrational levels of the ground and excited electronic states are very similar. The shift of the emission spectra to a longer wavelength is commonly called a Stokes shift and occurs because of the lower energy transitions of fluorescence (18).

The spectroscopic properties of conjugated polymers can be quite different from those seen in small molecules. The conjugation of  $\pi$ -orbitals can greatly increase the wavelength of both absorption and fluorescence. For example, while ethylene absorbs at 175 nm, 1,3-butadiene and 1,3,5-hexatriene absorb at 217 nm and 258 nm, respectively (16, 20).  $\beta$ -Carotene, a pigment found in plants, has a conjugated system of 11 bonds and absorbs at 465 nm (20). In addition to red-shifting the absorption spectra, more conjugation usually intensifies absorption (20). Theoretically, a molecule of PPV could be completely conjugated, resulting in a super-delocalized  $\pi$ -system which could absorb into the infrared (16). Realistically, the typical PPV chromophore consists of 10 to 15 repeating units of the polymer due to random bending of the polymer backbone as well as chemical defects (4, 5).

The chromophores found throughout a molecule of PPV are of varying lengths which are determined by the physical conformation as well as any physical defects of the polymer (4). The physical conformation of PPV can often be influenced by the technique used to prepare a sample and has been the cause of conflicting results in the past (4). Since longer conjugation lowers the energy of molecule, chromophores exist at varying energy levels. When a chromophore absorbs light and enters an excited state, the energy is often transferred to a nearby chromophore of lower energy. This energy can transfer to

both a neighboring chromophore as well as a chromophore on another molecule or another section of the same polymer that has been brought close in proximity due to chain coiling (21). Interchain or coiling intrachain energy transfer is often more facile than energy transfer along a polymer backbone (4). Sequential energy transfer ultimately deposits the migrating excited state, or exciton, to the lowest-energy chromophore (5, 21). This lowest-energy chromophore, also referred to as an energy trap, can be much lower in energy than the original photon absorbing chromophore and is the cause of the large Stokes shift seen in PPV and other conjugated polymers (4, 21).

The goal of this work has been to synthesize a new polymer which can selectively quench the fluorescence of PPV. This can be accomplished by covalently bonding a molecule to the polymer which, depending on the form of the molecule, can accept the energy from an exciton (17). This process is referred to as Fluorescence Resonance Energy Transfer, or FRET (17). Reversibility of quenching can be obtained by using a molecule which accepts energy only when under the influence of an outside stimulus and otherwise doesn't quench. If the energy acceptor is fluorescent itself, it can be used to tune the fluorescence color of a PPV sample; otherwise, the energy acceptor can dissipate the energy vibrationally (8). FRET is a radiationless process whereby two chromophores become coupled, the ultimate result being the loss of energy from the donor and the gain of that energy to the acceptor. An important example of FRET seen in nature is the "energy hopping" between chlorophyll molecules during photosynthesis (22). One energy acceptor can effectively quench the fluorescence of many

chromophores due to the exciton migration detailed previously (5). To effectively quench fluorescence, FRET must take place more quickly than the timescale of fluorescence (21).

One factor which determines the amount of energy transferred in FRET is the distance between the energy donor and the energy acceptor. The distance at which energy transfer is 50% efficient commonly referred to as the Förster radius (17). This distance can be as high as 70 Å and explains why FRET is commonly used in biochemistry, since this is typically larger than a protein or a membrane (16, 17). FRET can also be employed as a “molecular ruler” to measure distances in biological systems (17, 22). Note that it is not necessary for an energy acceptor and energy donor to be in physical contact with each other.

Another important component of FRET is the spectral overlap between an energy donor and energy acceptor. Although FRET is a non-radiative process, the absorption spectra of the energy acceptor must have some overlap with the emission spectra of the energy donor for any energy transfer to take place. The integrated overlap of the experimental acceptor absorption and donor emission spectra is referred to as the overlap integral (23). Ignoring other variables, to quench fluorescence the acceptor absorption spectrum must overlap the emission spectrum of the donor.

While there are an enormous number of compounds that could satisfactorily quench the fluorescence of PPV, the Harbron lab endeavors to control both the presence of any quenching as well as the degree of quenching. The strategy thus far has been to use a photochromic molecule as the energy acceptor (10). First reported in the literature

by Fritzsche in 1867, photochromism is the reversible transformation of a chemical species to another form with a different absorption spectra (24-26). Photochromism is most often seen in ophthalmic lenses, where bright sunlight causes compounds on the lenses to absorb more light (27). Silver chloride was originally used for this purpose, but today organic dyes are used instead (25, 28). Another important use of photochromism is in erasable memory media, most commonly experienced with the organic dyes used in recordable compact disks (24).

Photochromism in organic molecules is typically produced by a change in physical conformation which causes a shift in its absorption. For a compound to be considered photochromic, it must be possible for back isomerization to take place. Often, heat will usually expedite this process, an example of the interplay between photochromism and thermochromism (25, 27). If a photochromic molecule is attached to a fluorophore, selective quenching can be accomplished if one form of the molecule has greater overlap with the emission spectra of the fluorophore. In the past, the Harbron lab has used the photochromic molecule azobenzene to selectively quench the fluorescence of PPV (5, 6, 8, 10).

Azobenzene, thermodynamically stable in the trans conformation, undergoes an isomerization to the cis conformation under UV irradiation (Figure 4) (8). Due to the steric hindrance of the phenyl groups of cis-azobenzene, they are forced out of the same plane which partially disrupts the full conjugation of the molecule. The absorption spectra of both isomers of azobenzene partially overlap the emission spectra of PPV,

making them candidates for energy accepters in FRET (8).

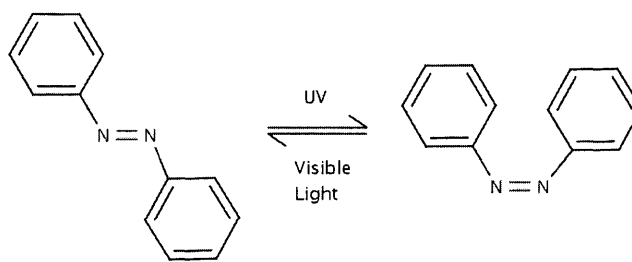


Figure 4 – Isomerization of Azobenzene

While the azobenzene isomers' spectra do overlap the emission spectra, the overlap is quite poor (Figure 5) (8). This eliminates azobenzene from being able to selectively quench PPV from an “on” to an “off” state, though the intensity of the fluorescence can be modulated to a certain extent. When azobenzene is covalently attached to PPV and in the trans conformation, fluorescence is diminished by 65%; after isomerization of about half of the azobenzene molecules, fluorescence is quenched by 79% (8). Harbron and co-workers found that the quenching of PPV fluorescence by azobenzene works in both films and solutions of PPV. While azobenzene can be useful in modulating the intensity of fluorescence, its poor overlap with the emission spectra of PPV eliminates its use as a true “switch” of fluorescence. Fortunately, there are other photochromic molecules better suited for the job.

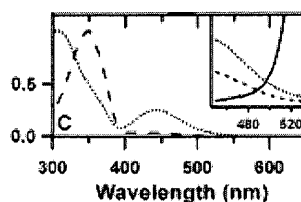


Figure 5 (8) – Poor Overlap of Azobenzene Absorption and PPV Emission Spectra; Cis-Azobenzene is dotted line, Trans-Azobenzene is dashed line, PPV Emission is Solid Line

Another class of highly studied photochromic molecules are spiropyrans and the related spirooxazines. First discovered in 1952, spiropyrans and spirooxazines are characterized by a spiro linkage which connects an indole and another conjugated subunit (29). Due to the  $sp^3$  hybridization of the spiro linkage, full conjugation of the molecules is interrupted and both are colorless solids. Upon irradiation with UV light, the spiro C-O bond breaks and the spiro carbon becomes  $sp^2$  hybridized (30). The molecule is then able to twist into the planer “merocyanine” conformation and become fully conjugated (Figure 6) (31). An example of the close relationship between photochromism and thermochromism, merocyanine reverts to the non-colored thermodynamically stable conformation upon heating (31).

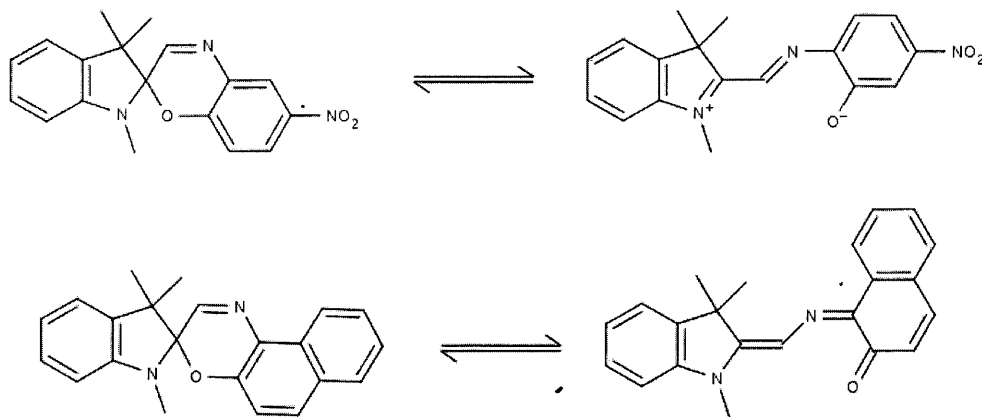


Figure 6 (20) – Different Conformations of Spiropyran and Spirooxazine

The greater conjugation of merocyanine lowers its electronic transition such that it absorbs in the visible part of the spectrum (30). The excited state of merocyanine formed from spirooxazine absorbs between 560-630 nm and the isomerization is complete within

50 picoseconds (27, 30). Though most spiropyrans form merocyanines that exist in a zwitterionic form, the spirooxazine dye described in this work has a merocyanine form which is in a more ketone-like state (30). The addition of substituents to spiropyrans and spirooxazines can cause either an increase or a decrease in photoresponsiveness; in particular, the addition of an alkoxy substituent at the 9'-carbon of spirooxazine has been shown to increase photoresponsiveness (30).

A common disadvantage in photochromic compounds is photobleaching, where alternative non-reversible reactions occur and effectively destroy the photochromaticity of a molecule. This process is referred to as "fatigue" and is most commonly caused by oxidation or the attack of a free radical (25, 30). While spiropyran and spirooxazine are both quite resistant to fatigue, spirooxazine is at least two to three orders of magnitude more resistant (27, 30). This is primarily due to the mechanism of spiropyran photochromaticity, which occurs via a triplet state (27). This triplet state leaves the molecule prone to free radical attack (30). The resulting adduct cannot close to the spiro form of the molecule and absorbs from 510 to 560 nm (30). The photochromic mechanism of spirooxazine does not proceed via a triplet state and thus is more stable. The resistance of spirooxazine (1,3,3-trimethylspiro[indoline-naphthoxazine]) to fatigue makes it a more viable candidate for many applications and is the photochromic molecule of interest in this project.

While the photochemical properties of spirooxazine make the molecule an excellent choice for the goals of this work, it can be quite difficult to covalently attach the

molecules to PPV. In the past, the Harbron lab has utilized the Gilch polymerization in the synthesis of polymers using a monomer that has already been functionalized with a photochromic molecule (Figure 7). The mechanism of the Gilch polymerization begins with the deprotonation of a hydrogen at the benzylic position, as it is the most acidic due to the resonance stabilization of the anion (Figure 8).

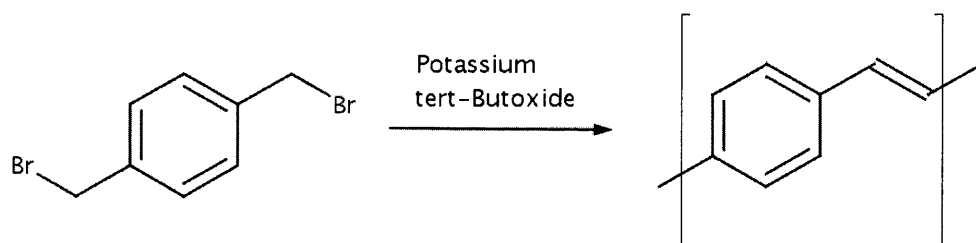


Figure 7 – The Gilch Polymerization

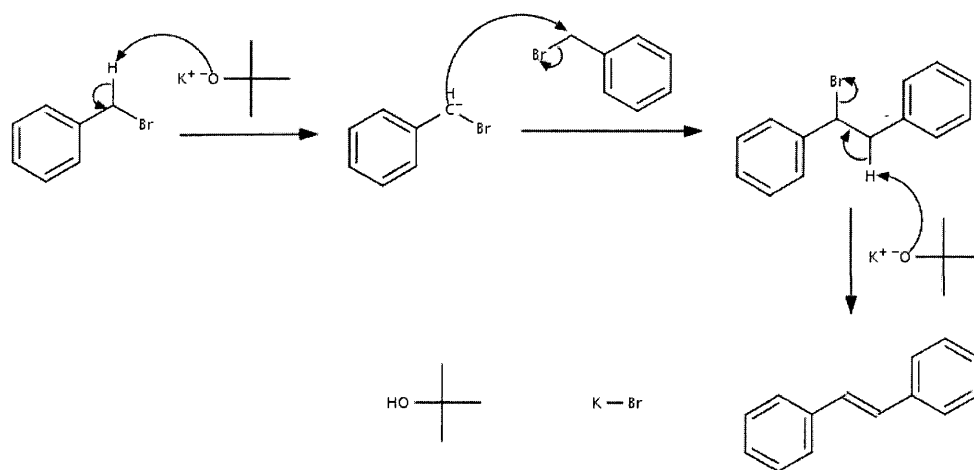


Figure 8 – Gilch Polymerization Mechanism

The carbanion quickly attacks the benzylic position of another molecule and a bromide ion leaves to complete the  $S_N2$  reaction. More base then catalyzes the  $E2$  reaction to form the vinyl group of PPV. Tert-butanol and potassium bromide are the side products of the

reaction. Unfortunately, spiropyrans haven't completely survived Gilch polymerizations in the past and it is believed that spirooxazines would show similar stabilities in the highly basic conditions. Several polymerizations have been investigated and the Heck polymerization was chosen for our purposes.

The Heck polymerization, a palladium-catalyzed coupling reaction, was discovered by Richard Heck in 1972 (32). The Heck reaction has mild reaction conditions making it a viable candidate for polymerizations in the presence of sensitive photochromic molecules. In the Heck reaction, an aryl or alkenyl halide is substituted with an alkene in the presence of catalytic amounts of palladium (Figure 9) (33).

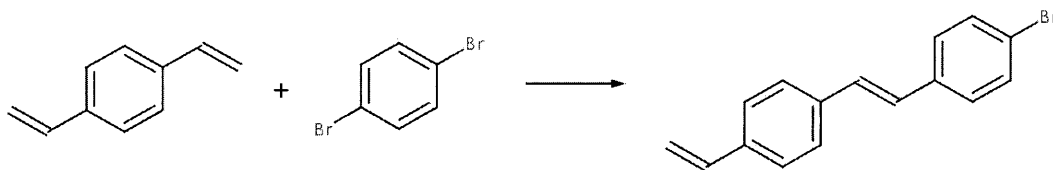


Figure 9 – The Heck Reaction

The reaction is typically carried out with a phosphine ligand and in the presence of a base which reduces reacted palladium back to its activated state (33). As seen in Figure 9, if an intermolecular Heck reaction is carried out using difunctionalized molecules, a growing polymer chain can result.

The mechanism of the Heck reaction is well understood (Figure 10) (33, 34). Palladium acetate is first reduced when the acetate groups are replaced by phosphine ligands in the presence of a Lewis base. Next, oxidative addition of an aryl halide leaves palladium with an oxidation state of +2. Palladium then forms a  $\pi$ -complex with an alkene which can later insert itself into the palladium-aryl bond.  $\beta$ -hydride elimination

forms the double bond in the product which is equivalent to the vinyl group in PPV and the product is ejected from the palladium complex. Finally, base (most commonly potassium carbonate) catalyzes the reductive elimination of the palladium complex which reduces palladium so that it can begin another cycle of the mechanism. Since palladium is recycled back to the active state at the end of the cycle, palladium acetate is only needed in catalytic amounts.

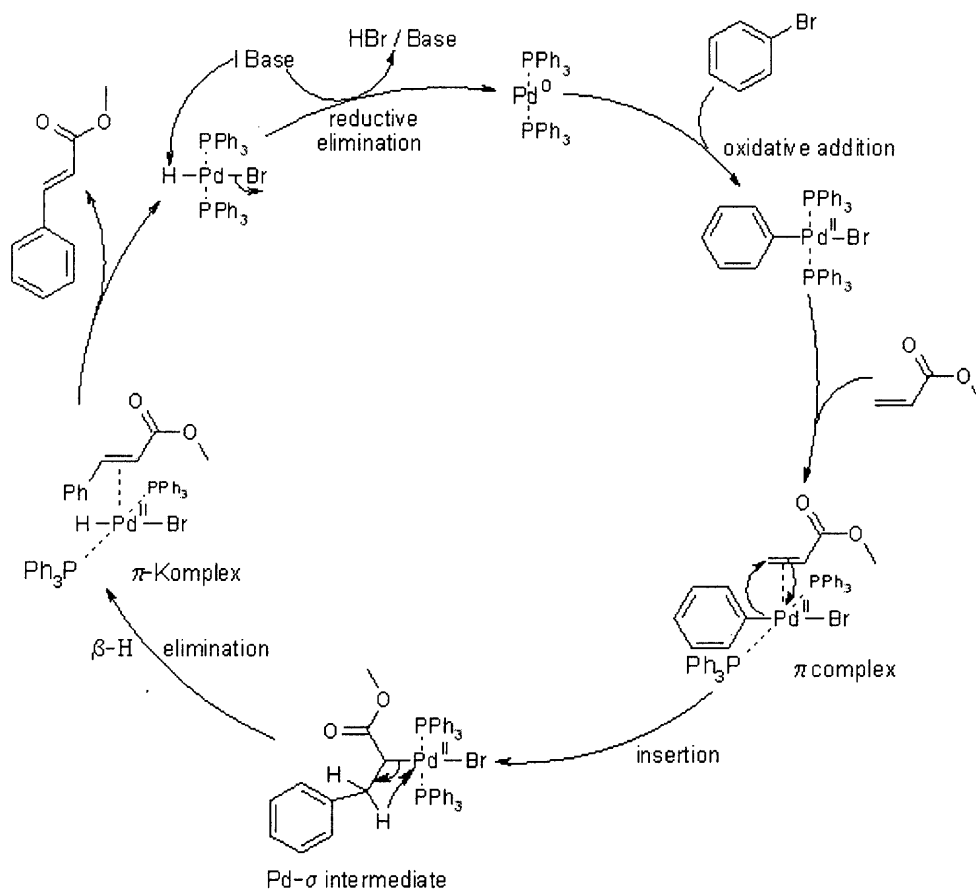


Figure 10 (34) – Mechanism of Heck Reaction

## Results and Discussion

### Monomer Synthesis

The polymer of interest was synthesized from three fragments which were themselves synthesized independently (Figure 11).

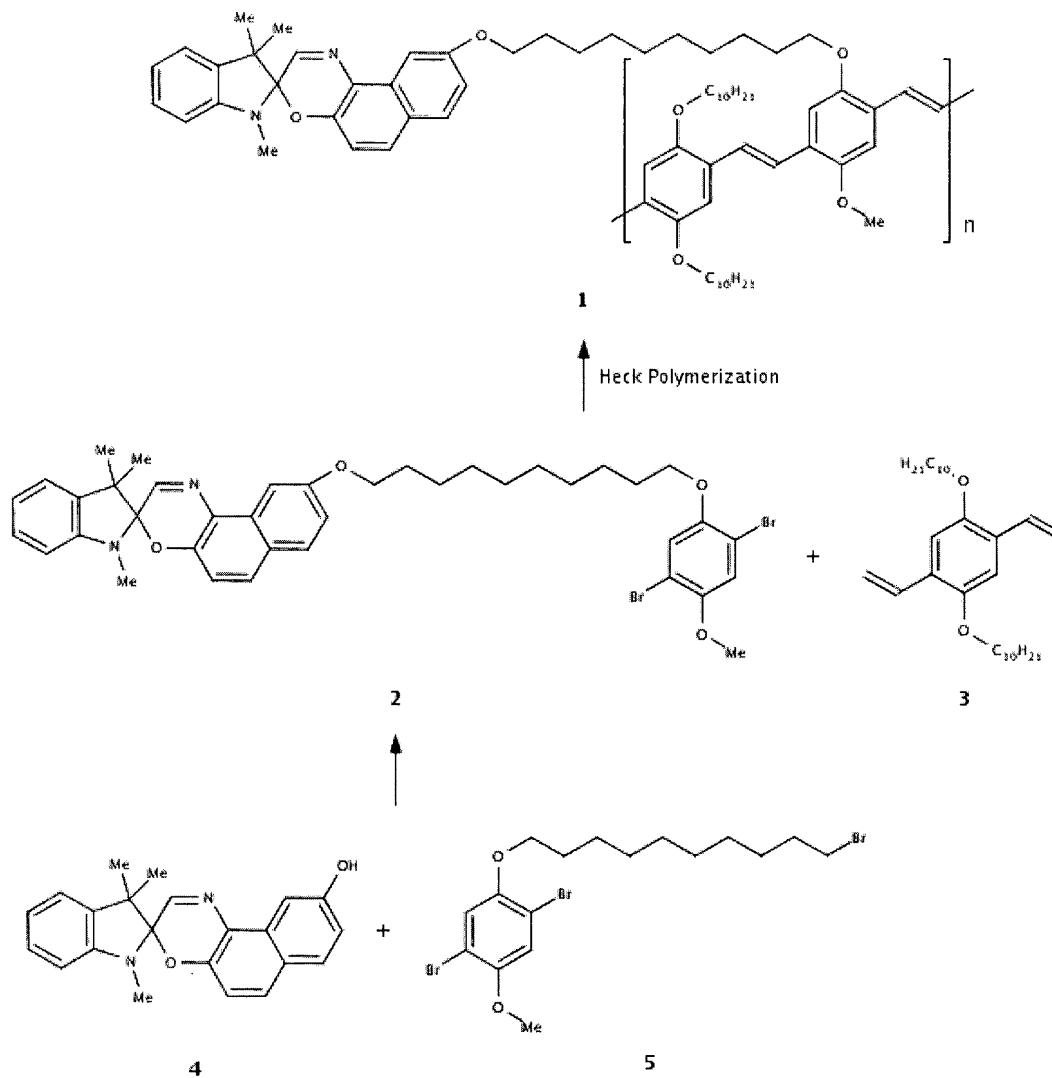


Figure 11 – Synthesis of SO-PPV

The Heck reaction was utilized to make the ABAB copolymer **1**. The functionalization of

the polymer with spirooxazine was chosen to occur on **5** mainly due to the difficulty of synthesizing **3** as well as its reactivity. Fragment **2** was synthesized by an  $S_N2$  reaction between **4** and **5**. The decyloxy groups on **3** ensured that the monomer as well as the polymer would be somewhat soluble in organic solvents. The synthesis of **3** was complicated due to the difficulty of obtaining a dialdehyde precursor.

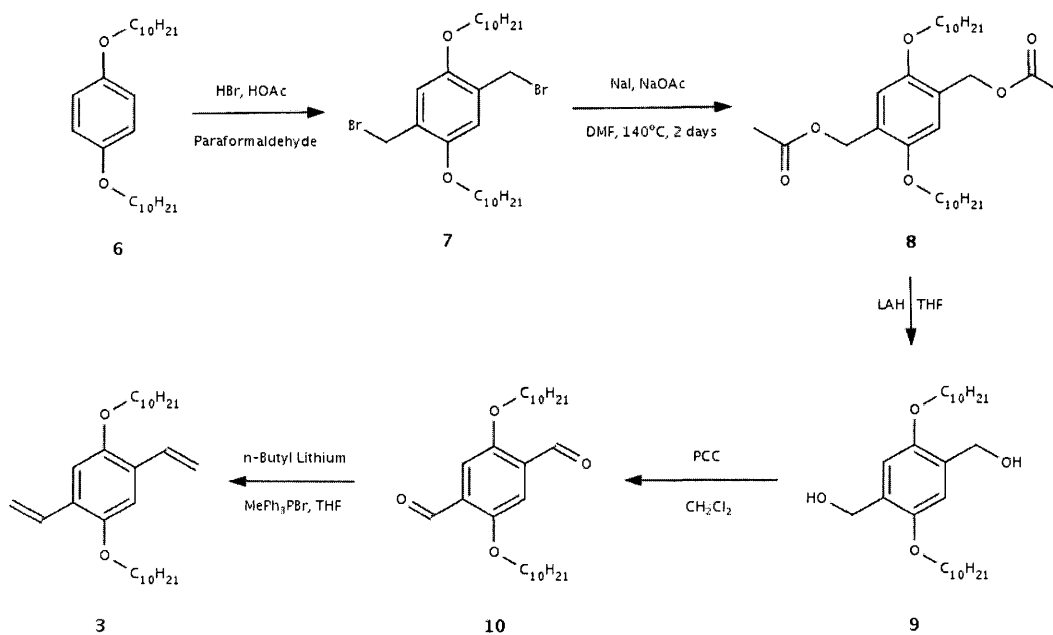


Figure 12 – Synthesis of 1,4-bis(decyloxy)-2,5-diethenylbenzene

Fragment **3** was obtained using a six step synthesis starting with commercially available **6** (Figure 12). Several pathways were investigated to form dialdehyde **10**; less successful attempts are described later in this work. Treatment of **6** with hydrogen bromide and paraformaldehyde yielded dibromomethylbenzene **7** in a 67% yield (35). Upon heating, paraformaldehyde decomposes to give the reaction mixture a source of

formaldehyde. Formaldehyde is then protonated in the acidic environment to give a carbocation, and an electrophilic aromatic substitution takes place on the alkyloxybenzene to give a benzylic alcohol (Figure 13) (36).

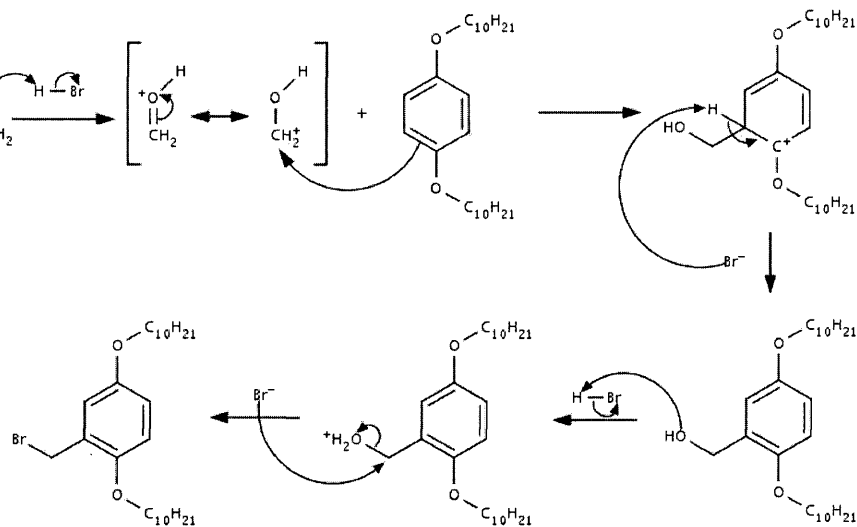


Figure 13 – Methylbromination Mechanism

During the substitution, the carbocation located on the ring is resonance stabilized by the lone pair from the alkoxy group. The benzylic alcohol is quickly protonated in the harshly acidic conditions and converted to a better leaving group. This protonated alcohol is then displaced by a bromide ion in a substitution reaction to give the final product. While early experiments showed that aqueous HBr can be used to give yields of ~6%, the reaction is most efficient when the HBr is dissolved in glacial acetic acid. The reaction showed little variation in repeated attempts and side products weren't apparent as long as enough HBr was present and the reaction was kept dry.

Next, dibromomethylbenzene **7** was converted to diacetyloxymethylbenzene **8** in

the presence of sodium acetate with a yield of 81% (37). The reaction proceeds via two successive S<sub>N</sub>2 reactions. The first reaction involves the substitution of bromine with the more labile iodine, which improves the overall reaction rate and yield (Figure 14) (38). This reaction is favored because sodium bromide is less soluble in DMF than sodium iodide, shifting the equilibrium in favor of forming the methyliodo compound by removing bromide ion from solution.

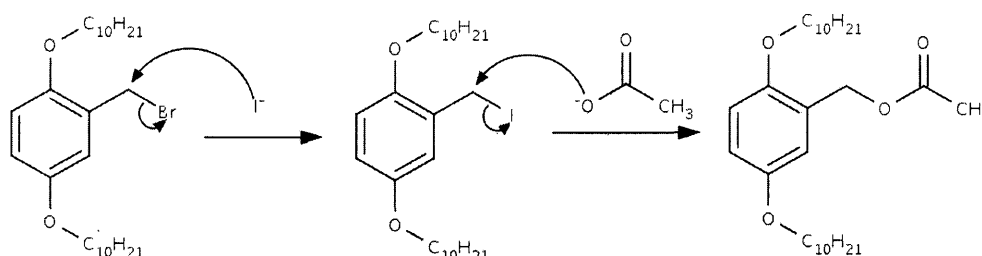


Figure 14 – Acetyloxymethyl Mechanism

To form the final product, the acetate anion substitutes for iodine. Although the reaction takes two days to compete, it was very successful and yields were only slightly less than stated in the literature.

Diacetyloxymethylbenzene **8** was reduced to dihydroxymethylbenzene **9** with lithium aluminum hydride in a greater than 96% yield (37, 39). LAH, a strong reducing agent of esters, acids, nitriles, and amides, donates a nucleophilic hydride anion which attacks the electrophilic carbonyl carbon atom of the ester in **8** (Figure 15) (34). An elimination then occurs when the carbonyl reforms to give an alkoxide and acetaldehyde. Quenching with H<sub>2</sub>O donates a hydrogen to the alkoxide to form an alcohol. Though the literature calls for quenching excess LAH with ethyl acetate, experiment showed that

water was required to successfully complete the quench.

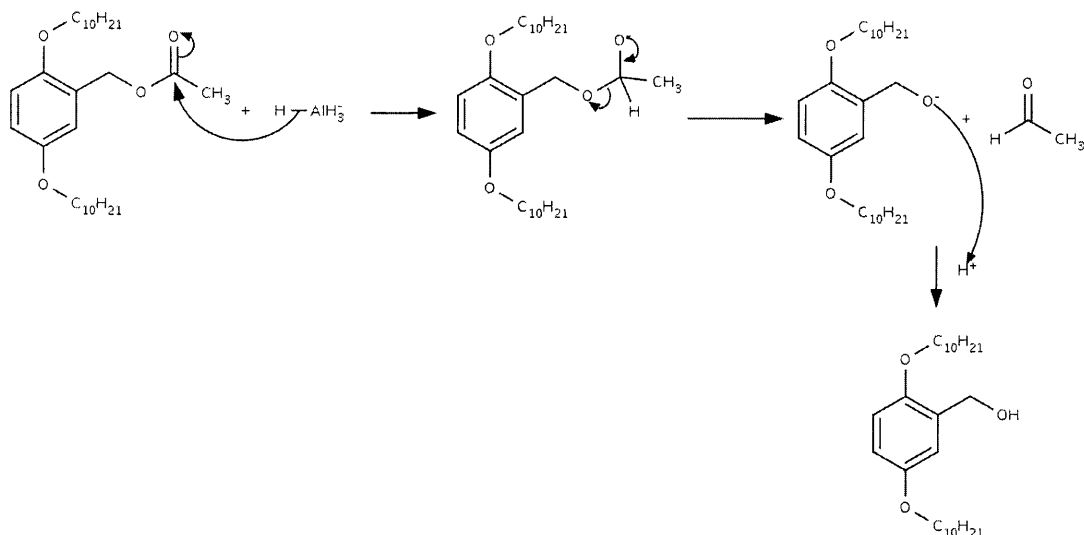


Figure 15 – Lithium Aluminum Hydride Ester Reduction Mechanism

Oxidation of dihydroxymethyl benzene **9** to dicarbaldehyde **10** was achieved using pyridinium chlorochromate (PCC) (37, 39). Chromium oxidants are the most widely used transition metal oxidants for alcohols, but unfortunately they contain Cr(III) which is both toxic and mutagenic (34). PCC must therefore be worked with very carefully and attempts should be made to use as little as stoichiometrically necessary. PCC works by coordinating with an alcohol and facilitating deprotonation of the alcoholic carbon (Figure 16) (34). First, the acidity of PCC causes the benzylic alcohol to become protonated. This protonated alcohol is now a good leaving group and can be displaced by the oxygen bearing a negative charge on the chromium reagent. Finally, water attacks the benzylic proton. The electrons from the carbon-hydrogen bond move to form a  $\pi$ -bond with oxygen which forces chromium to accept the electrons from its bond with oxygen

and become reduced.

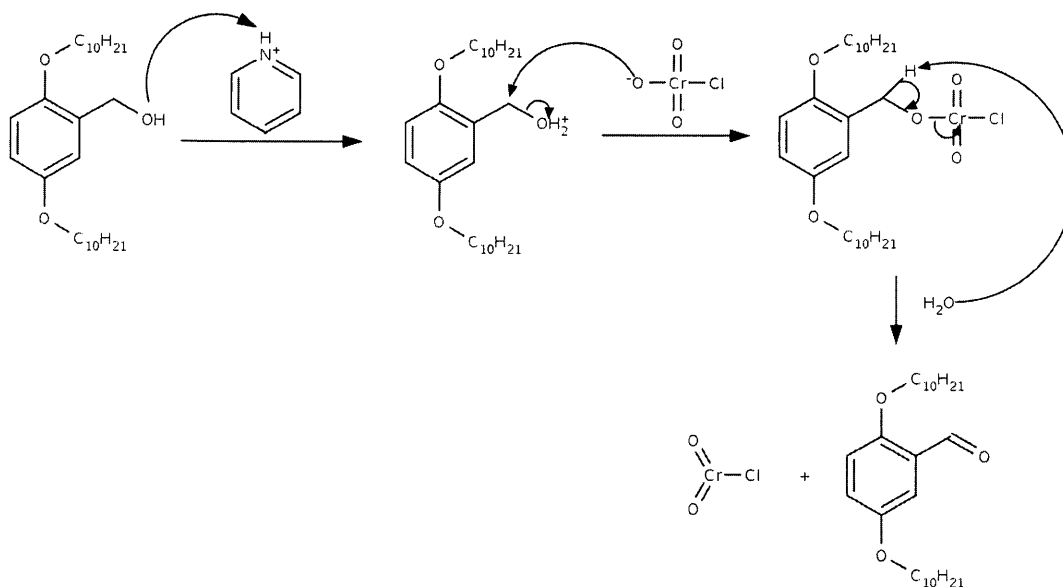


Figure 16 – Pyridinium Chlorochromate Oxidation Mechanism

The reaction is complicated by the formation of black, tarry chromium salts byproducts. Silica gel and molecular sieves are often added to a reaction mixture to absorb the salts (37). Fortunately, workup of **10** only required the use of a short chromatography column. As with the previous reaction, the yield was high at 88%. The high yields of these two steps made this particular pathway to **3** both viable and more dependable than other investigated pathways. Other syntheses of **10** were attempted and are described later in this work.

The final step in making fragment **3** is the Wittig reaction of dicarbaldehyde **10** (40). The first step of the Wittig reaction involves the deprotonation of the alpha carbon of the R-group next to phosphorus, in this case a methyl group (Figure 17). This

deprotonation forms an ylide, an intramolecular zwitterion where the charges are on adjacent atoms. The ylide in a Wittig reaction is the source of a carbon nucleophile that can attack carbonyl carbons. After attack, the negative charge on the former carbonyl oxygen is attracted to the positive charge on phosphorus and forms a four-membered ring intermediate. Due to the strength of the phosphine oxide bond, this intermediate quickly falls apart to form the alkene and the phosphine oxide. The strong driving force of the phosphine oxide bond prevents the intermediate from returning to an aldehyde. The yield of the Wittig reaction was quite low, 37%, which decreased the overall yield of fragment **3** to 17%. The low yields found with the Wittig reaction are possibly due to water getting into the reaction mixture, since that would provide a proton source to the ylide and allow the bromide salt to regenerate.

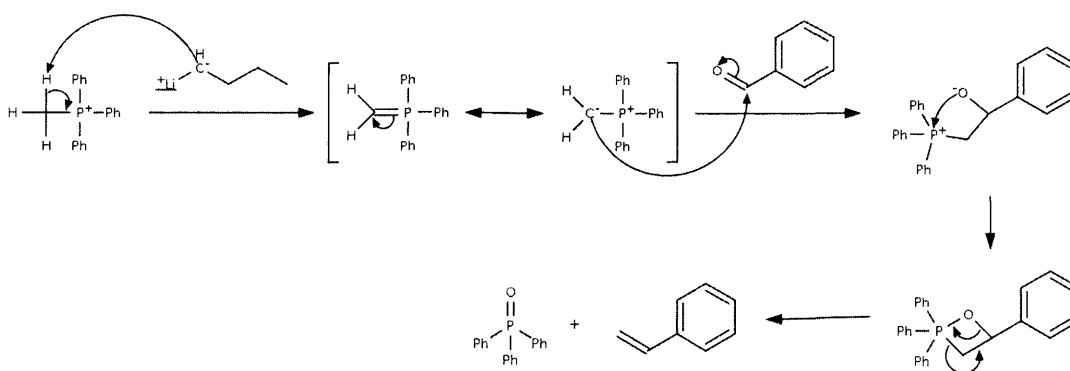


Figure 17 – Wittig Reaction Mechanism

The synthesis of fragment **4** was completed using the synthesis developed originally by Kakishita and refined by Durr (Figure 18) (41, 42). A short, two-step synthesis ensures that yield is high. While the synthesis is straightforward, much effort

was required to discover the most efficient purification due to a black, tarry by-product formation. Furthermore, identification of compound **12** was difficult and its successful synthesis was only known by continuing to the next step.

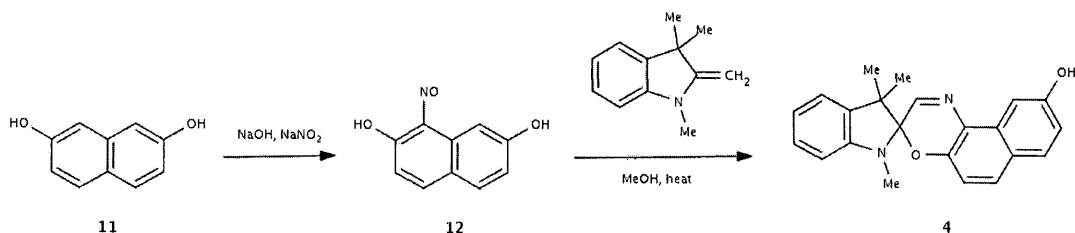


Figure 18 – Synthesis of Hydroxyspirooxazine **4**

Synthesis of nitrosonaphthalene **12** was completed with a yield of 98% (43, 44). Obtaining a NMR spectrum is quite difficult and confirmation that the synthesis is successful depends on continuing the synthesis to **4**. The deeply red solid obtained at the end of the reaction is very wet and the amount of water lost by drying in a vacuum oven often exceeds the amount of product recovered. The nitrosation proceeds via an electrophilic aromatic substitution mechanism (Figure 19). Since the reaction is run in water, one equivalent of sodium hydroxide is added to form the alkoxide of dihydroxynaphthalene, a much more soluble species. Sulfuric acid is added to form nitrous acid from sodium nitrite, and the acid is added dropwise to avoid a quick regeneration of the alcohol from the alkoxide. Excess acid is added to protonate nitrous acid, forcing a water molecule to leave and forming a positively charged intermediate. This intermediate is quickly attacked by the aromatic electron density of dihydroxynaphthalene. After deprotonation of the ring to regain aromaticity, more excess

acid protonates the alkoxide and the product precipitates out from the water.

Hydroxy groups at the 2 and 7 position can activate the ring and act as ortho/para directors due to their lone pairs, making the intended substitution position the only one where substitution is seen.

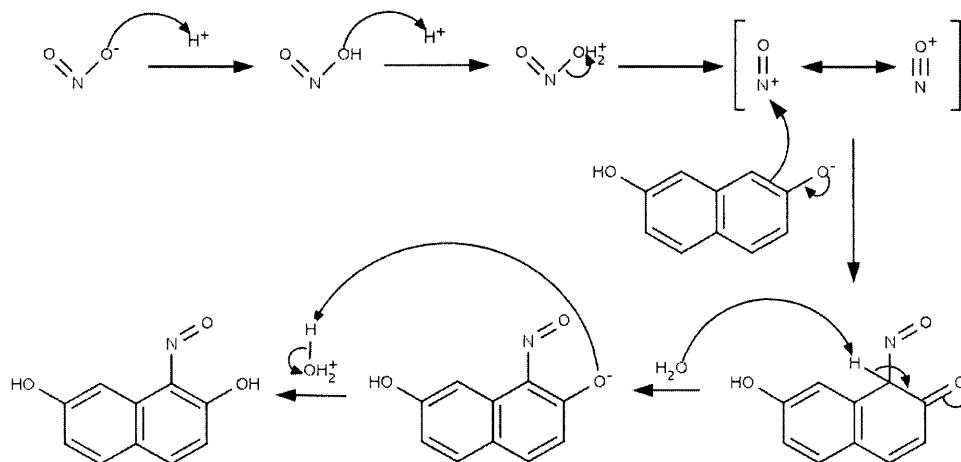


Figure 19 – Nitrosation Mechanism

The loss of aromaticity during the substitution is somewhat offset by carbonyl formation from the deprotonated hydroxy group. To ensure only mononitrosation occurs, stoichiometric amounts of sodium nitrite are used. Furthermore, the nitroso group is a weak electron withdrawing group which discourages further nitrosation.

The second step in the synthesis of **4** proceeds via a condensation reaction between **12** and a methylene base (Figure 20) (41, 42). It was this step that gave a goeey, black tar which proved difficult to purify. Several columns and recrystallizations were attempted before discovering that washing the crude product with a minimal volume of ethyl acetate dissolves impurities and allows isolation by filtering the mixture. The

condensation reaction forms the spiro-linkage which gives the photochromic compound its peculiar properties. The electron density of the methylene group first attacks the nitrogen of the nitrosonaphthalene much like it might the carbon of a carbonyl. The resulting carbocation is then attacked by the alcohol to create a six-membered ring. Through an intermolecular reaction, the acidic proton of the oxonium ion can be transferred to the oxygen now bearing a negative charge. Finally, an elimination takes place to give a water molecule and form the double bond which connects the two different conjugated regions. The reaction is driven by the thermodynamic stability of spirooxazine; the double bond with nitrogen extends the conjugation in the closed form and allows the open merocyanine form to exist.

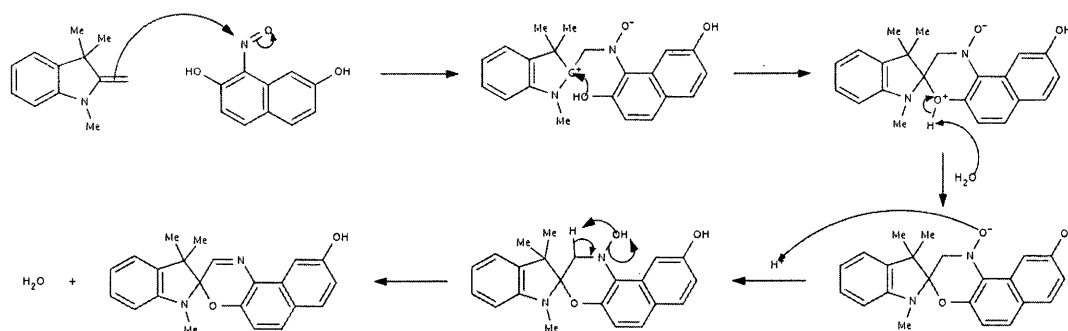


Figure 20 – Spirooxazine Condensation Mechanism

With the successful syntheses of **3** and **4**, all that remains is the synthesis of fragment **5** which serves as the linkage between the two. In the past, the Harbron lab has used a bromoalkoxy chain to attach azobenzenes to a phenyl group for PPV synthesis. The compound is utilized again in this synthesis, this time adapting the phenyl group with bromo substituents to allow for the Heck polymerization to proceed (Figure 21).

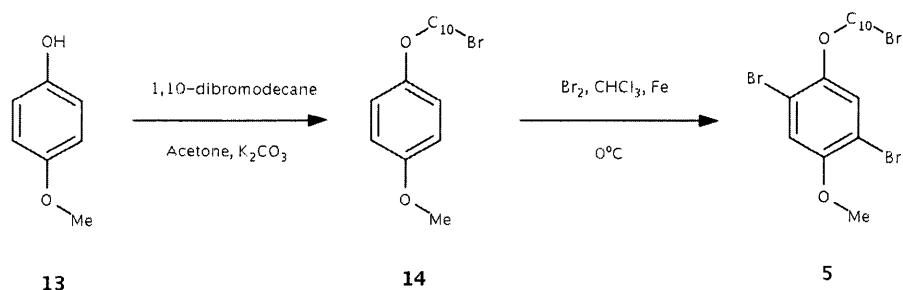


Figure 21 – Synthesis of Fragment 5

Synthesis of **14** proceeds via a Williamson ether synthesis (Figure 22).

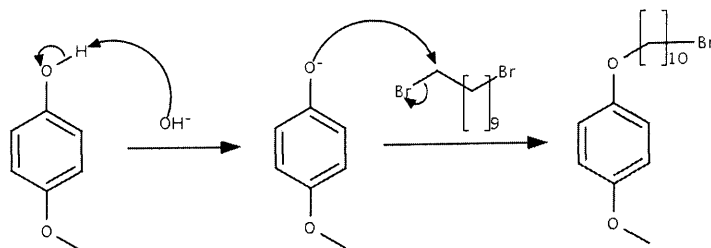


Figure 22 - Mechanism in Synthesis of **14**

Since 1,10-dibromodecane is functionalized at both ends, it is possible to simply link two phenyl rings together which wouldn't allow attachment of **3** (Figure 23). To avoid this, much higher amounts of 1,10-dibromodecane were used to decrease the risk of difunctionalized product forming. Despite the large excess, it is impossible to completely avoid some formation of difunctionalized product. Further complicating the reaction is the difficult separation of **14** and unreacted 1,10-dibromodecane. Several recrystallizations are necessary to ensure that the product is completely pure, since residual 1,10-dibromodecane would be reactive when attempting the synthesis of **2**. The reaction is rather slow and should be allowed to continue for at least a day. Yields can be

lower than expected (~30%) due to the repeated recrystallizations.

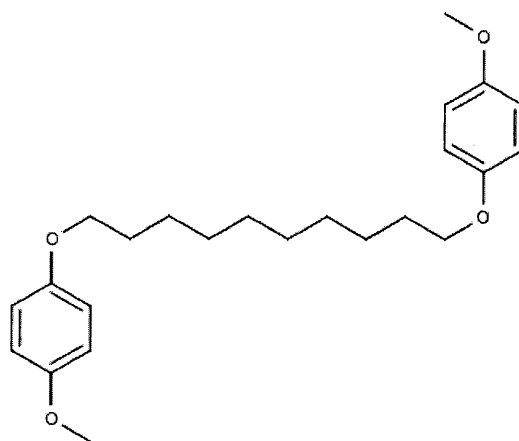


Figure 23 – Difunctionalized Side Product in Synthesis of **14**

Bromination of **14** yields **5** in high yields (92%) (45). The bromination proceeds via an electrophilic aromatic substitution mechanism where a bromine atom replaces a hydrogen and hydrogen bromide is given off as a by-product (Figure 24).

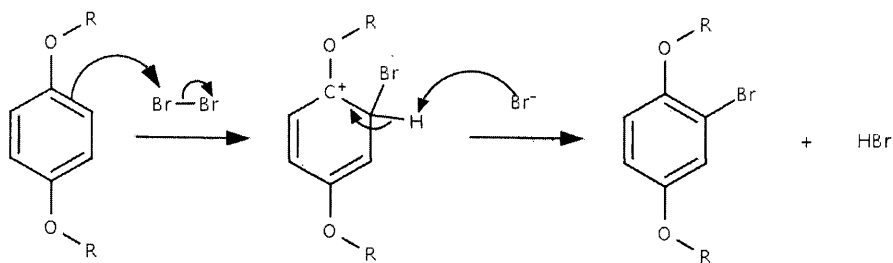


Figure 24 – Bromination Mechanism

Purification of **5** can be quite difficult. The crude product is contaminated with an unknown byproduct which is less soluble than **5** in all attempted solvent systems and is a liquid at room temperature. Recrystallization is therefore a trying exercise. Pipetting this liquid from the mixture at room temperature after dissolving everything in hot solvent

was the only successful manner in removing it, and reducing the temperature further usually gave pure product.

Successful syntheses of **3**, **4**, and **5** left only combinatorial steps to obtain the desired polymer. First, **4** and **5** were combined using another Williamson ether synthesis. The reaction was allowed to run for several days and it never went to completion, complicating purification since both starting materials were present in substantial amounts. Nonetheless, the yield was still high enough that reaction completion wasn't a concern (66%). Initially, purification was done using column chromatography with an eluent of methylene chloride. While the product was cleaned of all trace of **4**, it turned out that there was still a large amount of **5** present. After experimentation with many solvent systems, the only suitable separation of the product and **5** was using 3:2 toluene - pet ether. Successful synthesis of **2** as a yellow oil meant that the required monomers had been obtained and only polymerizations were left to attempt.

### Polymerizations

The Heck coupling reaction was utilized to synthesize poly(phenylene vinylene)s. A total of three polymers were made, two functionalized with spirooxazine as well as another to use as a control. The two functionalized polymers contained 50% and 25% functionalized monomers, respectively. 1,4-dibromo-2,5-didecyloxybenzene was used in 25% functionalized polymer to take the place of half of the functionalized monomers. In effect, all nonfunctionalized monomers were attached with two decyloxy groups.

The control polymer was the first attempt at using the Heck polymerizations to make PPV (Figure 25) (40, 46). **15** was a standard PPV with decyloxy groups to improve solubility.

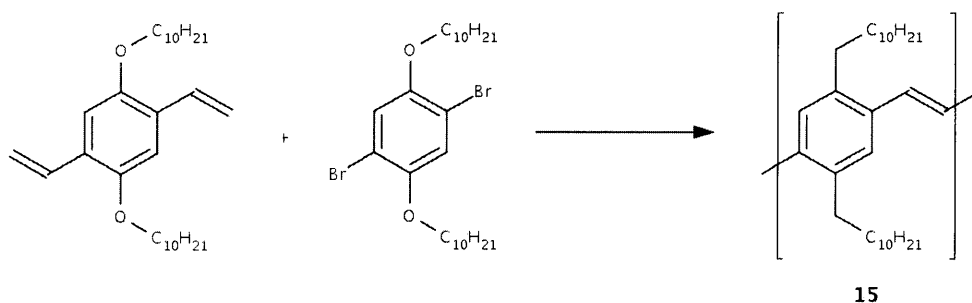


Figure 25 – Control Polymer **15**

The polymer was purified by Soxhlet extraction with methanol and hexanes. During the extractions, it was noticed that the solvents never stopped extracting some amount of colored material from the sample. This is possibly due to the hot solvents cutting the polymer into shorter oligomers which can then be dissolved and extracted. Despite this problem, the polymerization proceeded with a 47% yield.

Next, the polymerization of 50% functionalized PPV **1** was carried out. In contrast to the synthesis of the control polymer, Soxhlet extractions were not used to purify functionalized polymers for two reasons. In addition to the fear of the Soxhlet extractions degrading the polymer, it was also felt that the high temperatures needed to undergo Soxhlet extractions could harm the spirooxazine. Therefore, the polymer was purified using only precipitation into methanol. The color of the functionalized polymer was a dark green, much different from the control polymer. Yields of the polymerization were quite low (5%).

Finally, the synthesis of a 25% functionalized polymer was performed. To do this, half of the functionalized monomer was replaced with the 1,4-dibromo-2,5-dicycloxybenzene which was used in the control polymerization (Figure 26). Since the polymerization cannot distinguish between functionalized and nonfunctionalized brominated monomer, there is some randomization which occurs. Any particular point on a polymer chain may have a higher or lower concentration of functionalization. Purification of the polymer gave results which hindered the ability to study the polymer. The combination of a small scale, low yields, and the texture of the polymer made recovery of the precipitated polymer very difficult. Most often a precipitated polymer could not be cleanly filtered and required placing the filter paper into solvent to recover it. Upon evaporation of the solvent, the green polymer underwent a color change to orange. While a small amount of green polymer was kept separate from the purifications, the amount was extremely low. The yield was high enough to carry out fluorescence

experiments, but unfortunately the purity of the sample has to be treated as suspect since only one precipitation was possible.

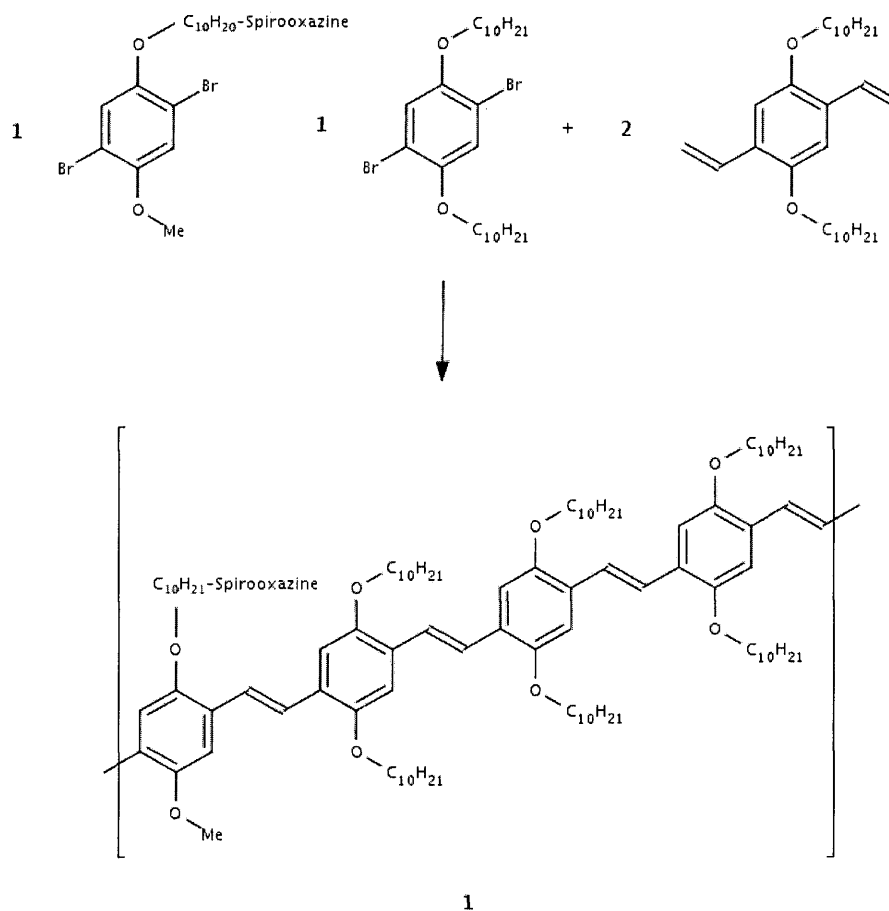


Figure 26 – Synthesis of 25% Functionalized PPV 16

### Early Fluorescence Studies

Although synthesis of the polymers took longer than expected, preliminary investigation of their fluorescence properties were conducted. The goal of this project was to reversibly quench the fluorescence of PPV. To that end, success of the project would have seen the fluorescence of the polymers completely quenched. While that goal was not met, there is evidence that the polymers are in fact photoresponsive.

The first polymer synthesized, control polymer **15**, showed that the Heck polymerization is suitable to making PPV. Absorption and fluorescence studies of **15** gave spectra indicative of PPV with a  $\lambda_{\text{max}}$  of 448 and 542 nm, respectively (Figure 27).

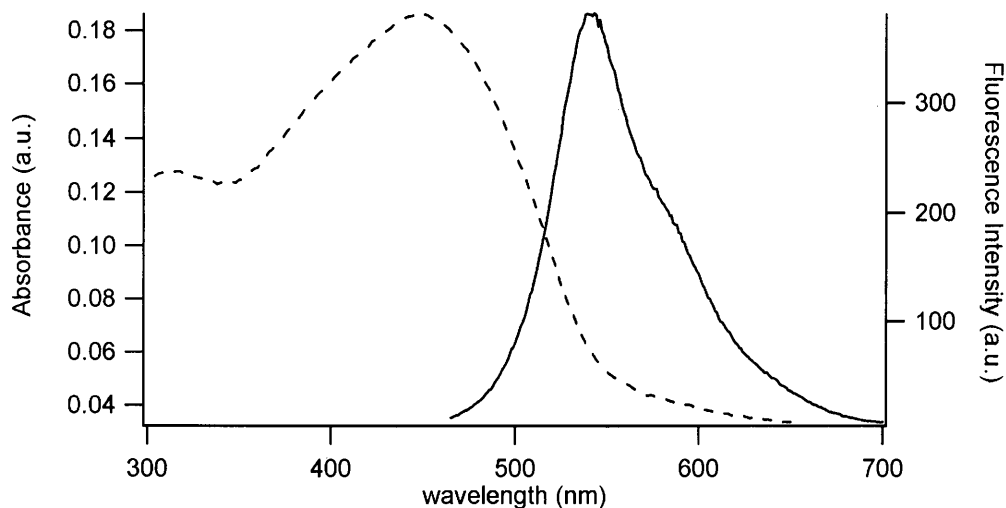


Figure 27 – Absorption and Emission Spectra of Control Polymer **15** in THF. Absorption is dashed, emission is solid.

There were two samples of control polymer **15** synthesized. One of these was dried in a vacuum oven at  $\sim 80^{\circ}\text{C}$  and became discolored, its bright orange color becoming a much more muted orange. Figure 27 shows the spectra of a sample that was not heated. The

color change indicated that **15** is quite sensitive to heat in the solid form and other functionalized polymers should be treated carefully to avoid unwanted side effects.

The absorption of SO-PPV **1** was much different from the control polymer (Figure 28).

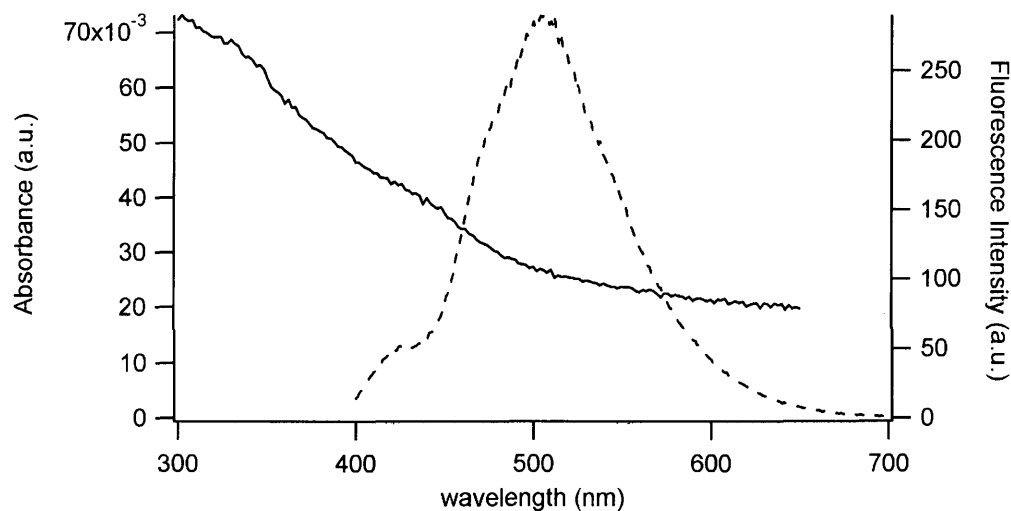


Figure 28 - Absorption and Emission Spectra of SO-PPV **1** in THF. Absorption is solid, emission is dashed.

Absorption of the polymer was little more than a slight hump at ~435 nm along the gradually declining baseline. This is an indication that the solubility of this polymer is quite low. Despite the low absorbance of this polymer, its fluorescence peak is clearly visible although more blue-shifted than the control polymer ( $\lambda_{\text{max}}$  is 505 nm). The apparent low solubility of the polymer doesn't eliminate the possibility of photochromic behavior, however.

SO-PPV appears to undergo a reversible decrease in fluorescence intensity upon exposure to UV light (Figure 29). Although the decrease in intensity is quite small, the

largest peak shows reversibility as fluorescence returns to pre-UV exposure intensities.

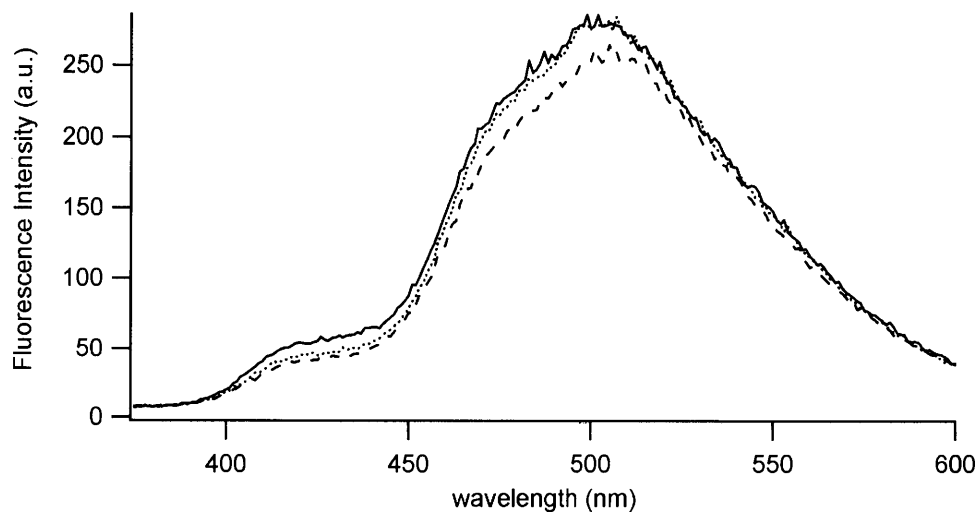


Figure 29 – Fluorescence of **1** (THF) before (solid), immediately after (dashed), and 60 seconds after (dotted) UV exposure.

Unfortunately, the shoulder from 400-450 nm shows little reversibility and may actually experience some photobleaching. The absorbance spectrum of SO-PPV **1** also shows some evidence that photochromic activity is taking place (Figure 30). Upon exposure to UV light, the 450-650 nm region ( $\lambda_{\text{max}}$  of 588 nm) of the absorption spectrum undergoes an increase in absorbance. This is likely due to spirooxazine entering the merocyanine conformation, causing an increase in the solubility of the polymer which then increases the absorbance. In fact, when the pre-UV absorption spectrum is subtracted from the post-UV spectrum, the resulting spectrum is very similar to a merocyanine absorption spectrum (Figure 30, inset). After 60 seconds, the merocyanine has relaxed back to the closed form and the absorbance is back to pre-exposure levels. This evidence, along with clear visual evidence of polymer suspended in THF, indicates that the 50% functionalized

SO-PPV isn't particularly soluble.

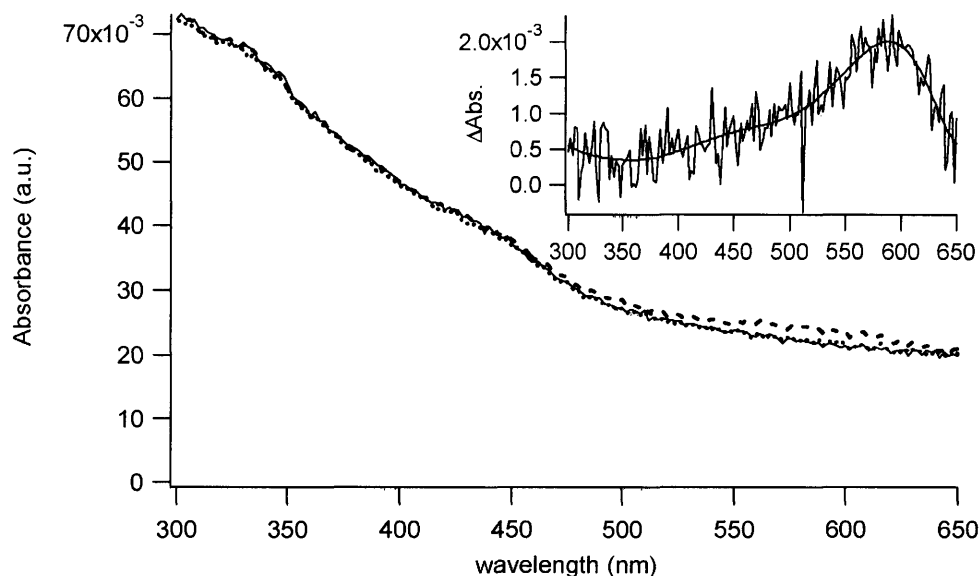


Figure 30 – Absorption of **1** (THF) before (solid), immediately after (dashed), and 60 seconds after (dotted) UV exposure. Inset is dashed minus solid.

Since the control polymer was shown to be fully soluble, a 25% functionalized SO-PPV **16** would likely be more soluble than **1** and hopefully still show some photoactivity. The spectra of **16**, particularly the absorption spectrum, is much more defined and indicative of PPV polymer (Figure 31). There are obvious differences in this spectrum and the spectra of **15** and **1**. Most obviously, the absorption spectrum of **16** is much more of a distinct peak than the small blip seen for **1**, indicating that the reduction in polymer functionalization did in fact increase the solubility. The absorption and fluorescence spectra of **16** are also blue-shifted ( $\lambda_{\max}$  of 421 and 482 nm, respectively) in comparison to the spectra of **15** and **1**. This is likely due to shorter chromophore lengths

in **16**. Furthermore, the spectra of **16** are more narrow, indicative of a smaller range of polymer lengths.

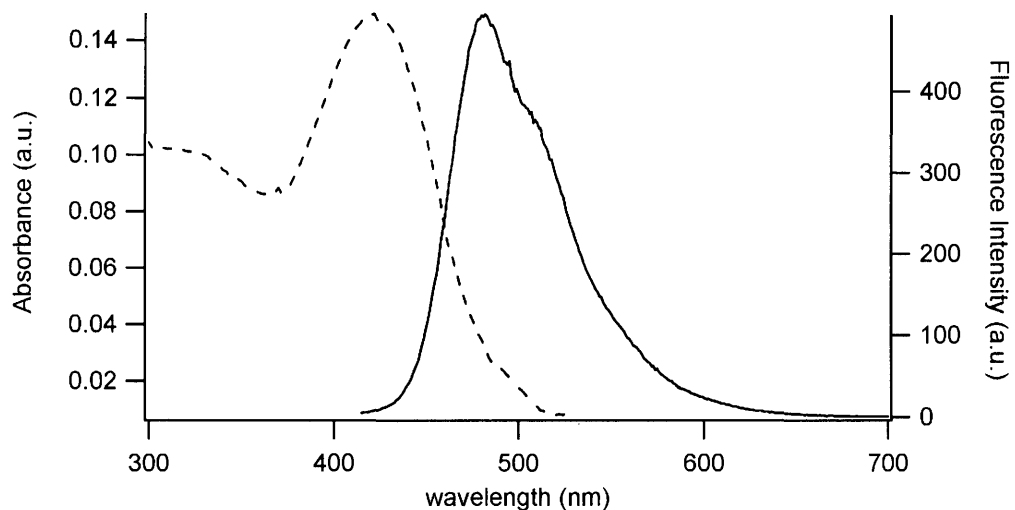


Figure 31 – Absorption and Emission Spectra of 25% Functionalized Polymer **16** in THF. Absorption is dashed, emission is solid.

While the solubility of the polymer was increased with the decrease in functionalization, unfortunately the photoactivity seen in **1** is no longer evident. Upon exposure to UV light, polymer **16** showed neither a change in fluorescence or absorption. It appears that, in this case, to fix the problem of solubility only creates another with the lack of photoactivity.

### Other Synthetic Routes

In the course of synthesizing PPV, several different routes were investigated and eventually set aside in deference to the routes previously described. The most difficult compound to synthesize in this work was the diethenylbenzene **3** needed to complete the polymerization. Unsurprisingly, most of time spent on the project centered on how to make this compound. Although the route used in the synthesis above is longer than some of the other routes, it has the advantages of producing yields in meaningful amounts as well as its product being easily purified.

The first attempt at making **3** utilized the Stille coupling using vinyltributyltin in the presence of tetrakis(triphenylphosphine)palladium(0) (Figure 32).

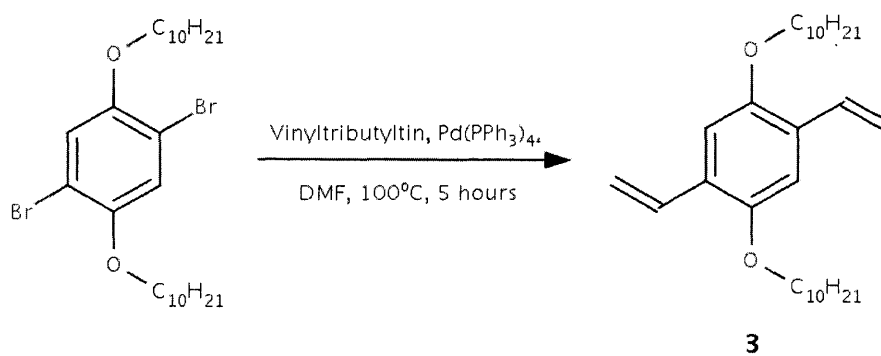


Figure 32 – Diethenylbenzene Synthesis Using Stille Coupling

While the reaction most certainly formed **3**, purification at the time was inadequate and the compound was never suitable for polymerization. Furthermore, using this method **3** seemed to be susceptible to self-polymerization, causing it to eventually form an orange solid during purification indicative of PPV oligomers. Extra benzylic peaks in the <sup>1</sup>H NMR were the largest concern during the purification of **3**. Furthermore, the expected

triplet at 4 ppm was shrouded in several other peaks. The yield of crude product in this reaction was only 2%, largely due to the removal of self-polymerization products.

The Stille coupling works in a similar fashion to the Heck reaction (Figure 33). The aryl bromide adds to palladium in an oxidative addition. The vinyl group of vinyltributyltin is a nucleophile and displaces the bromine on palladium. Finally, reductive elimination couples the phenyl ring and the vinyl group together to give **3**. In this step the palladium is reduced back to its catalytic form without requiring additional reagents.

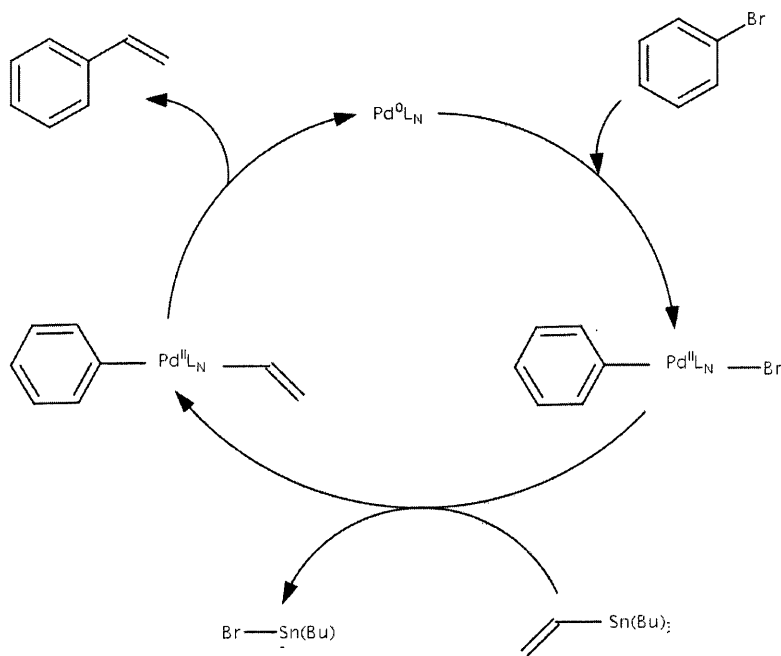


Figure 33 – Stille Coupling Mechanism

After purification of **3** via the Stille coupling proved unsuccessful, elimination of side products became the next goal. The ligands used in a palladium catalyst can have a substantial effect on the performance of its catalysis (48). Palladacycles, cyclic palladium

compounds, have been shown to be effective in Heck, Suzuki, and Sonogashira reactions (49). *Trans*-Di( $\mu$ -acetato)-bis[3-(diphenylphosphino)-4-styryl]dipalladium **17** has been shown to be particularly effective in these reactions (Figure 34) (50). Synthesis of palladacycle **17** is very short and the yield was found to be 42%.

Another Stille coupling was attempted using **17** as the catalyst, but unfortunately the same extra peaks were present in the  $^1\text{H}$  NMR spectrum (48). Although use of **17** failed to remove the side products seen with tetrakis(triphenylphosphine)palladium(0), crude yields were substantially larger (41%). The higher yields seemed to be due to little or no self-polymerization, as no orange solid was ever experienced.

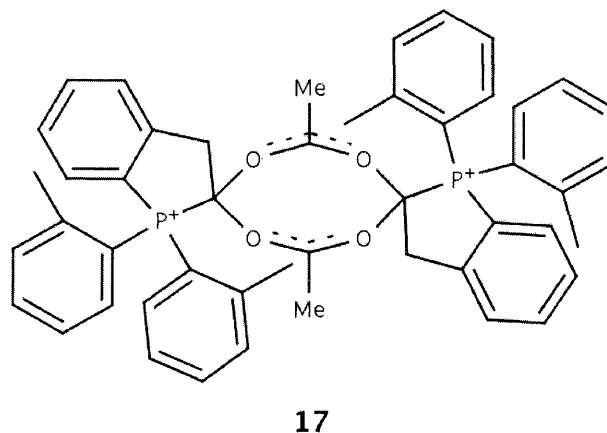


Figure 34 - *Trans*-Di( $\mu$ -acetato)-bis[3-(diphenylphosphino)-4-styryl]dipalladium

After the failures of the previous Stille couplings, other alterations to the reaction were explored. Replacement of the aryl bromines on 1,4-dibromo-2,5-didecyloxybenzene with iodines was conjectured to improve the reaction, since iodine is a better leaving group. Two different syntheses of 1,4-diiodo-2,5-didecyloxybenzene **18** were attempted

with mixed results. The first synthesis of **18** was attempted using bis(pyridine)iodonium tetrafluoroborate in the presence of triflic acid (Figure 35) (51).

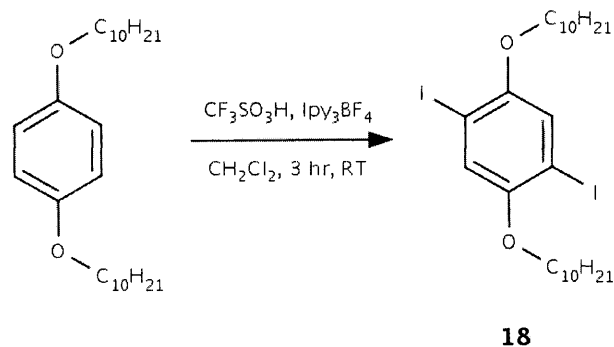


Figure 35 – Synthesis of Iodobenzene **18** Using Bis(pyridine)iodonium Tetrafluoroborate

While the reaction seems to have worked, a laboratory accident prevented the characterization of the product. Nevertheless, the reaction is easy to carry out and the conditions are mild. The reaction proceeds via an electrophilic aromatic substitution mechanism (Figure 36) (52). Triflic acid first protonates the bis(pyridine)iodonium to create an iodine electrophile. Next, the aromatic electron density attacks the iodine cation. Finally, deprotonation by tetrafluoroborate restores the aromaticity.

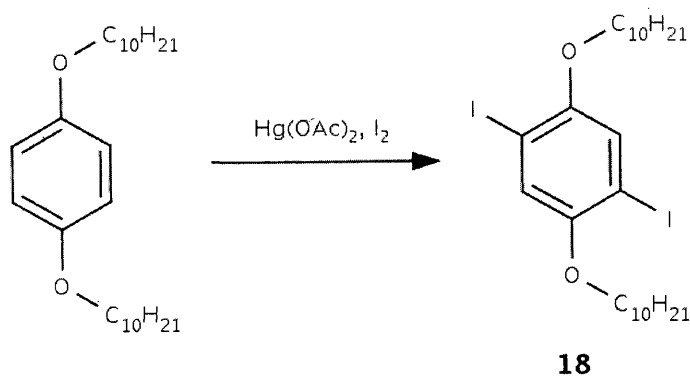


Figure 36 – Iodination Mechanism using Bis(pyridine)iodonium Tetrafluoroborate

The second attempted synthesis of diiodobenzene **18** utilized mercury(II) acetate in the presence of molecular iodine (Figure 37) (53).

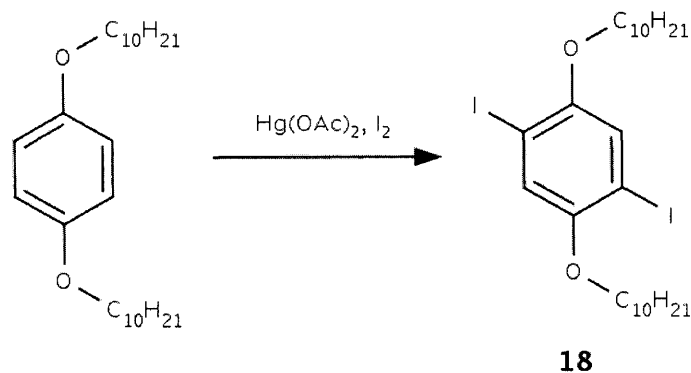


Figure 37 – Synthesis of Iodobenzene **18** Using Mercury Acetate

Interestingly, the reaction proceeds via an electrophilic aromatic substitution mechanism where an acyl hypobromite is used to make iodine an acceptable electrophile (Figure 38). In solution, mercury acetate can dissociate to form the monosubstituted mercury compound. The acetate anion can then attack molecular iodine. The positively charged mercury helps the molecular iodine bond to break by forming a bond when the extra iodine. Next, the acyl hypobromite is willing to give up iodine to the aromatic electron density of the ring. Finally, deprotonation of the ring restores the aromaticity. The reaction has a good yield (70%) which indicates that if further attempts of a Stille coupling are desired using iodinated reagents, this iodination would probably be the place to start.

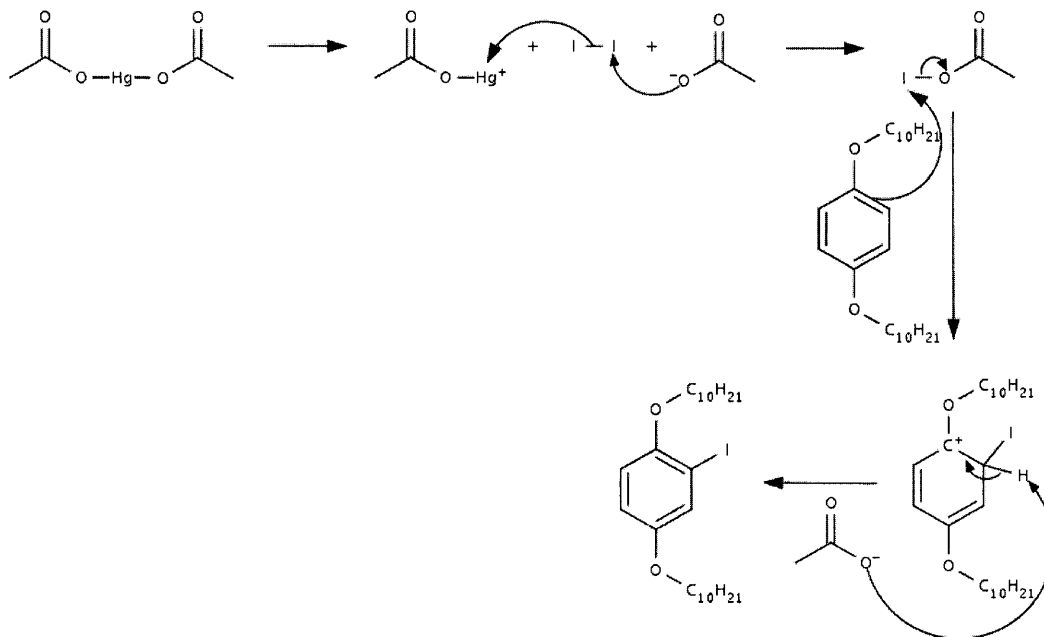


Figure 38 – Iodination Mechanism Using Mercury(II) Acetate

A Stille coupling was attempted using diiodobenzene **18** in hope that the side product experienced with the similar dibromobenzene starting material would not be seen (Figure 39). Unfortunately, the reaction improved very little. The erroneous peaks seen in previous Stille couplings were present. At this point, the Stille coupling didn't seem to be the answer in obtaining **3**. At the time, my skills in column chromatography were poor and this likely had to do with the failures of the reaction. I believe that with more experimentation, an acceptable purification technique would likely be found.

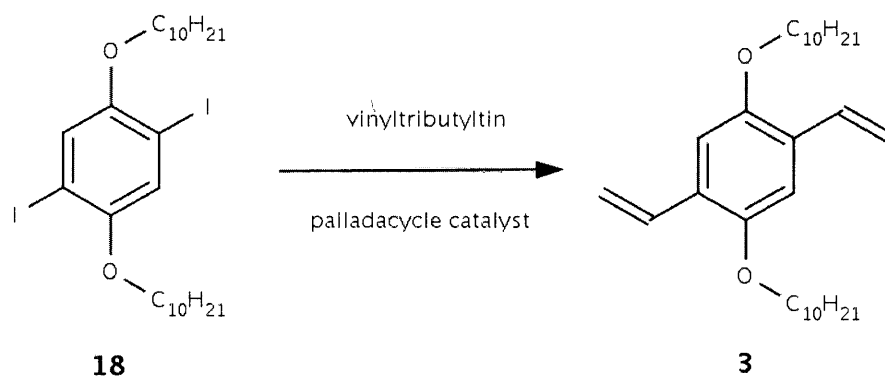


Figure 39 – Stille Coupling using **18**

With the success of the Wittig reaction in making **3**, it is important to have an efficient synthetic route to the terephthalaldehyde precursor **10**. The current route to **10**, though proceeding with a high yield, takes several steps. Previous to finding this route, three other attempts were made to acquire **10** (Figure 40). All three attempts had their shortcomings, typically a very low yield or the inability to obtain a pure product.

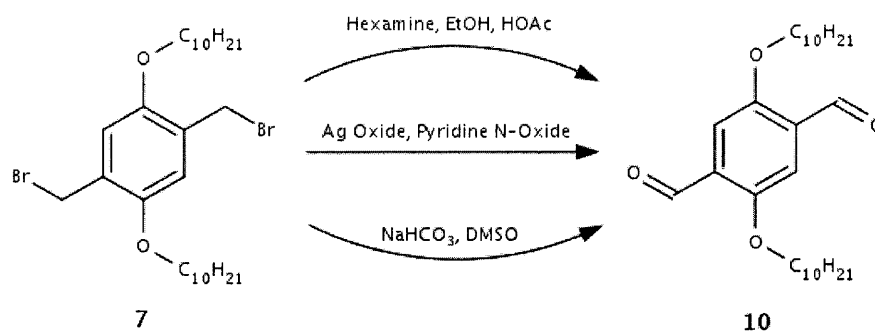


Figure 40 – Different Routes to Aldehyde **10**

The first attempt in obtaining **10** used hexamine in the presence of acetic acid, referred to as the Sommelet reaction (54). The Sommelet reaction works by first substituting hexamine for the benzylic bromine (Figure 41) (55). Next, the positive

charge on nitrogen is transferred to a nearby carbon by breaking the carbon-nitrogen bond. Hydride transfer to the carbocation is allowed due to the possible imine formation between nitrogen and the benzylic carbon. A water molecule then attacks the benzylic carbon which bears a partial positive charge through the resonance of the imine. Deprotonation of the oxonium ion forms the benzylic alcohol. Further deprotonation of this alcohol forms the double bond of the aldehyde and allows the reduced hexamine molecule to leave. While pure **10** was obtained using the Sommelet reaction, yields were very low (6%) and thus the reaction was not suitable for our purposes.

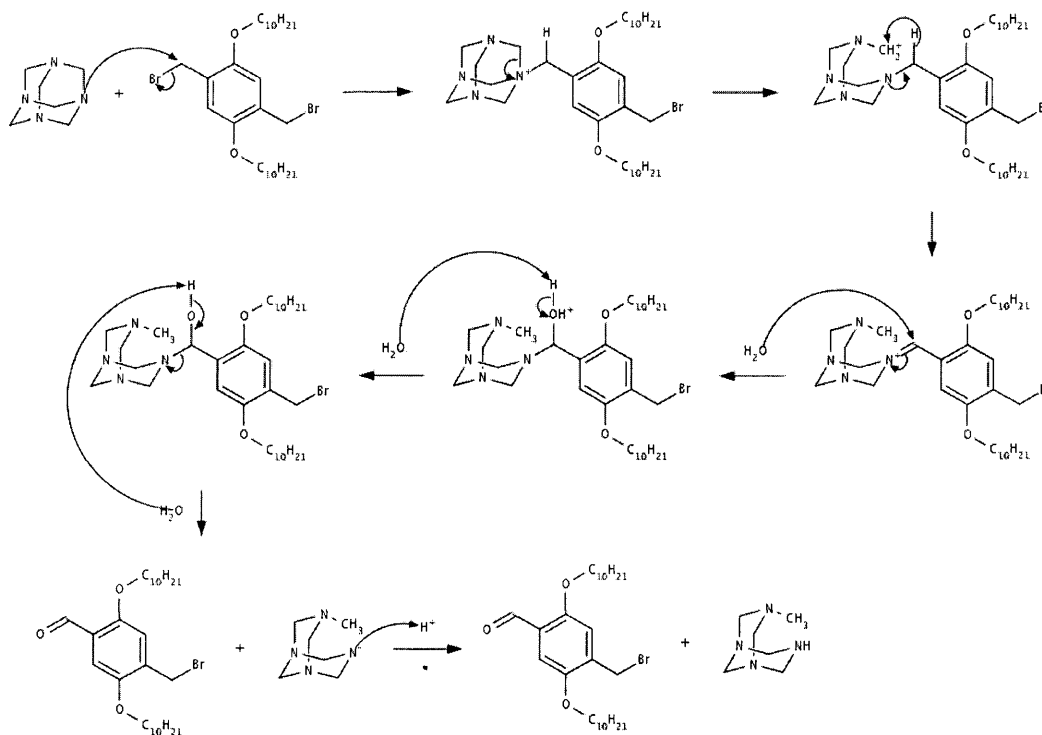


Figure 41 – Oxidation Mechanism Using Hexamine

Next, the synthesis of **10** using silver(I) oxide and pyridine N-oxide was attempted

(56). The first step of this oxidation is the substitution of bromine with pyridine N-oxide (Figure 42). Next, deprotonation of the benzylic proton forms the aldehyde and releases pyridine. Pure **10** was again obtained, but like the Sommelet reactions the yield was low (11%). Despite the small increase in yield, the 11% yield was still not large enough to be useful in the coming steps.

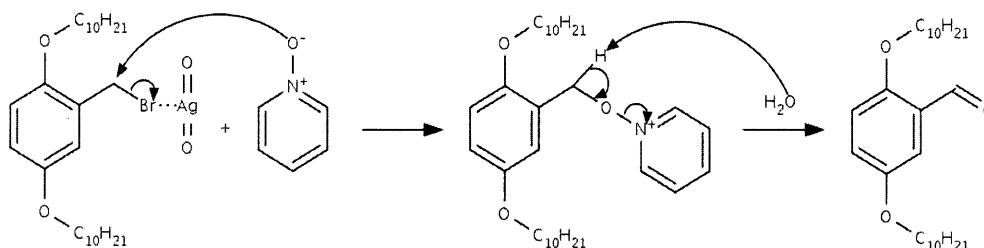


Figure 42 – Oxidation Mechanism using pyridine N-oxide

Finally, an oxidation using DMSO and sodium bicarbonate was attempted (57).

This reaction likely proceeds via the following mechanism (Figure 43).

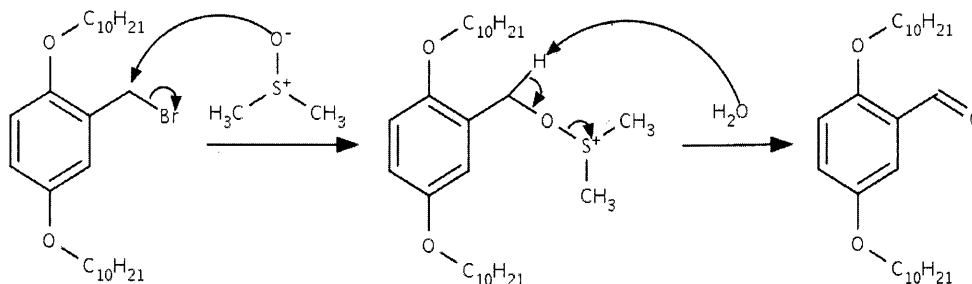


Figure 43 – Oxidation Mechanism using DMSO

The nucleophilic oxygen in DMSO can displace the benzylic bromine. The large excess of sodium bicarbonate can then deprotonate the benzylic proton to form an aldehyde.

One fact that contradicts this mechanism is that at no time was the presence of dimethyl

sulfide detected. While the reaction appears to convert most of the dimethylbromo precursor to **10**, an orange side product is also formed during the reaction which can be extremely hard to separate. At the time, column chromatography was only able to give pure yields of 11%. This oxidation doesn't improve on the previous oxidations' low yields and thus was also bypassed.

The route ultimately used to obtain **10** took much more time and two more steps than these oxidations. Despite these shortcomings, yields were much higher and purification of the compound was very easy. Of three oxidations, the DMSO-based oxidation is the best candidate for future use. With more careful chromatography, it's possible that higher yields can be obtained which would significantly shorten the time needed to synthesize the monomers necessary to making PPV.

## Conclusions

The project was successful in showing that the selective, reversible quenching of PPV can be accomplished using the photochromic properties of a spirooxazine. A successful polymer synthesis has been outlined that allows modification to obtain a desired polymer. While substantial quenching was not achieved, the groundwork has been laid for future research into improving the phenomenon.

Synthesis of SO-PPV is a time consuming process which, at a minimum, takes 11 steps. The low yields associated with a synthesis of this length make purification of the final product an arduous and sometimes even prohibitive exercise. If SO-PPV can be obtained in higher yields, I believe purification can safely be carried using Soxhlet extraction. This technique was a success in purifying the control polymer, but the decreased yields of SO-PPV made the extraction of marginal value. Greater yields of SO-PPV would most certainly improve its purity.

The easiest way to improve the yields of SO-PPV would be to reduce the number of steps needed or to improve the efficiency of the less productive steps. The first place to look is in the synthesis of diethenylbenzene **3**. The ultimate failure of the Stille coupling could have likely been avoided with better column chromatography technique. There is no doubt that the reaction successfully made **3**, and with proper purification yields would likely be high. The use of iodine as the aryl halogen in the coupling gave little improvement and the use of dibromomethylbenzene **7** is likely suitable.

If the Stille coupling cannot be improved upon, further development of the

oxidation of **7** to **10** would substantially increase the overall yield of the synthesis. The reaction is very short and seems to give high yields. The difficulty of the reaction is removing the sticky orange side-product which is invariably present after the reaction. The literature recommends the reaction be heated for half an hour; I found twenty minutes to be suitable for the reaction. Further heating appears to only increase the amount of side product. Again, better chromatography technique would likely give **10** in a high yield, avoiding the two additional steps of the current procedure. Use of this oxidation would also avoid the necessary handling of dangerous or toxic materials such as LAH and PCC.

The other parts of the synthesis are likely as efficient as they can be made. Synthesis of spirooxazine **4** takes only two steps and the reactions are suitable for large scales. The synthesis of **5** is also as short as it can be, though the purification of some of the compounds can be exasperating. With a successful purification from the Stille coupling, the overall reaction can be shortened to eight steps.

Although only minor quenching was seen with the synthesized polymers, the quenching was reversible and full fluorescence returned within about a minute. While the lack of full quenching from the polymers is obvious, the reason for it is not. In polymer **1**, only minor quenching takes place in solution. The lack of more substantial quenching is troubling. If it was an artifact of the limited solubility of the polymer, it's even more astounding that in the more soluble polymer **16** there was no photoactivity. Future research must determine the reason for this lack of photoactivity. With luck, the synthetic

scheme developed in this work will withstand the modifications needed to selectively and reversibly quench PPV fluorescence.

## Experimental

**Synthesis of 1, 4-bis(bromomethyl)-2,5-bis(decyloxy)benzene [7] (35).** To a solution consisting of 42 mL (170 mmol, 2.6 equiv) of 33% HBr and 200 mL of glacial acetic acid, 25.8 g (66 mmol, 1 equiv) of 1,4-bis(didecyloxy)benzene and 7.9 g (264 mmol, 4 equiv) paraformaldehyde were added. The slurry was heated to 70°C which resulted in the dissolution of all solids. The reaction was stirred at 70°C overnight, during which time solid salts precipitated. Precipitation of organic product occurred as the solution was allowed to cool to room temperature. Chloroform (~400 mL) was added to dissolve organic material and the mixture was washed with water to dissolve salts. Neutralization of the solution was then achieved with the slow addition of aqueous sodium bicarbonate and it was then washed with brine. The organic layer was dried with MgSO<sub>4</sub> and the solvent was evaporated to give an off-white colored solid. This was recrystallized in ~400 mL of hexanes to yield 25.5 g (67%) of the product as a white solid. <sup>1</sup>H NMR (400 MHz, CDCl<sub>3</sub>) δ 6.85 (s, 2H), 4.53 (s, 6H), 3.98 (t, 4H), 1.81 (quint, 4H), 1.49 (quint, 4H), 1.2-1.4 (br, 24H), 0.88 (t, 6H). <sup>13</sup>C NMR (400 MHz, CDCl<sub>3</sub>) δ 150.87, 127.72, 114.84, 69.21, 32.15, 29.83, 29.80, 29.60, 29.58, 29.56, 29.03, 26.32, 22.93, 14.38.

**Synthesis of 1,4-bis(acetyloxymethyl)-2,5-bis(decyloxy)benzene [8] (37).** A flask was charged with 5.0 g (8.6 mmol, 1 equiv) **7**, 2.6 g (17.3 mmol, 2 equiv) sodium iodide, 4.3 g (52 mmol, 6 equiv) anhydrous sodium acetate, and 90 mL DMF. The mixture was heated to 140°C and stirred for two days. After cooling to room temperature, the solution was poured into ~600 mL H<sub>2</sub>O and extracted with 3 x 150 mL ethyl acetate.

The organic layer was washed with H<sub>2</sub>O, brine, and dried with MgSO<sub>4</sub>. The solvent was evaporated to give a yellow solid. This solid was recrystallized in ~50 mL of ethyl acetate to yield 3.74 g (81%) of the product as a light yellow solid. <sup>1</sup>H NMR (400 MHz, CDCl<sub>3</sub>) δ 6.88 (s, 2H), 5.14 (s, 4H), 3.94 (t, 4H), 2.10 (s, 6H), 1.76 (quint, 4 H), 1.44 (quint, 4H), 1.2-1.4 (br, 24H), 0.88 (t, 6H). <sup>13</sup>C NMR (400 MHz, CDCl<sub>3</sub>) δ 171.20, 151.04, 125.34, 114.06, 69.28, 61.94, 32.13, 29.85, 29.81, 29.63, 29.59, 29.57, 26.31, 22.92, 21.33, 14.37.

**Synthesis of 1,4-bis(hydroxymethyl)-2,5-bis(decyloxy)benzene [9]** (37, 39). 0.5 g (13.2 mmol, 4.6 equiv) LAH was suspended in 10 mL of anhydrous THF. 1.55 g (2.9 mmol, 1 equiv) compound **8** was dissolved in anhydrous THF and added dropwise. The mixture was then stirred for two hours. LAH was then quenched, first by the slow addition of ethyl acetate and later by the addition of H<sub>2</sub>O to complete the quench. This solution was extracted with 3 x 75 mL chloroform and the organic layer was washed with H<sub>2</sub>O (2 x 100 mL) and then dried using MgSO<sub>4</sub>. Evaporation of the solvent yielded 1.26 g (96.6%) of the product as a white solid. <sup>1</sup>H NMR (400 MHz, CDCl<sub>3</sub>) δ 6.84 (s, 4H), 4.67 (s, 4H), 3.98 (t, 4H), 2.0 (br s, 2H), 1.78 (quint, 4H), 1.44 (quint, 4H), 1.2-1.4 (br, 24H), 0.89 (t, 6H). <sup>13</sup>C NMR (400 MHz, CDCl<sub>3</sub>) δ 150.84, 129.24, 112.52, 68.96, 62.42, 32.12, 29.81, 29.79, 29.64, 29.60, 29.55, 26.37, 22.92, 14.35.

**Synthesis of 2,5-bis(decyloxy)-1,4-dicarbaldehyde [10]** (39). A flask was charged with 1.23 g (2.73 mmol, 1 equiv) **9**, 2.35 g (10.9 mmol, 4 equiv) PCC, and 100 mL methylene chloride and stirred at room temperature for two hours. The now black mixture was carefully poured onto a short silica column and washed with chloroform.

The yellow solution was collected and the solvent evaporated to yield 1.22 g (88%) of the product as a yellow solid.  $^1\text{H}$  NMR (400 MHz,  $\text{CDCl}_3$ )  $\delta$  11.52 (s, 2H), 7.43 (s, 2H), 4.08 (t, 4H), 1.84 (quint, 4H), 1.47 (quint, 4H), 1.2-1.4 (br, 24H), 0.88 (t, 6H).  $^{13}\text{C}$  NMR (400 MHz,  $\text{CDCl}_3$ )  $\delta$  189.65, 155.43, 129.45, 111.79, 69.43, 32.10, 29.77, 29.76, 29.53, 29.27, 26.24, 22.90, 14.45

**Synthesis of 1,4-bis(decyloxy)-2,5-diethenylbenzene [3] (40).** In a flask charged with argon, 4.45 g methyltriphenylphosphonium bromide (12.5 mmol, 2.2 equiv) was suspended in 25 mL anhydrous THF and cooled to 0°C. 7.4 mL of 1.6M n-butyllithium in hexanes (12 mmol, 2.1 equiv) was slowly added and the yellow solution was stirred at room temperature for ½ hour. 2.53 g **10** (5.7 mmol, 1 equiv) was dissolved in 20 mL and slowly added and the resulting solution was refluxed for four hours. The solution was then cooled to room temperature and poured into 50 mL  $\text{H}_2\text{O}$ . This mixture was extracted with 100 mL diethyl ether, washed with brine, and the organic layer was dried with  $\text{MgSO}_4$ . The solvent was evaporated to leave a light yellow solid. This solid was purified using silica gel chromatography (1:6 methylene chloride - hexanes) and the colorless, fluorescent product was collected. Evaporation of the eluent yielded 0.93 g (37%) as a white, fluorescent solid.  $^1\text{H}$  NMR (400 MHz,  $\text{CDCl}_3$ )  $\delta$  7.04 (d of d, 2H), 6.98 (s, 2H), 5.72 (d, 2H), 5.25 (d, 2H), 3.96 (t, 4H), 1.79 (quint, 4H), 1.47 (quint, 4H), 1.2-1.4 (br, 24H), 0.88 (t, 6H).  $^{13}\text{C}$  NMR (400 MHz,  $\text{CDCl}_3$ )  $\delta$  150.86, 131.78, 127.39, 114.24, 110.74, 69.56, 32.15, 29.82, 29.80, 29.68, 29.65, 29.57, 26.38, 22.92, 14.37.

**Synthesis of 1-nitrosonaphthalene-2,7-diol [12] (43, 44).** 2.5 g (62.5 mmol, 1

equiv) was added to a flask and stirred until it completely dissolved. 10.0 g (62.5 mmol, 1 equiv) 2,7-dihydroxynaphthalene and 4.47 g (64.8 mmol, 1.04 equiv) sodium nitrite were added to the solution and stirred at 60°C for one hour. The solution was cooled to 0°C in an ice bath and 25 mL of a 6 M sulfuric acid solution was added dropwise. The acidified solution was then stirred for an additional hour and the precipitate was filtered and washed several times with water to give a wet powder. This wet powder was dried in a vacuum oven for six hours to yield 11.6 g (98%) of a bright, deep red powder. Note: Characterization of **12** proved to be very difficult.

#### **Synthesis of 1,1,3-trimethyl-1,3-dihydrospiro[indole-2,3'-naphtho[2,1-b]**

**[1,4]oxazine]-9'-ol [4]** (41, 42). 1.88 g (10.0 mmol, 1 equiv) **12** was suspended in 50 mL absolute methanol and stirred with gentle reflux. 1.99 g (11.5 mmol, 1.15 equiv) of 1,3,3-trimethyl-2-methylidene-2,3-dihydro-1H-indole was dissolved in 5 mL absolute methanol and added dropwise. The reaction was refluxed for another two hours and the solvent was removed to leave a dark purple, viscous oil. This oil was rinsed with a minimal amount of ethyl acetate (enough to remove it from the walls of the flask) and then filtered to give a light brown powder. This light brown powder was further purified by a recrystallization in ethanol to yield 0.974 g (28%) of the product as a tan powder. <sup>1</sup>H NMR (400 MHz, CDCl<sub>3</sub>) δ 7.87 (d, 1H), 7.71 (s, 1H), 7.65 (d, 1H), 7.58 (d, 1H), 7.22 (t, 1H), 7.08 (d, 1H), 7.02, (d, 1H), 6.90 (t, 1H), 6.84 (d, 1H), 6.58 (d, 1H), 5.53 (s, 1H), 2.76 (s, 3H), 1.35 (s, 6H). <sup>13</sup>C NMR (400 MHz, CDCl<sub>3</sub>) δ 155.26, 150.68, 147.81, 145.22, 136.08, 132.60, 130.44, 130.27, 128.25, 124.92, 122.15, 121.72, 120.07, 116.04, 114.44, 107.37, 103.95,

98.85, 52.03, 29.89, 25.68, 21.02.

**Synthesis of 1-(10-bromodecyloxy)-4-methoxybenzene [14].** 6.0 g (48.3 mmol, 1 equiv) 4-methoxyphenol, 100 g (333 mmol, 6.9 equiv) 1,10-dibromodecane, and 47.7 g (346 mmol, 7.2 equiv) potassium carbonate were added to a flask and dissolved in 225 mL distilled acetone. The solution was heated to reflux and stirred overnight. After cooling it to room temperature, salt by-products were filtered out and the solvent was evaporated to leave a liquid of primarily 1,10-dibromodecane. This liquid was poured into 350 mL hexanes, allowed to stand for 15 minutes, and filtered. The filtrate was then placed in the refrigerator and then filtered to give a solid. This solid was recrystallized from hexanes once more to yield 5.20 g (31%) of the product as a white solid.  $^1\text{H}$  NMR (400 MHz,  $\text{CDCl}_3$ )  $\delta$  6.83 (s, 4H), 3.90 (t, 2H), 3.77 (s, 3H), 3.41 (t, 2H), 1.85 (quint, 2H), 1.75 (quint, 2H), 1.4-1.5 (br, 4H), 1.3-1.4 (br, 8H).  $^{13}\text{C}$  NMR (400 MHz,  $\text{CDCl}_3$ )  $\delta$  153.70, 153.33, 115.56, 114.74, 68.88, 56.01, 34.34, 33.15, 29.77, 29.71, 29.68, 29.07, 28.49, 26.38.

**Synthesis of 1,4-dibromo-2-(10-bromodecyloxy)-5-methoxybenzene [5] (45).** 1.1 g (3.2 mmol, 1 equiv) **14** was added to a flask and dissolved in a minimal volume of chloroform. The solution was cooled to 0°C and 1.07 g (6.7 mmol, 2.1 equiv) bromine dissolved in 5 ml of chloroform was added dropwise. The dark orange solution was then stirred at room temperature for two hours. Residual bromine was removed by washes with water, an aqueous saturated sodium thiosulfate solution, and brine. The organic layer was dried with sodium sulfate and the solvent evaporated to give an off-white solid.

This solid was recrystallized from petroleum ether, carefully removing the bottom layer of by-product as the solution cooled. Further cooling yielded 1.48 g (92%) of the product as a white solid. <sup>1</sup>H NMR (400 MHz, CDCl<sub>3</sub>) δ 7.09 (s, 2H), 3.94 (t, 2H), 3.84 (s, 3H), 3.40 (t, 2H), 1.75-1.90 (m, 4H), 1.4-1.5 (m, 4H), 1.25-1.40 (br, 8H). <sup>13</sup>C NMR (400 MHz, CDCl<sub>3</sub>) δ 150.60, 150.26, 118.83, 117.23, 111.46, 110.61, 70.62, 57.32, 34.35, 33.20, 29.76, 29.70, 29.58, 29.48, 29.10, 28.54, 26.29.

**Synthesis of 9'-[10-(2,5-dibromo-4-methoxyphenoxy)decyloxy]-1,3,3-trimethyl-1,3-dihydrospiro[indole-2,3'-naphtho[2,1-b][1,4]oxazine] (2).** 0.94 g (2.8 mmol, 1 equiv) **4**, 1.82 g (3.6 mmol, 1.3 equiv) **5**, and 2.7 g (20 mmol, 7 equiv) potassium carbonate were added to a flask with 30 mL of acetone and heated to 80°C. The reaction was allowed to reflux for three days. After cooling to room temperature, the reaction was poured into water and extracted with methylene chloride. The organic layer was dried with MgSO<sub>4</sub> and the solvent was evaporated to give a dark yellow oil. The yellow oil was purified using silica gel chromatography (3:2 toluene – petroleum ether) to yield 1.42 g (66%) of product as a yellow oil. <sup>1</sup>H NMR (400 MHz, CDCl<sub>3</sub>) δ 7.86 (s, 1H), 7.73 (s, 1H), 7.63 (d, 1H), 7.57 (d, 1H), 7.22 (t, 1H), 7.10 (s, 2H), 7.09 (d, 1H), 7.05 (d, 1H), 6.90 (t, 1H), 6.84 (d, 1H), 6.58 (d, 1H), 4.18 (t, 2H), 3.96 (t, 2H), 3.84 (s, 3H), 2.77 (s, 3H), 1.89 (quint, 2H), 1.82 (quint, 2H), 1.45-1.60 (br, 4H), 1.30-1.45 (br, 12H). <sup>13</sup>C NMR (400 MHz, CDCl<sub>3</sub>) δ 158.80, 150.68, 150.46, 150.39, 147.90, 145.08, 136.16, 132.71, 130.27, 129.66, 128.30, 124.84, 122.63, 121.77, 120.11, 118.78, 117.53, 117.19, 114.14, 111.49, 110.65, 107.41, 100.65, 98.77, 70.52, 68.32, 57.20, 52.02, 30.02, 29.93, 29.81, 29.80,

29.70, 29.59, 29.41, 26.43, 26.24, 25.74, 21.09.

**Synthesis of poly(2,5-didecyloxyphenylene-4-vinylene) [15]** (40, 46). 0.48 g (1.1 mmol, 1 equiv) **3**, 0.62 g (1.1 mmol, 1 equiv) 1,4-dibromo-2,5-didecyloxybenzene, 20 mg (0.09 mmol, 0.08 equiv) palladium(II) acetate, 160 mg (0.53 mmol, 0.48 equiv) tri(*o*-tolyl)phosphine, 15 mL DMF, and 6 mL triethylamine were placed in a flask and the mixture was charged with argon. The flask was stirred at 90°C for 24 hours and heated to 110°C for another 24 hours. The mixture was cooled to room temperature and poured into 50 mL methanol, stirred for five minutes, and poured into a Soxhlet thimble. Soxhlet extractions were done using methanol, hexanes, and finally THF to extract the polymer from the thimble. The solvent was evaporated to give an orange solid which was redissolved in THF and poured into methanol. This mixture was filtered to yield 0.54 g (47%) of the product as an orange, fluorescent solid.

**Synthesis of [1]** (40, 46). 0.82 g (1.1 mmol, 1 equiv) **2**, 0.48 g (1.1 mmol, 1 equiv) **3**, 20 mg (0.09 mmol, 0.08 equiv) palladium(II) acetate, 160 mg (0.53 mmol, 0.48 equiv) tri(*o*-tolyl)phosphine, 15 mL DMF, and 6 mL triethylamine were placed in a flask and the mixture was charged with argon. The flask was stirred at 90°C for 24 hours and heated to 110°C for another 24 hours. The mixture was cooled to room temperature and poured into 50 mL methanol. The precipitate was filtered to yield a green solid. This solid was twice dissolved into THF and precipitated into methanol to yield 75 mg (5%) of the polymer as a green solid.

**Synthesis of [16]** (40, 46). 0.22 g (0.29 mmol, 1 equiv) **2**, 0.16 g (0.29 mmol, 1

equiv) 1,4-dibromo-2,5-didecyloxybenzene, 0.26 g (0.59 mmol, 2 equiv) **3**, 5 mg (0.02 mmol, 0.07 equiv) palladium (II) acetate, 45 mg (0.15 mmol, 0.51 equiv) tri(*o*-tolyl)phosphine, 10 ml DMF, and 4 mL triethylamine were placed in a flask and the mixture was charged with argon. The flask was stirred at 90°C for 24 hours and heated to 110°C for another 24 hours. The mixture was cooled to room temperature and poured into 30 mL methanol. The precipitate was filtered to yield 50 mg (8%) of the polymer as a green solid.

**Attempted Synthesis of [2] using the Stille Coupling (47).** 2.0 g (3.6 mmol, 1 equiv) 1,4-dibromo-2,5-didecyloxybenzene, 2.31 g (7.3 mmol, 2.03 equiv) vinyltributyltin, and 160 mg (0.14 mmol, 0.04 equiv) tetrakis(triphenylphosphine)palladium(0) were dissolved in DMF and the flask was charged with nitrogen. The solution was stirred at 100°C for five hours. After cooling to room temperature, the bluish green mixture was filtered. The filtrate was washed with water (x3) and extracted with methylene chloride. The organic layer was then dried using MgSO<sub>4</sub>. The solvent was evaporated to give a yellow solid. This solid was purified using silica gel chromatography (30:1 hexanes – ethyl acetate) and recrystallization from ethanol. Approximately 40 mg (2%) of the crude product was obtained.

**Synthesis of *trans*-Di( $\mu$ -acetato)-bis[3-(diphenylphosphino)-4-styryl]dipalladium [17] (49, 50).** 0.45 g (2.0 mmol, 1 equiv) palladium(II) acetate and 0.81 g (6.3 mmol, 3.2 equiv) tri(*o*-tolyl)phosphine were dissolved in toluene and heated to 50°C for five minutes. The orange solution was cooled to room temperature to give a

yellow solution. The solvent was reduced by half using a vacuum manifold and 50 mL of pentane was introduced. The resulting precipitate was filtered to give a yellow solid. This solid was recrystallized from 1:1 methylene chloride – pentane to yield 0.39 g (42%) of the product as a yellow solid.

**Attempted synthesis of 1,4-bis(decyloxy)-2,5-diethenylbenzene [2] using palladacycle catalyst (48).** 1.5 g (2.8 mmol, 1 equiv) 1,4-dibromo-2,5-didecyloxybenzene, 1.8 mL (5.8 mmol, 2.1 equiv) vinyltributyltin, and 30 mg (0.03 mmol, 0.01 equiv) **17** were dissolved in toluene and heated to 90°C for three hours. An additional 30 mg (0.03 mmol, 0.01 equiv) **17** was added and the solution was stirred at 90°C for another 36 hours. The dark blue mixture was cooled to room temperature and washed with 100 mL of ether saturated with potassium fluoride. This mixture was filtered through Celite and the solvents were evaporated to leave a dark green solid. This solid was purified using silica gel chromatography (1:6 methylene – chloride) and recrystallization from ethanol. 0.5 g (41%) of the crude product was obtained.

**Attempted synthesis of 1,4-diiodo-2,5-didecyloxybenzene [18] using bis(pyridine)iodonium tetrafluoroborate (51).** 0.50 g (1.3 mmol, 1 equiv) 1,4-didecyloxybenzene, 0.48 mL (5.4 mmol, 4.2 equiv) triflic acid, and 1.0 g (2.7 mmol, 2.1 equiv) bis(pyridine)iodonium tetrafluoroborate were dissolved in 6 mL methylene chloride. The flask was charged with argon and the solution was stirred at room temperature for three hours. The dark purple solution was poured into water and extracted three times with methylene chloride followed by extraction with ethyl acetate

three times. The organic layers were combined and washed with a saturated sodium thiosulfate solution. The organic layer was then dried with sodium sulfate the the solvent was evaporated to yield a crude orange/purple solid.

**Synthesis of 1,4-diiodo-2,5-didecyloxybenzene [18] using mercury acetate**

(53). 3.0 g (7.7 mmol, 1 equiv) 1,4-didecyloxybenzene, 6.1 g (19 mmol, 2.5 equiv) mercury acetate, and 4.9 g (19 mmol, 2.5 equiv) iodine dissolved in 110 mL methylene chloride. This solution was stirred at room temperature for three days. Solids were removed by filtering through a short silica column. The pomegranate solution was washed with an aqueous saturated sodium thiosulfate solution. The yellow solution was then washed with an aqueous sodium bicarbonate solution, water, and brine. Evaporation of the organic layer yielded a yellow solid. This solid was recrystallized from ethanol to yield 3.0 g (70%) of the product as a white solid.  $^1\text{H}$  NMR (400 MHz,  $\text{CDCl}_3$ )  $\delta$  7.16 (s, 2H), 3.92 (t, 4H), 1.79 (quint, 4H), 1.49 (quint, 4H), 1.20-1.40 (br, 30H), 0.88 (t, 4H).  $^{13}\text{C}$  NMR (400 MHz,  $\text{CDCl}_3$ )  $\delta$  153.12, 123.06, 86.55, 70.61, 32.13, 29.78, 29.55, 29.51, 29.38, 26.26, 22.91, 14.34.

**Attempted synthesis of 1,4-bis(decyloxy)-2,5-diethenylbenzene [2] using**

**Palladacycle Catalyst (48).** 3.0 g (4.7mmol, 1 equiv) **18**, 3.3 g (10.3 mmol, 2.2 equiv) vinyltributyltin, and 51 mg (0.02 mmol, 0.05 equiv) **17** were dissolved in 250 mL toluene and stirred at 90°C under a nitrogen atmosphere for three hours. An additional 50 mg (0.02 mmol, 0.05 equiv) **17** was added and the reaction was stirred at 90°C for three days. The mixture was introduced with an ether solution saturated with potassium fluoride and

allowed to stir overnight. The solvent was evaporated to yield an orange/yellow solid.

This solid was recrystallized from ethanol to yield a crude yellow solid.

**Synthesis of 2,5-bis(decyloxy)-1,4-dicarbaldehyde [10] via Sommelet reaction**

(54). 3.9 g (6.8 mmol, 1 equiv) **7** and 3.4 g (24 mmol, 3.6 equiv) hexamine were suspended in 160 mL ethanol and heated to reflux. Over two hours, 130 mL a 50% aqueous acetic acid solution was added dropwise. The solution was then refluxed for an additional half hour. After cooling to room temperature, the yellow solution was poured into water and extracted with methylene chloride. The organic layer was washed with a saturated aqueous solution of sodium bicarbonate and dried with MgSO<sub>4</sub>. The solvent was evaporated to give a yellow solid. This solid was purified using silica gel chromatography (1:1 methylene chloride – petroleum ether) to give 0.18 g (6%) of the product as a yellow solid.

**Synthesis of 2,5-bis(decyloxy)-1,4-dicarbaldehyde [10] using silver oxide (56).**

1.0 g (1.7 mmol, 1 equiv) **7**, 0.16 g (1.7 mmol, 1 equiv) pyridine N-oxide, and 0.20 g (0.87 mmol, 0.5 equiv) silver(I) oxide were suspended in 5 mL toluene and stirred overnight at 50°C. The mixture was cooled to room temperature and filtered through Celite to give a dark orange liquid. The liquid was placed onto a silica gel chromatography column, rinsed with hexanes, and washed off of the column using methylene chloride to give 0.089 g (11%) of the product as a yellow solid.

**Synthesis of 2,5-bis(decyloxy)-1,4-dicarbaldehyde [10] using DMSO (57).**

2.0 g (3.5, 1 equiv) **7** and 4.4 g (52 mmol, 15 equiv) sodium bicarbonate were suspended in

50 mL DMSO and stirred at 115°C for 25 minutes. The yellow solution was then poured into 1 L of water and the resulting precipitate was filtered to give a heterogeneous mixture of yellow and orange solids. The mixture was purified using silica gel chromatography (1:1 methylene chloride – petroleum ether) to yield 0.166 g (11%) of the product as a yellow solid.

## References

- 1 – Friend, R.H.; Gymer, R.W.; Holmes, A.B.; Burroughes, R.N.; Marks, R.N.; Taliani, C.; Bradley, D.D.C.; Dos Santos, D.A.; Brédas, J.L.; Löglund, M.; Salaneck, W.R. Electroluminescence in Conjugated Polymers. *Nature*, **1999**, 397, 121-128.
- 2 – Heeger, A.J. Semiconducting and Metallic Polymers: The Fourth Generation of Polymeric Materials. *J. Phys. Chem. B*, **2001**, 105 (36), 8475-8491
- 3 – Fumitomo, H.; Díaz-García, M.A.; Schwartz, B.J.; Heeger, A.J. New Developments in the Photonic Applications of Conjugated Polymers. *Acc. Chem. Res.* **2001**, 30 (10), 430-436.
- 4 – Schwartz, B.J. Conjugated Polymers as Molecular Materials: How Chain Conformation and Film Morphology Influence Energy Transfer and Interchain Interactions. *Annu. Rev. Phys. Chem.* **2003**, 54, 141-172.
- 5 – Grimes, A.F.; Call, S.E.; Harbron, E.J.; English, D.S. Wavelength-Resolved Studies of Förster Energy Transfer in Azobenzene-Modified Conjugated Polymers: The Competing Roles of Exciton Migration and Spectral Resonance. *J. Phys. Chem. C*. **2007**, 111 (38), 14257-14265.
- 6 – Lewis, S.M.; Harbron, E.J. Photomodulated PPV Emission in a Photochromic Polymer Film. *J. Phys. Chem. C*. **2007**, 111 (11), 4425-4430.
- 7 – Harbron, E.J.; Hadley, D.H.; Imm, M.R. Solvent Effects on Phototriggered Conformational Changes in an Azobenzene Functionalized poly(*p*-phenylene vinylene). *J. Photochem. Photobiol. A: Chem.* **2007**, 186, 151-157.
- 8 – Grimes, A.F.; Call, S.E.; Vicente, D.A.; English, D.S.; Harbron, E.J. Toward Efficient Photomodulation of Conjugated Polymer Emission: Optimizing Differential Energy Transfer in Azobenzene-Substituted PPV Derivatives. *J. Phys. Chem. B*. **2006**, 110, 19183-19190.
- 9 – Harbron, E.J.; Vicente, D.A.; Hadley, D.H.; Imm, M.R. Phototriggered Fluorescence Color Changes in Azobenzene-Functionalized Conjugated Polymers. *J. Phys. Chem. A*. **2005**, 109, 10846-10853.
- 10 – Harbron, E.J.; Vicente, D.A.; Hoyt, M.T. Fluorescence Modulation via Isomer-Dependent Energy Transfer in an Azobenzene-Functionalized PPV Derivative. *J. Phys. Chem. B*. **2004**, 108, 18789-18792.
- 11 – Blythe, T.; Bloor, D. *Electrical Properties of Polymers, Second Edition*; Cambridge University Press: Cambridge, 2005.
- 12 – Nalwa, H.S. *Handbook of Organic Conductive Molecules and Polymers*; Chichester: New York, 1997.
- 13 – Gettinger, C.L.; Heeger, A.J.; Drake, J.M.; Pie, D.J. A Photoluminescence Study of Poly(Phenylene Vinylene) Derivatives: The Effect of Intrinsic Persistence Length. *J. Chem. Phys.*, **1994**, 101, 1673-1679.
- 14 – Zhiqiang, R.L. *Organic Light-Emitting Materials and Devices*; CRC/Taylor & Francis: Boca Raton, 2007.

- 15 – Aime, J.P.; Ramakrishnan, S.; Chance, R.R.; Kim, M.W. The Effect of Substituent Groups on Polymer Conformation in Good Solvent; Polyoctene and Polydecene. *J. Phys. France*. **1990**, 51, 963-975.
- 16 – Sharma, A. *Introduction to Fluorescence Spectroscopy*; Wiley: New York, 1999.
- 17 – Lakowicz, J.R. *Principles of Fluorescence Spectroscopy*; Springer: New York, 2006.
- 18 – Levine, I.N. *Physical Chemistry, Fifth Edition*; McGraw Hill: Brooklyn, 2002.
- 19 – <http://www.ocf.berkeley.edu/~bramall/work/astrobiology/images/Jablonski-Diagram.jpg>
- 20 – Pavie, D.L. *Introduction to Spectroscopy: A Guide for Students of Organic Chemistry*; W.B. Saunders Co.: Philadelphia, 1979
- 21 – Rabek, J.F. *Mechanisms of Photophysical Processes and Photochemical Reactions in Polymers-Theory and Applications*; John Wiley & Sons: New York, 1987.
- 22 – Andrews, D.L.; Bradshaw, D.S. Virtual Photons, Dipole Fields, and Energy Transfer: A Quantum Electrodynamical Approach. *Eur. J. Phys.* **2004**, 25, 845-858.
- 23 – Turro, N.J. *Modern Molecular Photochemistry*; Benjamin/Cummings Pub. Co.: Menlo Park, 1978.
- 24 – Irie, M. Spiropyrans and Spirooxazines for Memories and Switches. *Chem. Rev.* **2000**, 100 (5), 1741-1754.
- 25 – Bouas-Laurent, H.; Dürr, H. Organic Photochromism (IUPAC Technical Report). *Pure Appl. Chem.* **2001**, 73 (4), 639-665.
- 26 – Konorov, S.O.; Sidorov-Biryukov, D.A.; Bugar, I.; Chorvat, D.; Chorva, D.; Zheltikov, A.M. Quantum Control of Two-Photon Photochromism in the Solid Phase. *JETP Letters*. **2003**, 78 (4), 246-249.
- 27 – Zollinger, H. *Color Chemistry: Syntheses, Properties, and Applications of Organic Dyes and Pigments, Third, Revised Edition*. VCH Publishers: New York, 2003.
- 28 – Dotsenko, A.V.; Glebov, L.B.; Tsekhomsky, V.A. Physics and Chemistry of Photochromic Glasses. Dotsenko et al, *Physics & Chemistry of Photochromic Glasses*. CRC Press: Boca Raton, 1997.
- 29 – Berkovic, G.; Krongauz, V.; Weiss, V. Spiropyrans and Spirooxazines for Memories and Switches. *Chem. Rev.* **2000**, 100 (5), 1741-1754.
- 30 – Crano, J.C.; Guglielmetti, R.J. *Organic Photochromic and Thermochemical Compounds: Main Photochromic Families*. Springer: New York, 1999
- 31 – Such, G.K.; Evans, R.A.; Davis, T.P. Rapid Photochromic Switching in a Rigid Polymer Matrix Using Living Radical Polymerization. *Macromolecules*, **2006**, 39 (4), 1391-1396.
- 32 – Heck, R.F.; Nolley, J.P. Palladium-Catalyzed Vinylic Hydrogen Substitution Reactions with Aryl, Benzyl, and Styryl Halides. *J. Org. Chem.* **1972**, 37 (14), 2320-2322.
- 33 – Carey, F.A.; Sundberg, R.J. *Advanced Organic Chemistry, Part B: Reactions and Synthesis, Fifth Edition*. Springer: New York, 2007.
- 34 – <http://www.organic-chemistry.org/namedreactions/heck-reaction.shtm>
- 35 – Thompson, B.C.; Kim, Y.G.; McCarley, T.D.; Reynolds, J.R. Soluble Narrow Band

- Gap and Blue Propylenedioxythiophene-Cyanovinylene Polymers as Multifunctional Materials for Photovoltaic and Electrochromic Applications. *J. Am. Chem. Soc.* **2006**, 128 (39), 12714-12725.
- 36 – Nazarov, I.N.; Semenovskiy, A.V. Mechanism of Halomethylation. *Russ. Chem. Bull.* **1957**, 6 (8), 997-999.
- 37 – Chen, Z.K.; Meng, H.; Lai, Y.H.; Huang, W. Photoluminescent Poly(*p*-phenylenevinylene)s with an Aromatic Oxadiazole Moiety as the Side Chain: Synthesis, Electrochemistry, and Spectroscopy Study. *Macromolecules*, **1999**, 32 (13), 4351-4358.
- 38 – Bordwell, F.G.; Brannen, W.T. The Effect of the Carbonyl and Related Groups on the Reactivity of Halides in SN2 Reactions. *J. Am. Chem. Soc.* **1964**, 86 (21), 4645-4650.
- 39 – Wang, B.; Wasielewski, M.R. Design and Synthesis of Metal Ion-Recognition-Induced Conjugated Polymers: An Approach to Metal Ion Sensory Materials. *J. Am. Chem. Soc.* **1997**, 119 (1), 12-21.
- 40 – Kim, J.H.; Lee, H. Synthesis, Electrochemistry, and Electroluminescence of Novel Red-Emitting Poly(*p*-phenylenevinylene) Derivative with 2-Pyran-4-ylidene-Malononitrile Obtained by the Heck Reaction. *Chem. Mater.* **2002**, 14, 2270-2275.
- 41 – Kakishita, T.; Matsumoto, K.; Kiyotsukuri, T. Synthesis and NMR Study of 9'-Substituted Spiroindolinonaphthoxazine Derivatives. *J. Heterocycl. Chem.* **1992**, 29, 1709-1715.
- 42 – Dürr, H.; Ma, Y.; Cortellaro, G. Preparation of Photochromic Molecules with Polymerizable Organic Functionalities. *Synthesis*, **1995**, 294-298.
- 43 – Son, Y.A.; Park, Y.M.; Choi, M.S.; Kim, S.H. Synthesis of Hetero-bi-functional Dye Having Photochromism and Electrochromism. Part 1: Characteristics and its Sensing Properties. *Dyes Pigm.* **2007**, 75 (2), 279-282.
- 44 – Deligeorgiev, T.; Minkovska, S.; Jejiaskova, B.; Rakovsky, S. Synthesis of Photochromic Chelating Spiro-naphthoxazines. *Dyes Pigm.* **2002**, 53 (2), 101-108.
- 45 – He, F.; Tang, Y.; Yu, M.; Wang, S. A Strategy for the Detection of Diels-Alder Reactions Using Fluorescence Quenching of Conjugated Polymers. *Adv. Funct. Mater.* **2007**, 17 (6), 996-1002.
- 46 – Xu, B.; Zhang, J.; Pan, Y.; Peng, Z. Syntheses and Optical Properties of poly(*o*-phenylenevinylene)s. *Synth. Met.* **1999**, 107, 47-51.
- 47 – Peng, Z.; Galvin, M.E. Polymers with High Electron Affinities for Light-Emitting Diodes. *Chem. Mater.* **1998**, 10, 1785-1788.
- 48 – Daoud, W.A.; Turner, M.L. Efficient Synthesis of 1,4-Dialkoxy and 1,4-Dialkyl Substituted 2,5-Divinylbenzenes via the Stille Reaction. *Bull. Chem. Soc. Jpn.* **2005**, 78, 367-369.
- 49 – Luo, F.T.; Xue, C.; Ko, S.L.; Shao, Y.D.; Wu, C.J.; Kuo, Y.M. Preparation of Polystyrene-Supported Soluble Palladacycle Catalyst for Heck and Suzuki Reactions. *Tetrahedron*, **2005**, 61, 6040-6045.

- 50 – Herrmann, W.A.; Brossmer, C.; Öfele, K.; Reisinger, C.P.; Priermeier, T.; Beller, M.; Fischer, H. Palladacycles as Structurally Defined Catalysts for the Heck Olefination of Chloro- and Bromoarenes. *Angew. Chem. Int. Ed. Engl.* **1995**, *34*, 1844-1848.
- 51 – López-Alvarado, P.; Avendaño, C.; Menéndez, J.C. Efficient, Multigram-Scale Synthesis of Three 2,5-Dihalobenzoquinones. *Synth. Commun.* **2002**, *32* (20), 3233-3239.
- 52 – Barluenga, J.; Campos, P.J.; González, J.M.; Suárez, J.L. Regio- and Stereoselective Iodofluorination of Alkenes with Bis(pyridine)iodonium(I) Tetrafluoroborate. *J. Org. Chem.* **1991**, *56*, 2234-2237.
- 53 – Shi, Z.F.; Wang, L.J.; Wang, H.; Cao, X.P.; Zhang, H.L. Synthesis of Oligo(phenylene ethynylene)s with Dendrimer “Shells” for Molecular Electronics. *Org. Lett.* **2007**, *9* (4), 595-598.
- 54 – Jin, J.Y.; Jin, Z.Z.; Xia, Y.; Zhou, Z.Y.; Uw, X.; Zhu, D.X.; Su, Z.M. Design and Synthesis of 1,4-bis[4-(1,1-dicyanovinyl)styryl]-2,5-bis(alkoxy)benzenes as red organic electroluminescent PPV analogs. *Polymer*, **2007**, *48*, 4028-4033.
- 55 – Li, J.J.; Corey, E.J. *Name Reactions for Functional Group Transformations*. John Wiley & Sons, Inc: New York, 2007.
- 56 – Chen, D.X.; Ho, C.M.; Wu, Q.Y.R.; Wu, P.R.; Wong, F.M.; Wu, W. Convenient Oxidation of Benzylic and Allylic Halides to Aldehydes and Ketones. *Tetrahedron Lett.*, **2008**, *49*, 4147-4148.
- 57 – Shao, P.; Li, Z.; Luo, J.; Wang, H.; Qin, J. A Convenient Synthetic Route to 2,5-Dialkoxyterephthalaldehyde. *Synth. Commun.*, **2005**, *35*, 49-53.

# Appendix

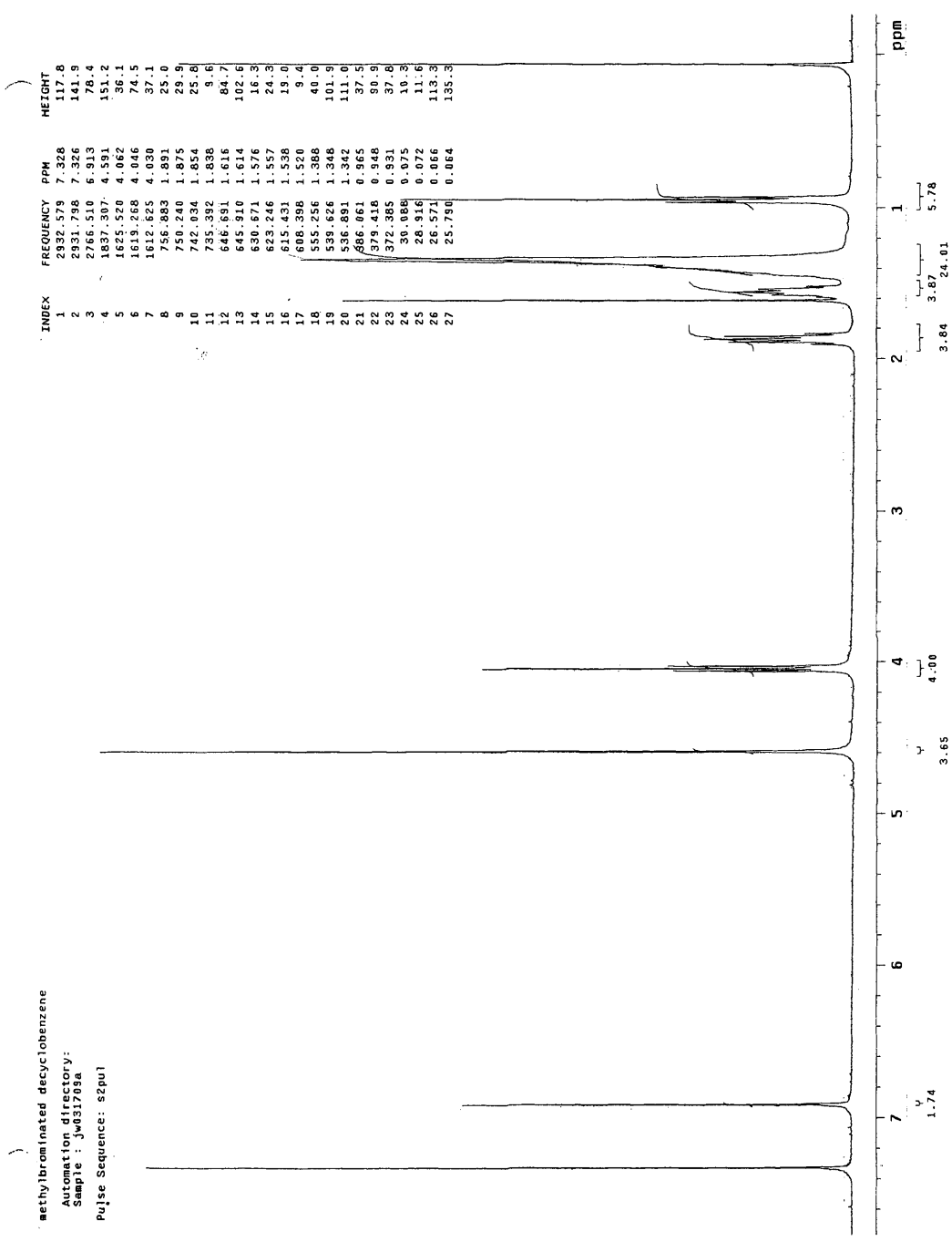


Figure 44 – <sup>1</sup>H NMR Spectrum of Dibromomethylbenzene 7

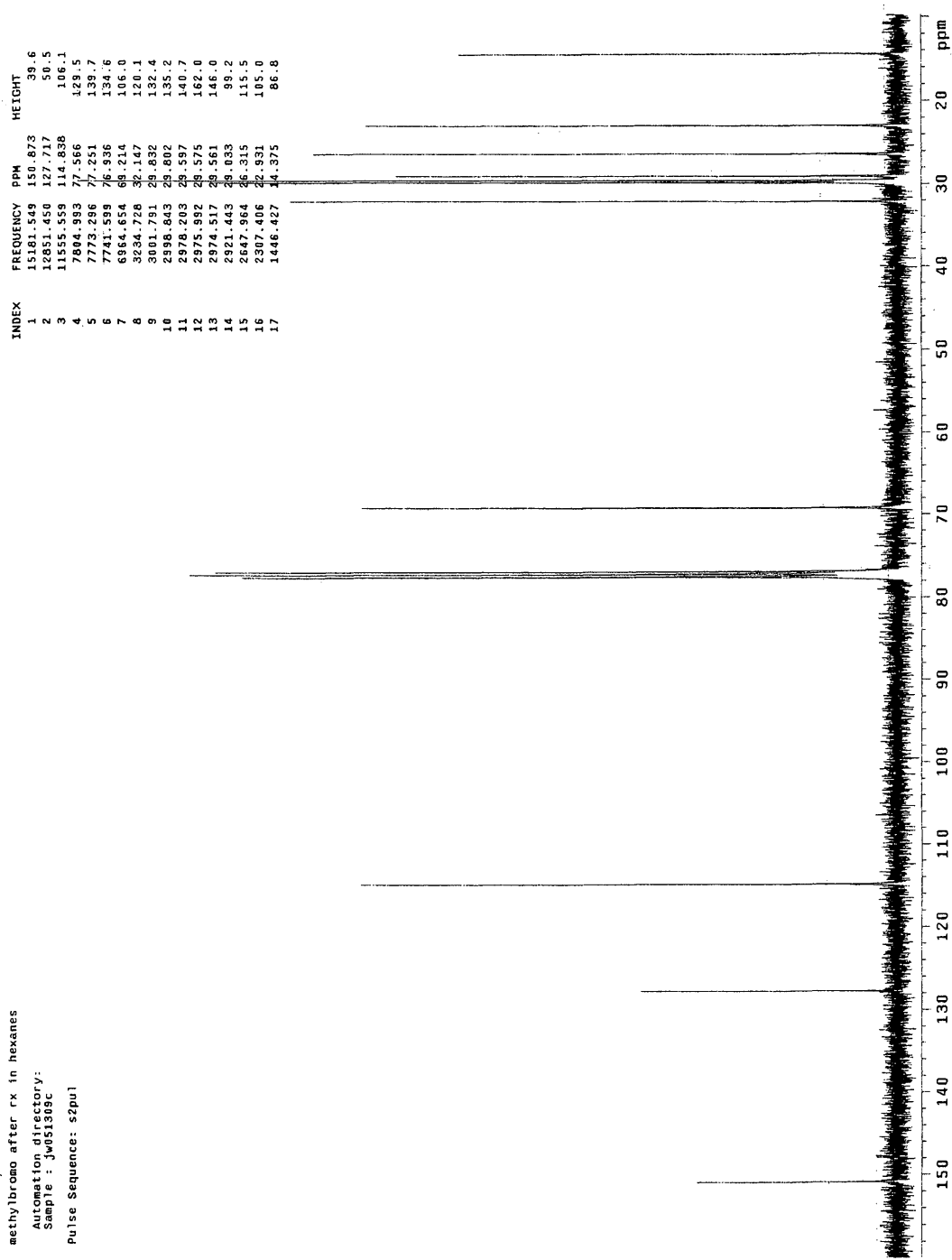


Figure 45 – <sup>13</sup>C NMR Spectrum of Dibromomethylbenzene 7

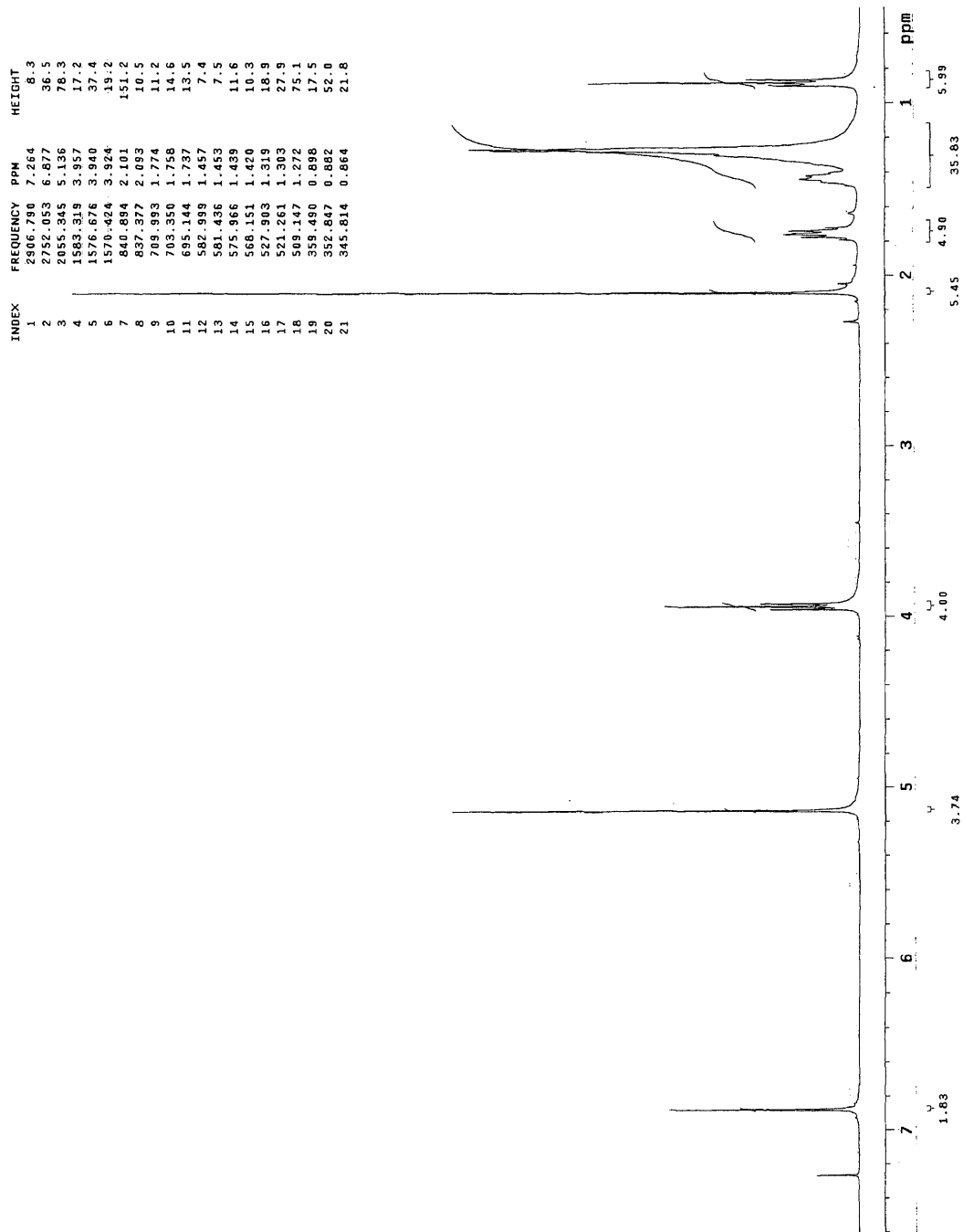


Figure 46 – <sup>1</sup>H NMR Spectrum of Diacetyloxybenzene **8**

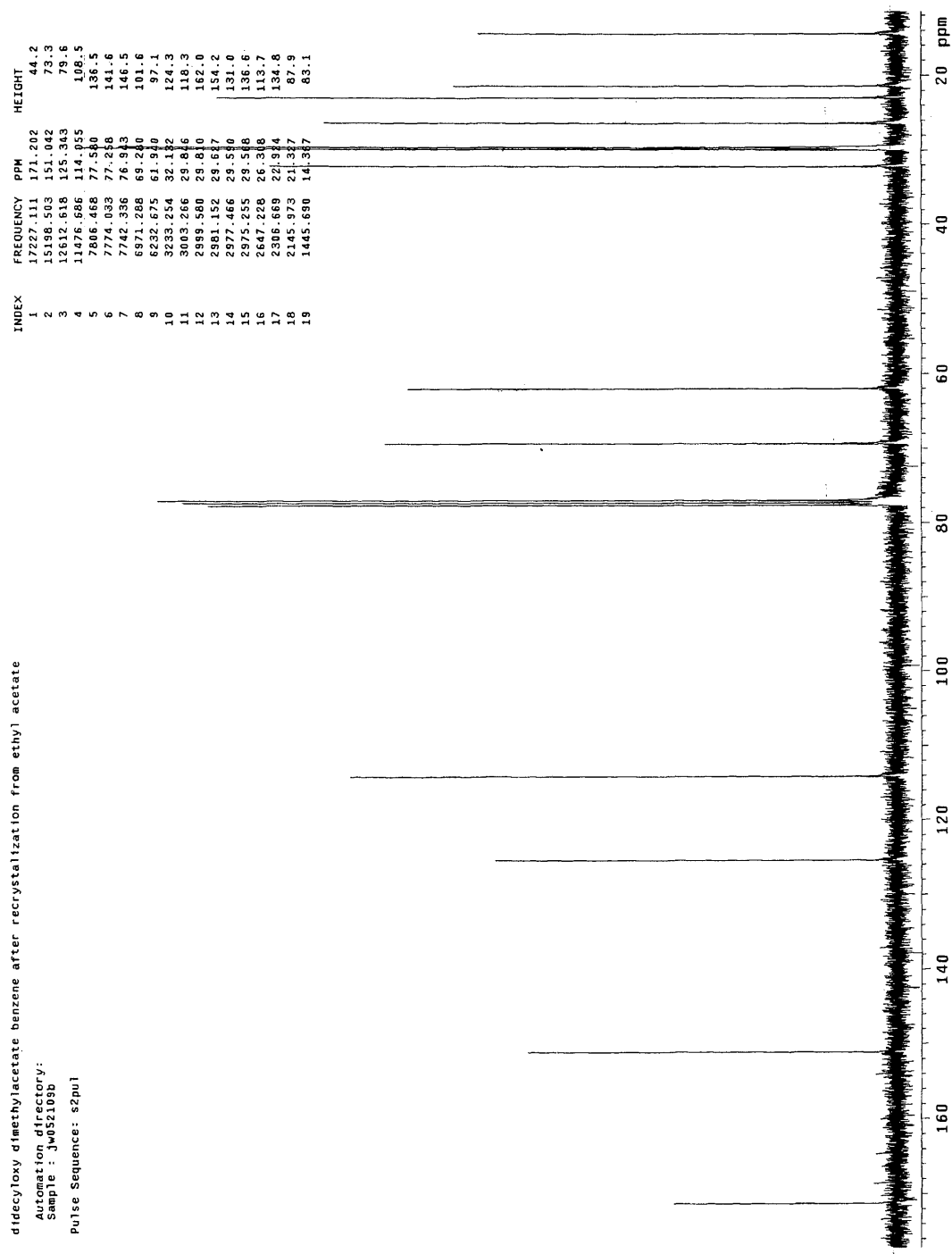


Figure 47 – <sup>13</sup>C NMR Spectrum of Diacetyloxybenzene 8

dimethylhydroxy using LAH with Date on bottle

Automation directory:

Sample : jw053009a

Pulse Sequence: s2pu1

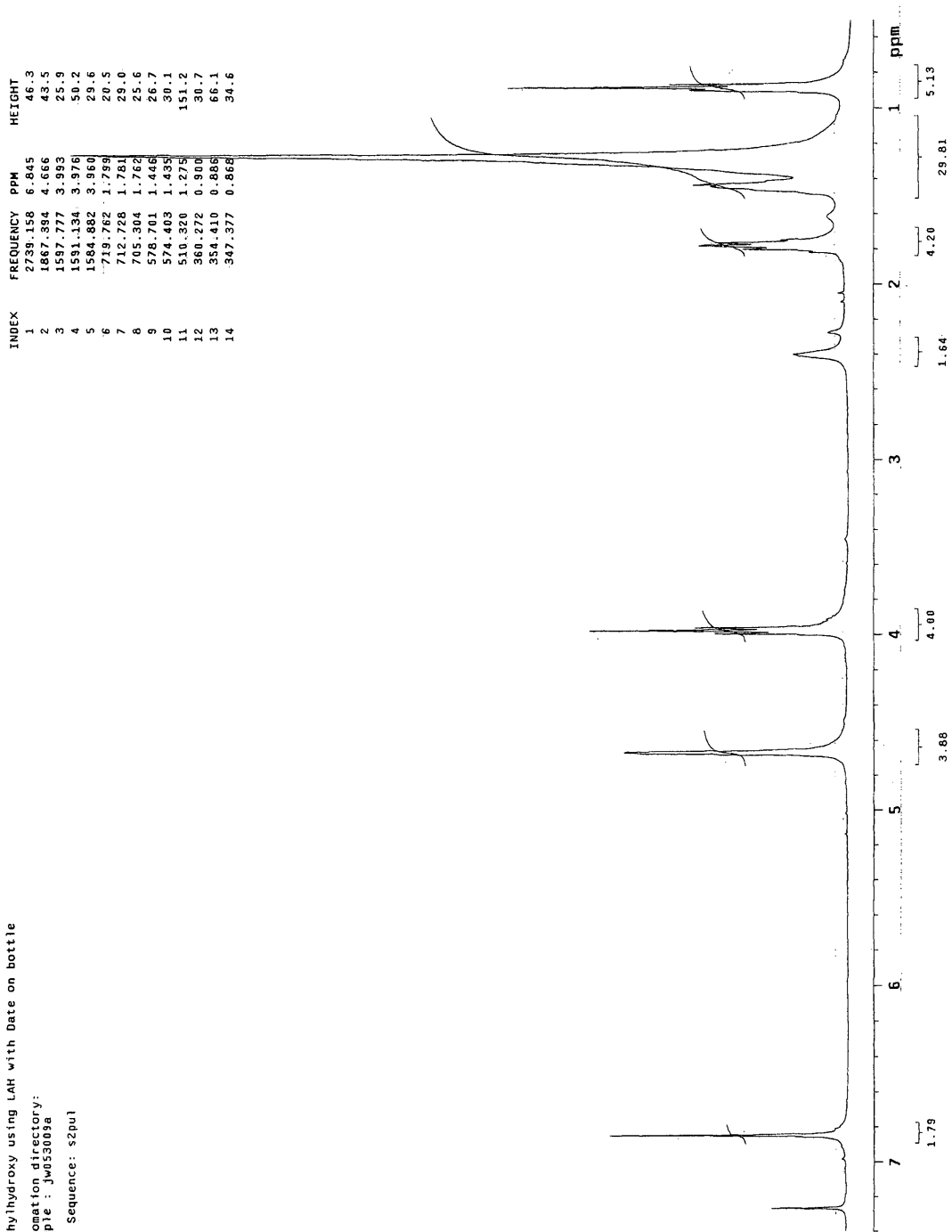


Figure 48 – <sup>1</sup>H NMR Spectrum of Dihydroxymethylbenzene **9**

dimethylhydroxy benzene using LAH with date on bottle

Automation directory:

Sample : JW55309B

Pulse Sequence: szpu1

INDEX	FREQUENCY	PPM	HEIGHT
1	15178.600	150.844	30.4
2	13004.776	128.241	33.1
3	1321.686	12.516	82.0
4	7804.933	77.566	156.6
5	7773.296	77.251	157.9
6	7740.662	76.928	162.0
7	6936.854	68.958	76.1
8	6281.325	62.423	66.6
9	3231.779	32.117	70.0
10	2989.580	29.810	115.9
11	2997.369	29.788	114.9
12	2982.626	29.641	91.3
13	2978.941	29.605	101.2
14	2973.043	29.546	93.8
15	2653.862	26.374	91.5
16	2305.832	22.516	76.3
17	1444.216	14.353	73.3

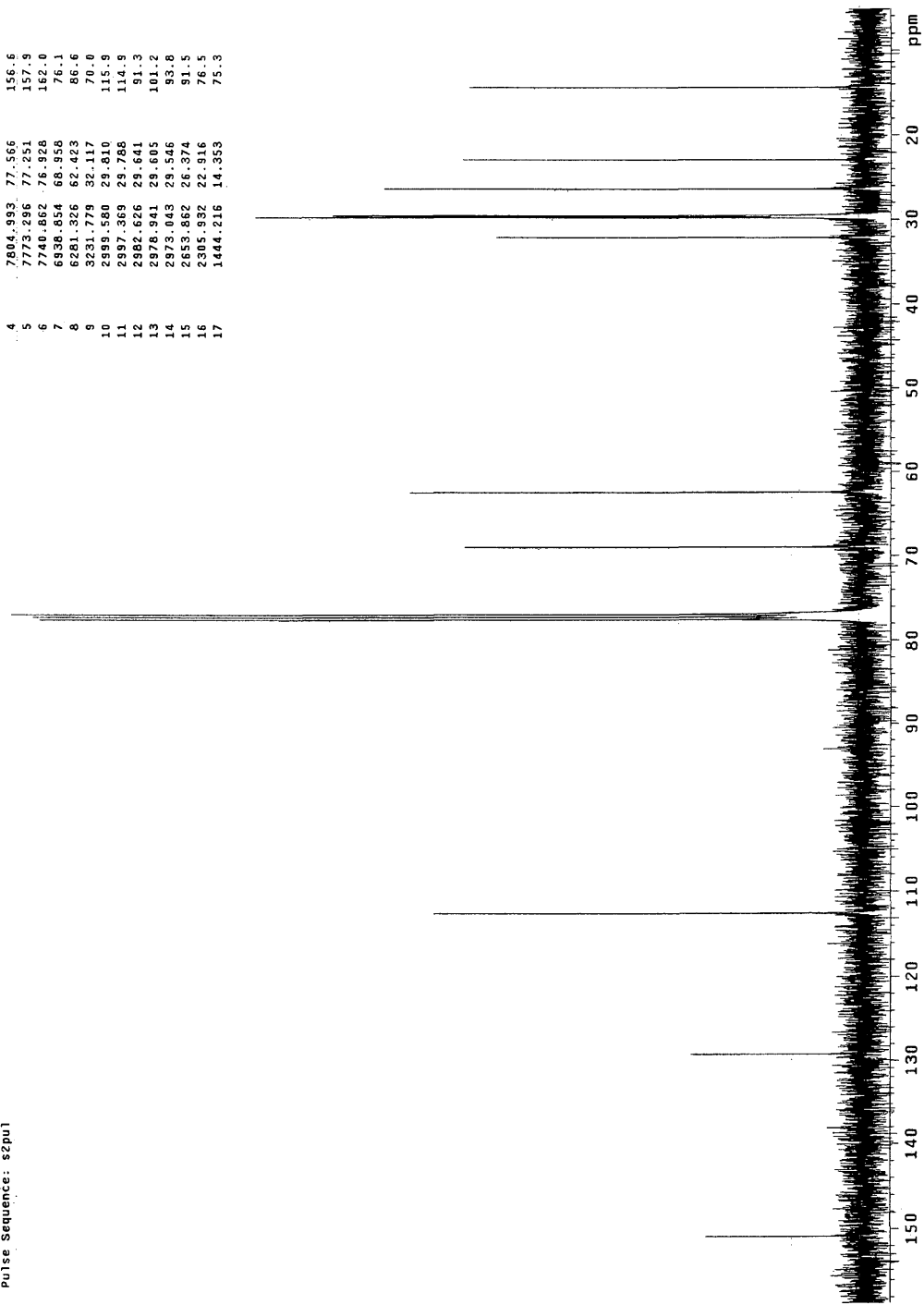


Figure 49 –  $^{13}\text{C}$  NMR Spectrum of Dihydroxymethylbenzene **9**

Aldehyde using PCC  
Automation directory:  
Sample : jw053109A  
Pulse Sequence: szpul

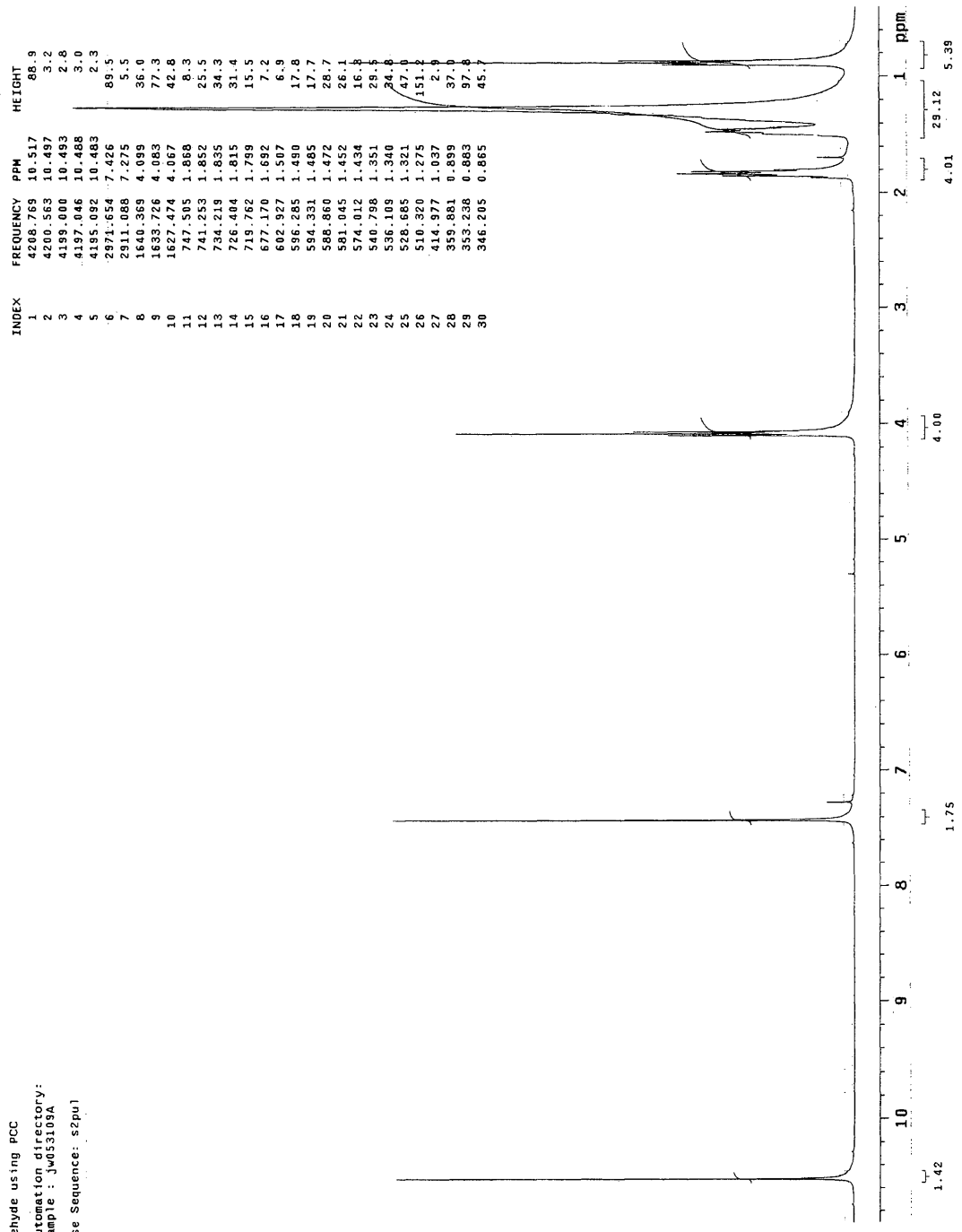


Figure 50 – <sup>1</sup>H NMR Spectrum of Dicarbaldehyde 10

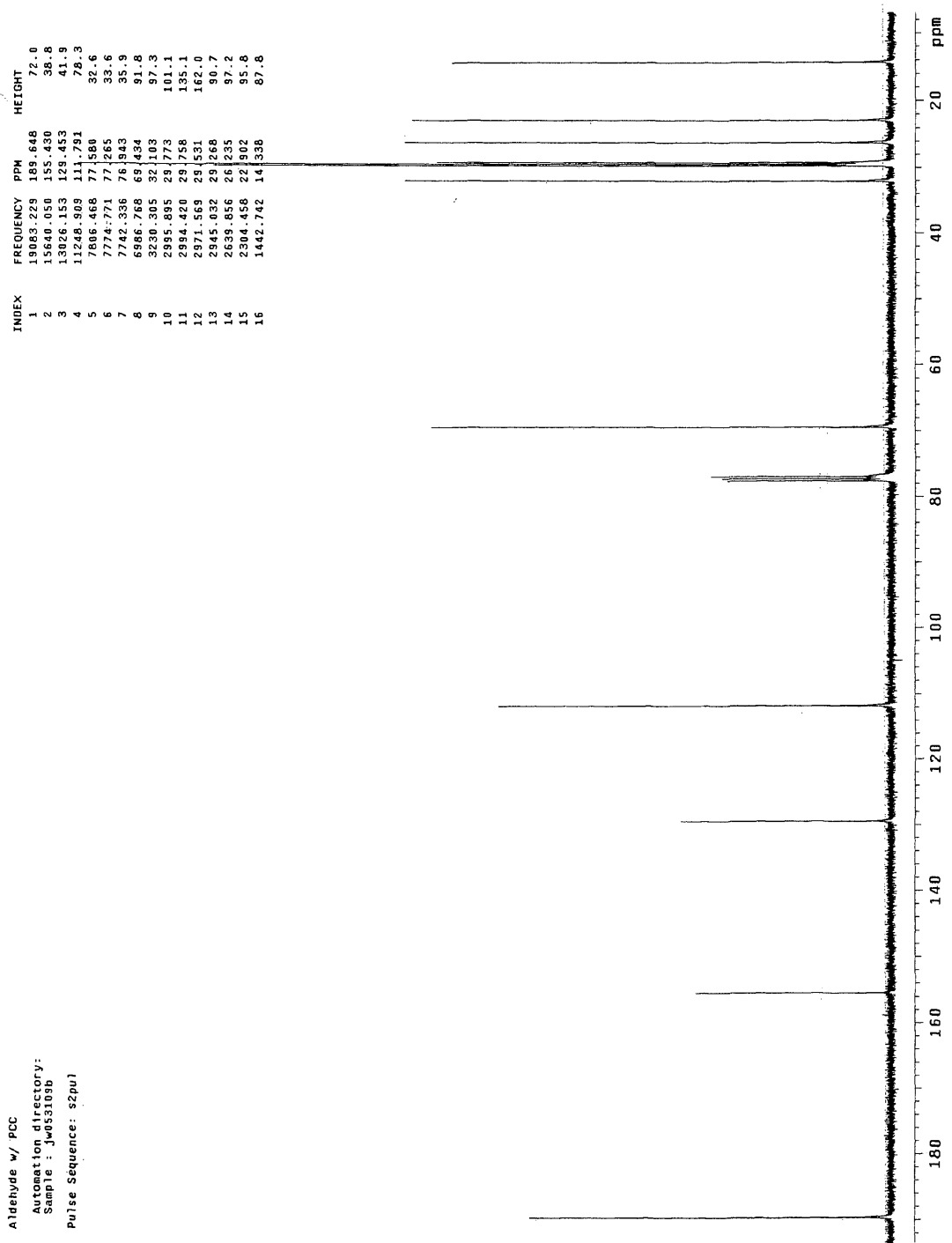


Figure 51 – <sup>13</sup>C NMR Spectrum of Dicarbaldehyde 10

Diviny/ benzene after column, 1st fraction  
 Automation directory:  
 Sample : jw012109a6  
 Pulse Sequence: s2bu1

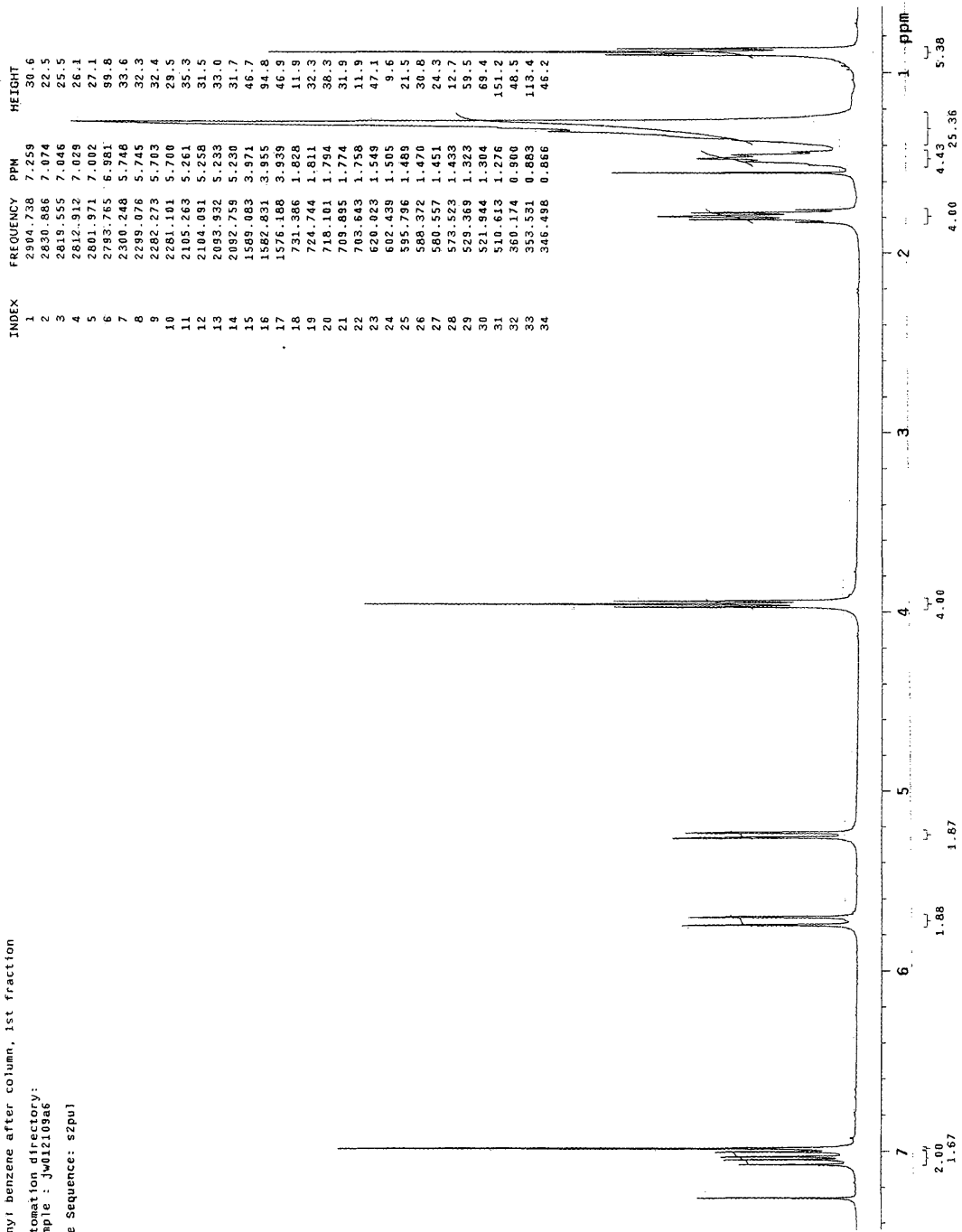


Figure 52 – <sup>1</sup>H NMR Spectrum of Diethenylbenzene 3

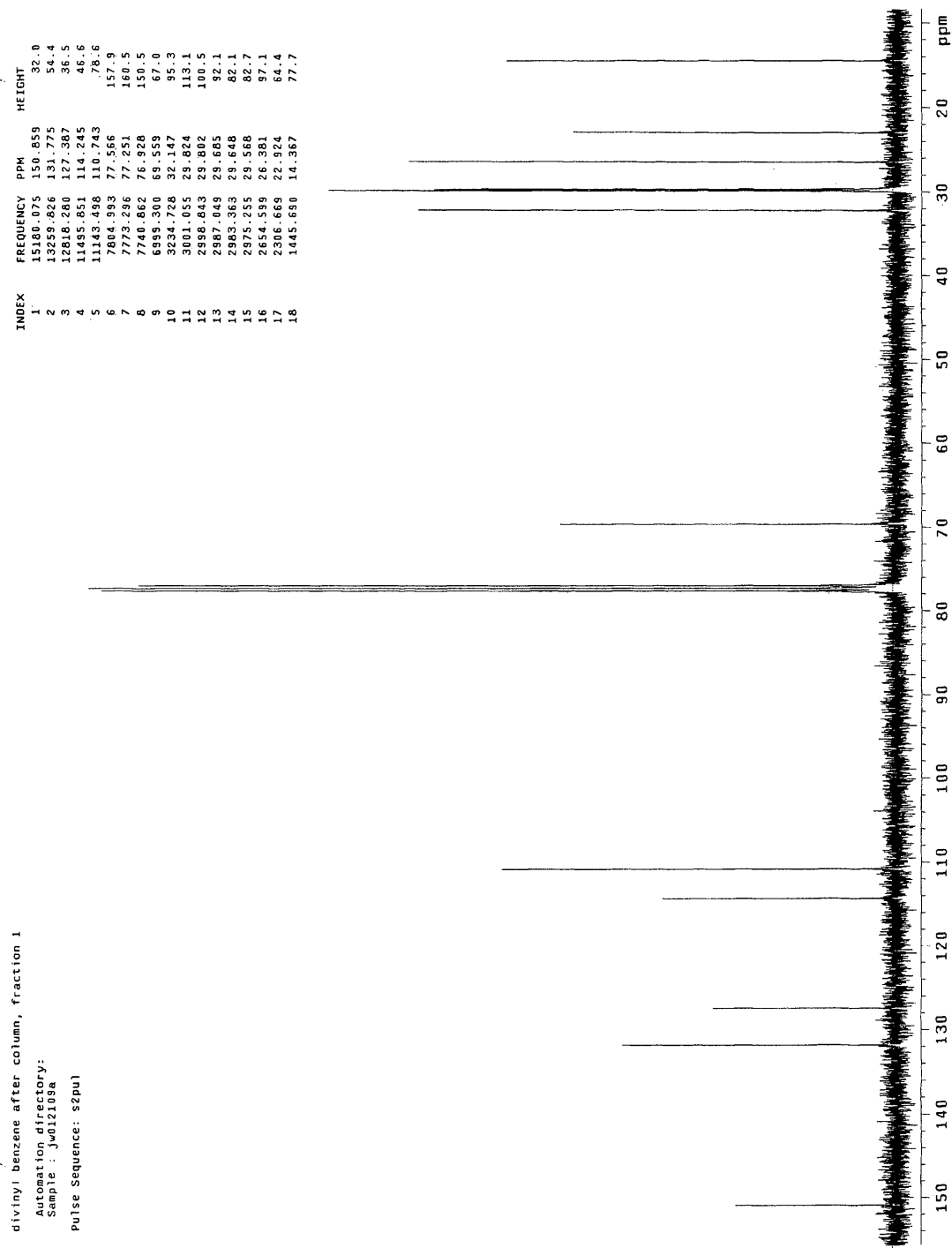


Figure 53 –  $^{13}\text{C}$  NMR Spectrum of Diethenylbenzene 3

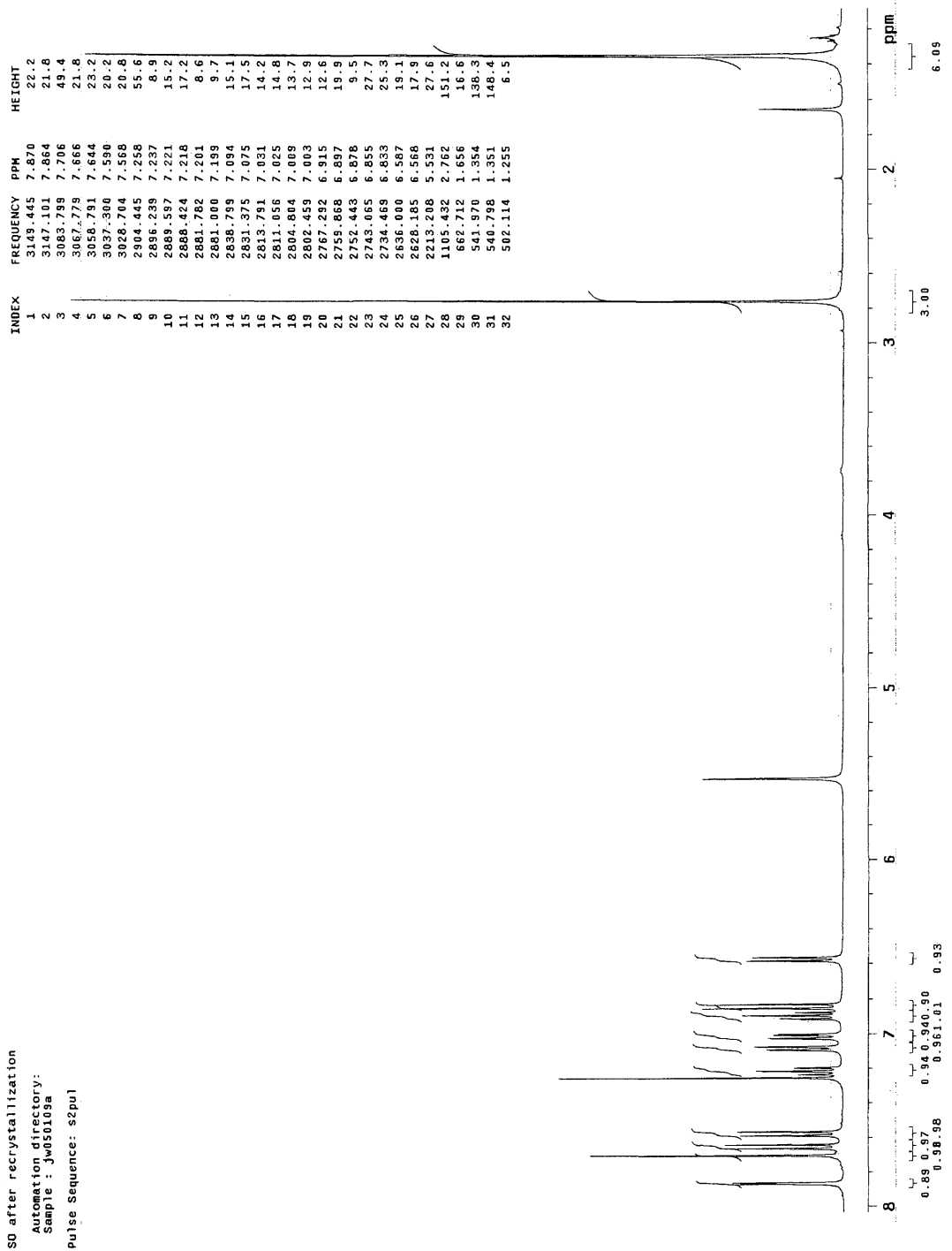


Figure 54 – <sup>1</sup>H NMR Spectrum of Hydroxyspiroxazine 4

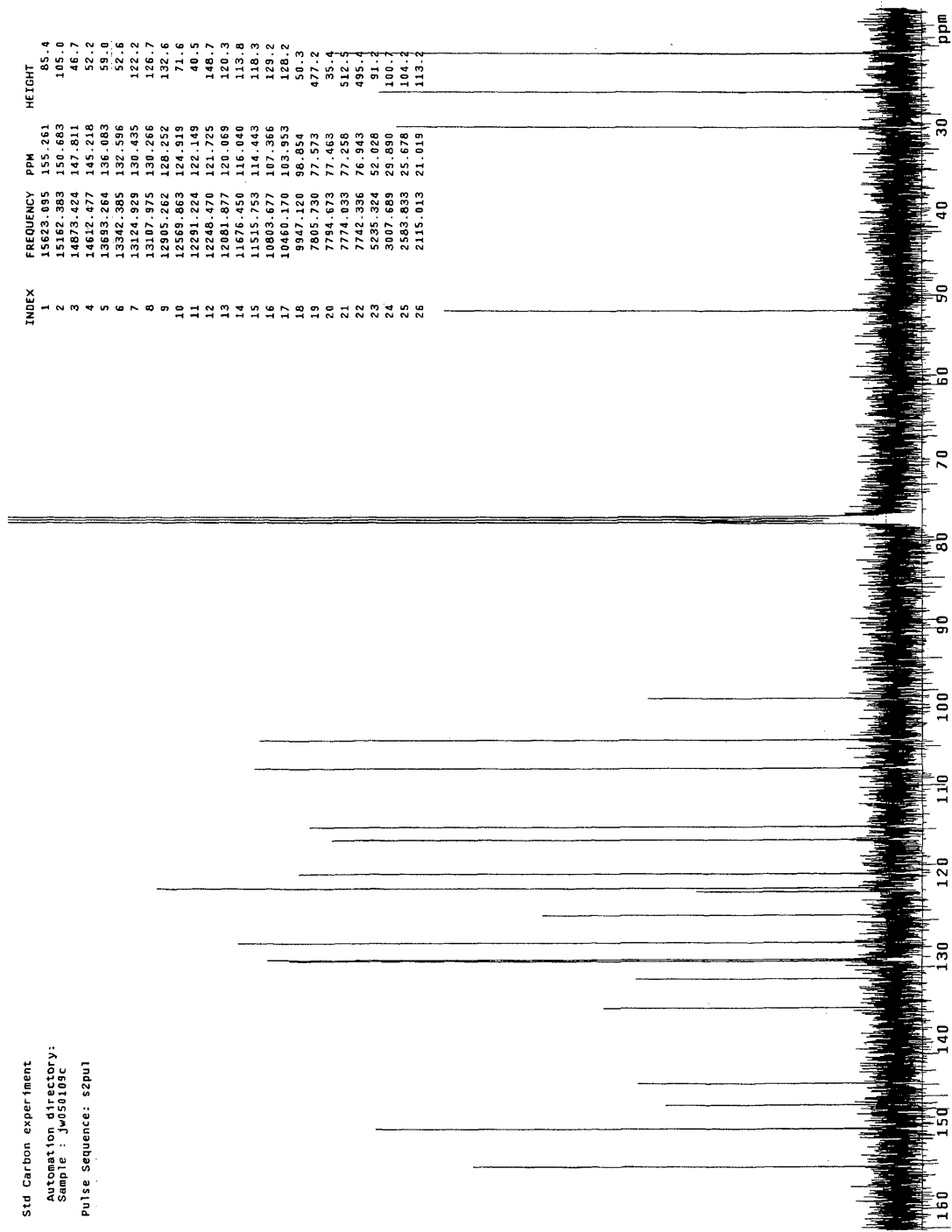


Figure 55 –  $^{13}\text{C}$  NMR Spectrum of Hydroxyspirooxazine 4

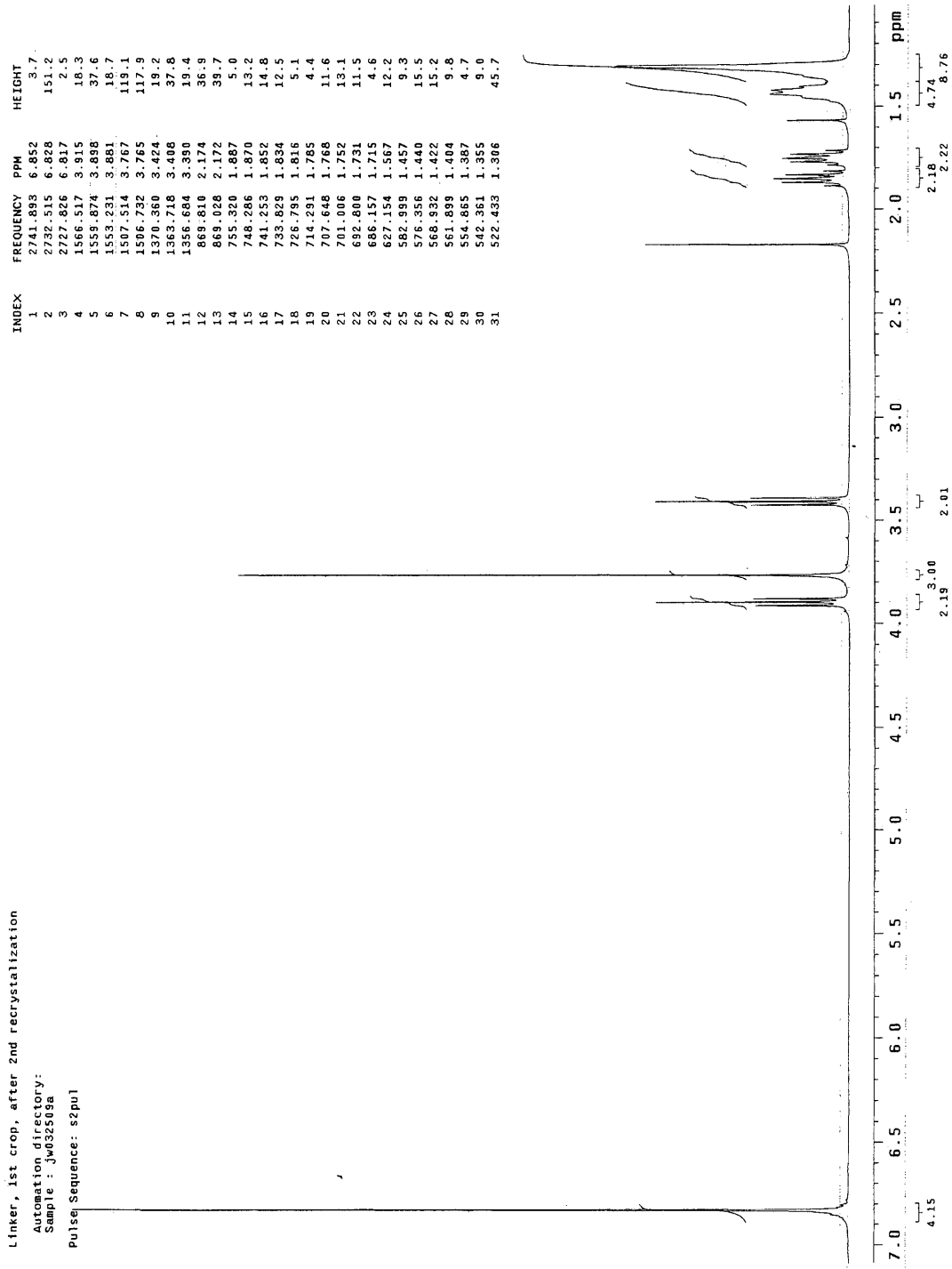


Figure 56 – <sup>1</sup>H NMR Spectrum of Bromodecyloxybenzene 14

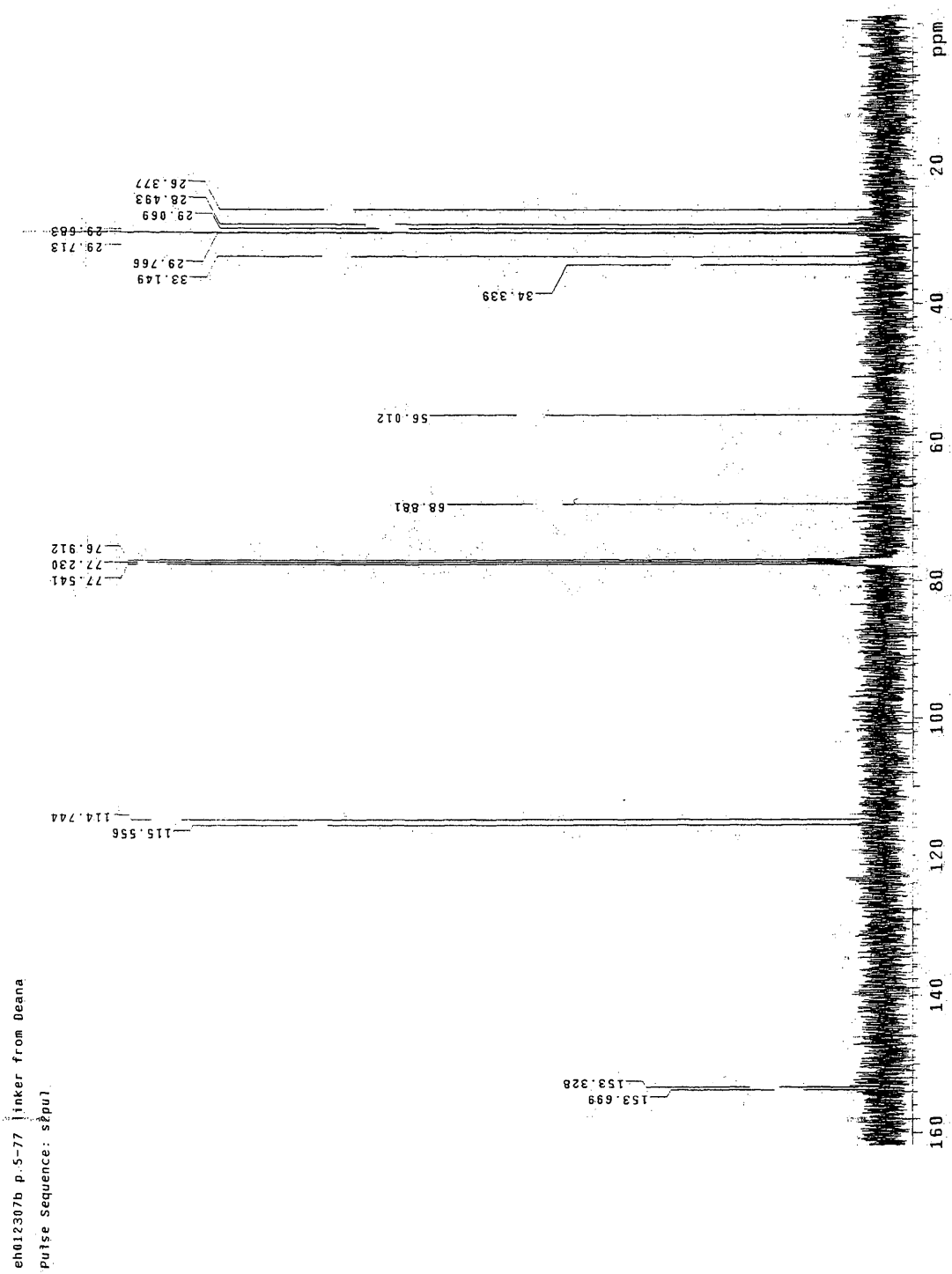


Figure 57 –  $^{13}\text{C}$  NMR Spectrum of Bromodecyloxybenzene 14

1,4-dibromo-2-bromodecylbenzene

Automation directory:

Sample : JW52203c

Pulse Sequence: s2pu1

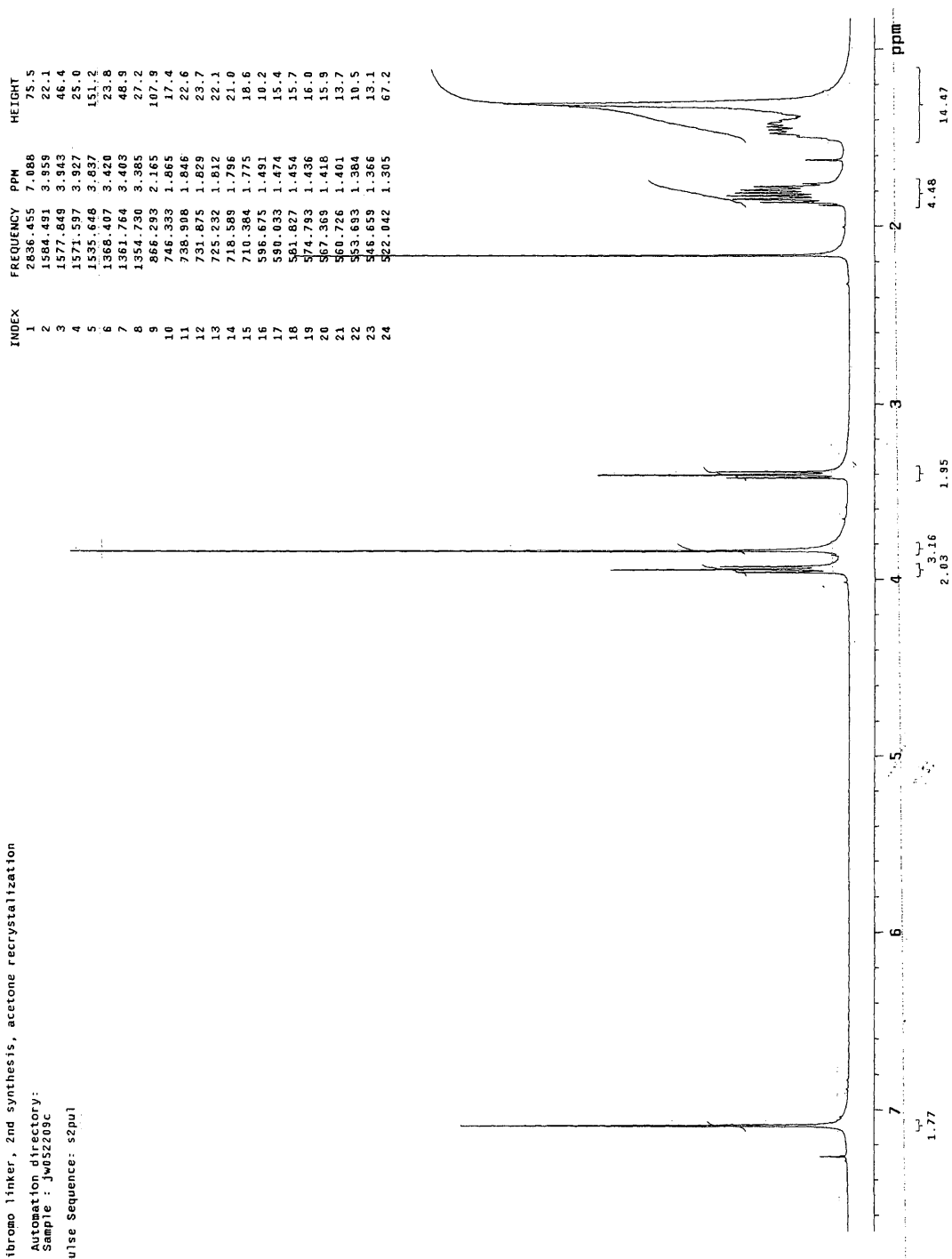


Figure 58 – <sup>1</sup>H NMR Spectrum of 1,4-dibromo-2-bromodecylbenzene 5

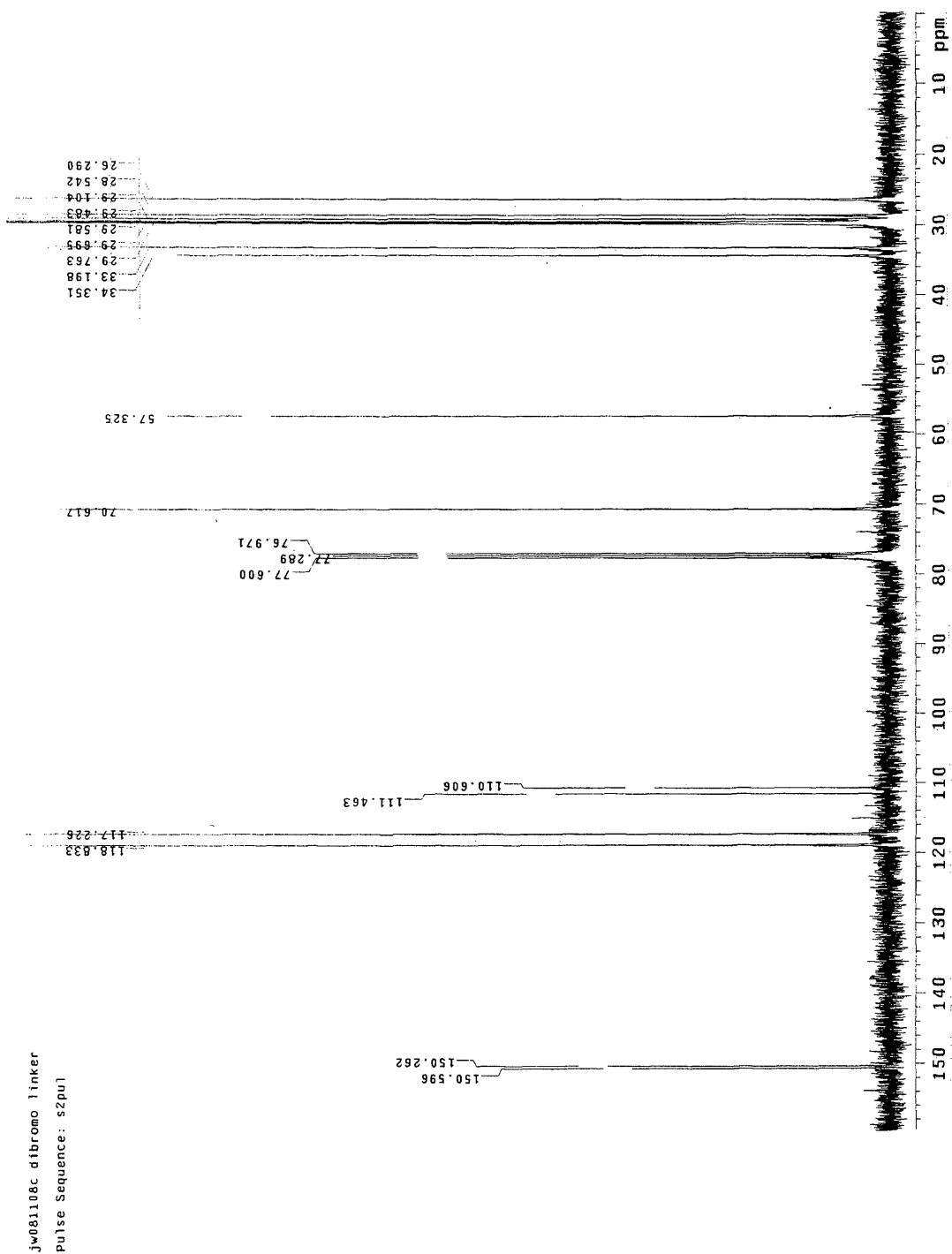


Figure 59 –  $^{13}\text{C}$  NMR Spectrum of 1,4-dibromo-2-bromodecyloxybenzene **5**

toluene/ pet ether column product- SO Linker

Automation directory:

Sample : kp070105a

Pulse Sequence: s2pu1

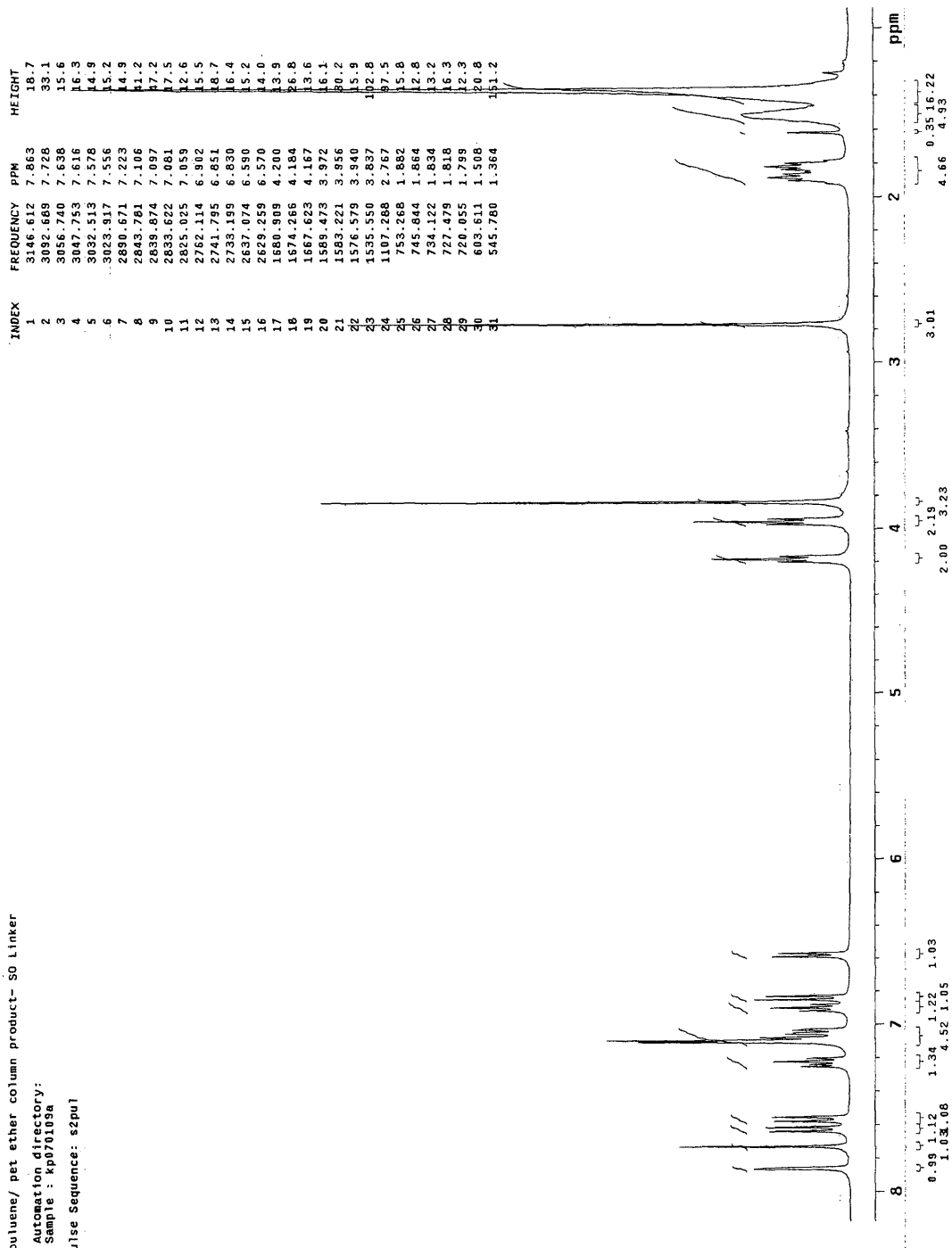


Figure 60 -  $^1\text{H}$  NMR Spectrum of 2

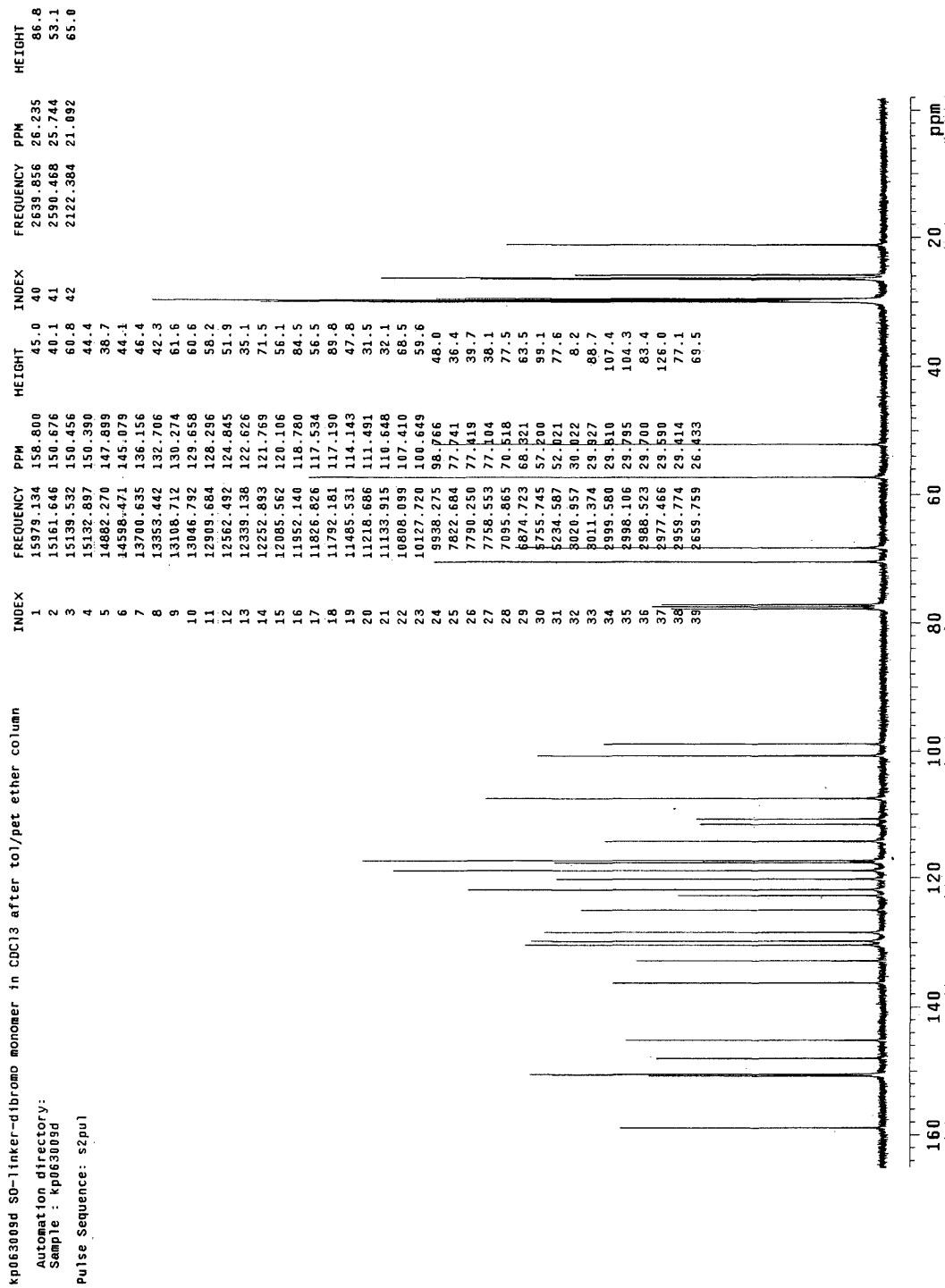


Figure 61 – <sup>13</sup>C NMR Spectrum of 2

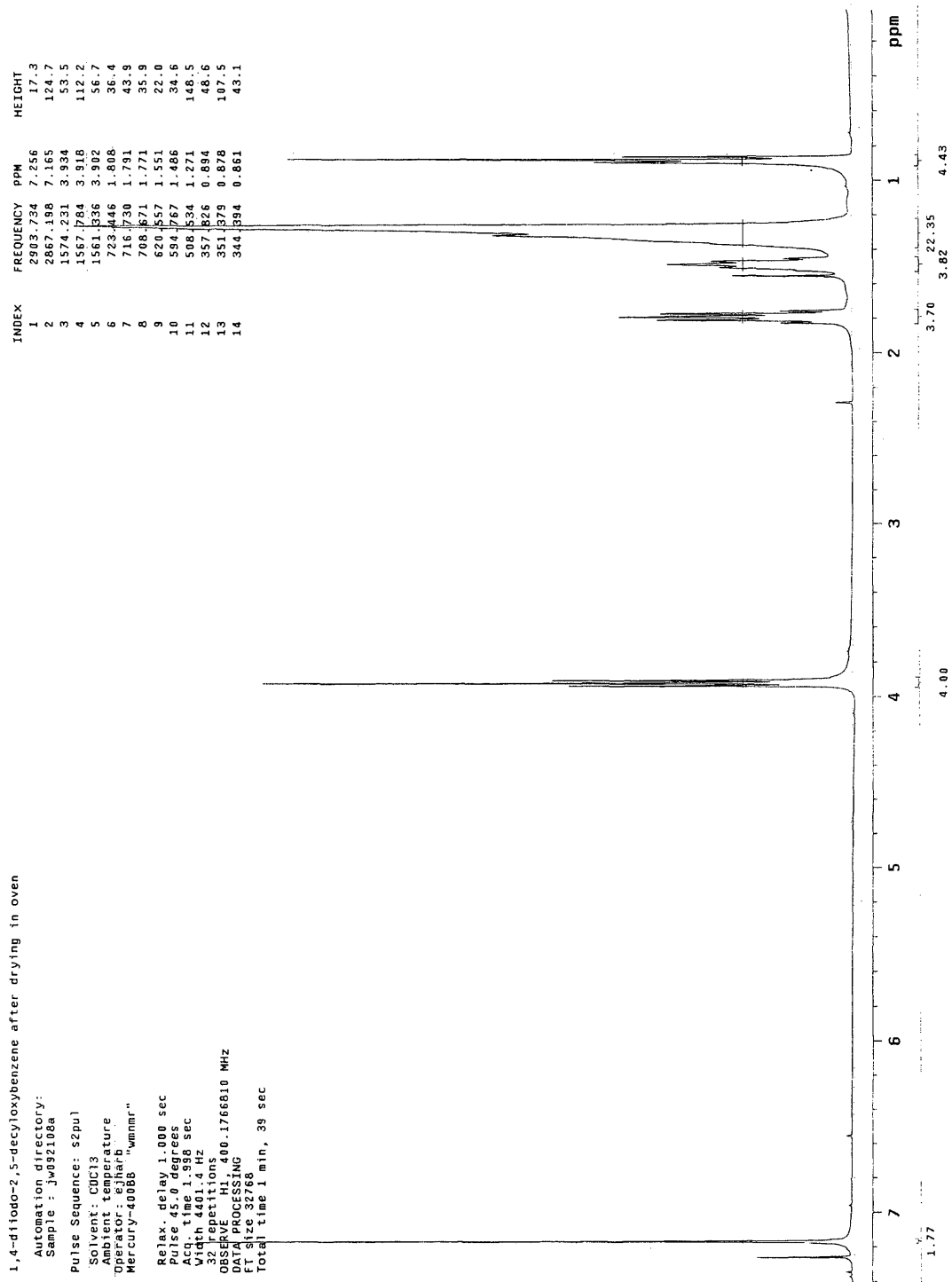


Figure 62 – <sup>1</sup>H NMR Spectrum of Diiodobenzene 18

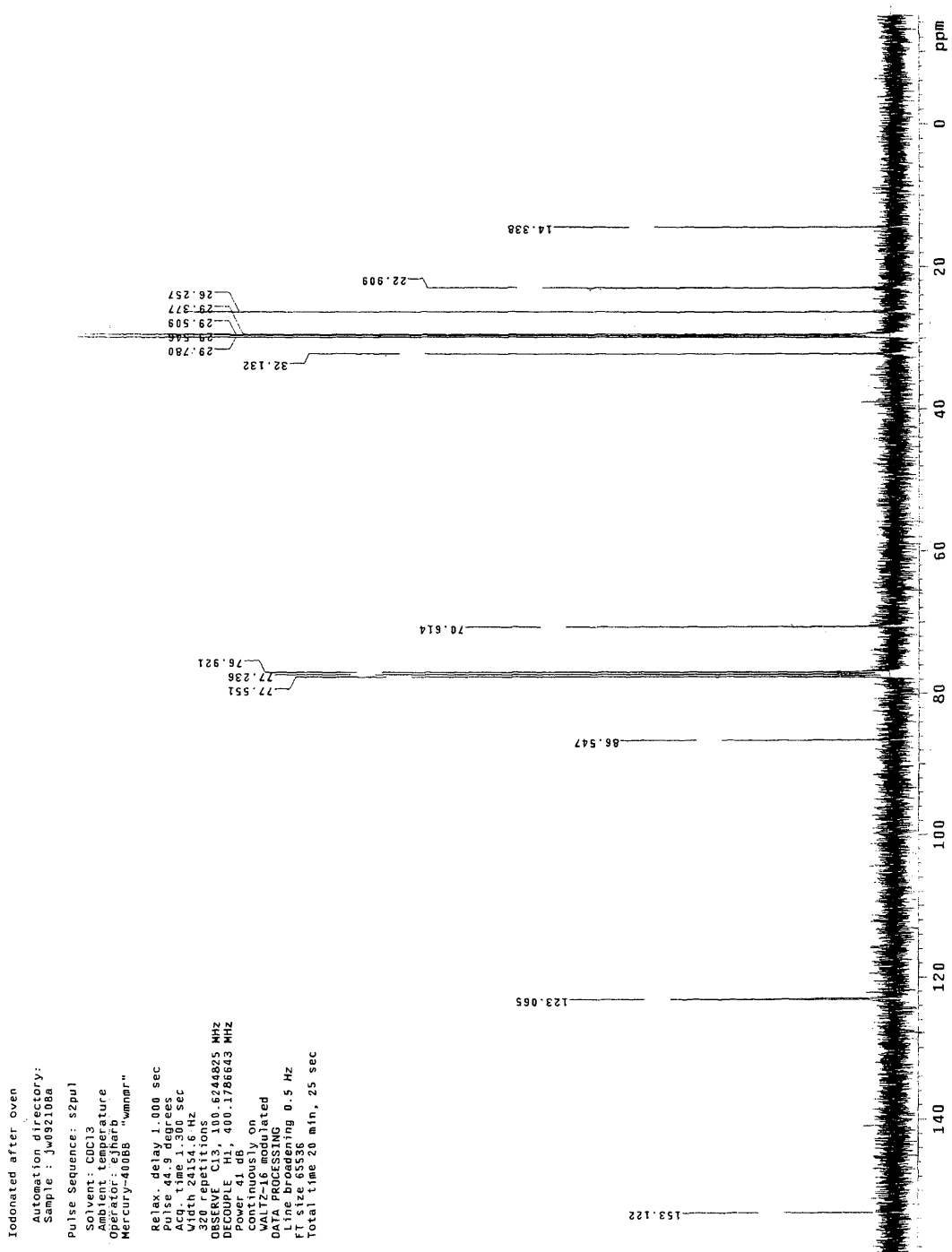


Figure 63 – <sup>13</sup>C NMR Spectrum of Diiodobenzene 18